CHARACTERIZATION OF THE MOLECULAR CHAPERONE HSP90 COHORTS, $p50^{CDC37}$ AND PROTEIN PHOSPHATASE 5, AND THEIR DIFFERENTIAL REGULATION OF THE BIOGENESIS OF THE HEME-REGULATED eIF2α KINASE

By

JIEYA SHAO

Bachelor of Science

Nankai University

Tianjin, China

1996

Submitted to the Faculty of the
Graduate College of the
Oklahoma State University
in partial fulfillment of
the requirements for
the Degree of
DOCTOR OF PHILOSOPHY
December, 2002

CHARACTERIZATION OF THE MOLECULAR CHAPERONE HSP90 COHORTS, $p50^{CDC37}$ AND PROTEIN PHOSPHATASE 5, AND THEIR DIFFERENTIAL REGULATION OF THE BIOGENESIS OF THE HEME-REGULATED eIF2α KINASE

Thesis Approved:

Robert L Matts

Thesis Adivisor

Elden C Nelson

Richard C Cooley

Dr. Lucas

Jeff Hadwiger

Timothy D. Pettitt

Dean of the Graduate College

PREFACE

The 90-kDa heat shock protein (Hsp90) is a highly conserved and ubiquitous molecular chaperone that plays a pivotal role in the functional regulation of various signaling proteins, including protein kinases and steroid hormone receptors, in the eukaryotic cells. Whereas the mechanistic details of Hsp90 function remain to be fully unveiled, the correct folding and acquisition of the ultimate biological activities of its client proteins rely on their physical interactions with Hsp90. Moreover, rather than working alone, Hsp90 forms dynamic heterocomplexes (referred to as the Hsp90 machinery) with a group of cofactors or co-chaperones *in vivo*, which acts to assist as well as regulate its chaperone activity in a controlled and ordered fashion. Here, two of these Hsp90 co-chaperones, $p50^{cdc37}$ and protein phosphatase 5 (PP5), were analyzed in this study. Their different roles in regulating the biogenesis of the previously described Hsp90 client, the heme-regulated eIF2α kinase (HRI), were investigated. These studies not only enriched our limited understanding in the functional aspects of both $p50^{cdc37}$ and PP5, but also suggested a model in which the overall chaperone activity of Hsp90 machinery, towards its substrates, is coordinated by the opposing effects of these two different Hsp90 cohorts *in vivo*. Furthermore, in an attempt to better understand these two Hsp90 cohorts, the domain structure of $p50^{cdc37}$ and potential post-translational phosphorylation sites of PP5 were studied, respectively. Whereas many questions still remain to be answered, these studies shed new light on our current understanding of the

Hsp90 chaperone machinery and unveiled several novel directions for future investigations.

I would like to give my sincere appreciation to my advisor, Dr. Robert Matts, who showed me the door to the exciting world of science and guided me throughout the entire course of study. He not only taught me the knowledge, but also the true passion for science, optimism as well as strength that are indispensable for a successful career and life. I would also like to thank the other members of my committee, Dr. Richard Essenberg, Dr. Eldon Nelson, Dr. Jose Soulages and Dr. Jeffrey Hadwiger for their critical reading of my dissertation and insightful suggestions for my research. My special thanks go to Dr. Steven Hartson, whose constant assistance and encouragement are invaluable to me. I also like to express my gratitude to those who helped me tremendously during the course of my study in each of their own ways: Dr. Uma Sheri, Dr. Bradley Scroggins, Yanwen Guo, Wenjun Huang, Bo-Geon Yun, Thomas Prince, Angela Irwin, Janet Rogers, SueAnn Hudiburg, and all the faculties and staffs in the department of Biochemistry and Molecular Biology that taught me science and helped my research in all different aspects.

Finally, I am truly grateful to my parents, my sister, and my boyfriend Jian Zhu whose unconditional love and support are the ultimate driving force of my life.

TABLE OF CONTENTS

LIST OF TABLES

LIST OF FIGURES

NOMENCLATURE

AA	arachidonic acid
ACN	acetonitrile
ANP	atrial natriuretic peptide
ATA	aurintricarboxylic acid
ATP	adenosine triphosphate
ADP	adenosine diphosphate
AP	alkaline phosphatase
APC	anaphase-promoting complex
ASK1	apoptosis signal-regulating kinase 1
Bag	Bcl-2 (B cell lymphoma gene-2)-associated protein
cAMP	adenosine 3',5'-cyclophosphoric acid
CBP	CREB binding protein
Cdc	cell division cycle
Cdk	cyclin-dependent protein kinases
CREB	cyclic AMP response element binding protein
Cyp40	40-KDa cyclosporine A-binding protein
DMSO	dimethyl sulfoxide
DTT	dithiothreitol
EDTA	ethylenediaminetetraacetic acid
EGTA	ethylene glycol-bis(2-aminoethyl)-N,N,N',N'-tetraacetic acid
eIF2α	α subunit of the eukaryotic initiation factor 2
FKBP	FK506 binding protein
FLAG-tag	octa-amino acid peptide-DYKDDDDK
GA	geldanamycin
GaG-agarose	goat anti-mouse IgG cross-linked to agarose
GANG/MCM3	germinal center-associated DNA primase associated with minichromosome maintenance 3 gene product
GCN2	general control non-derepressible-2
GDP	guanosine diphosphate
GimC	genes involved in microtubule biogenesis complex
grp94	94-KDa glucose-regulated protein
GST	glutathione-*S*-transferase
GTP	guanosine triphosphate
Hck	hemopoietic cell kinase
HEPES	4-(2-Hydroxyethyl)piperazine-1-ethanesulfonic acid
Hip	Hsp70-interacting protein
Hop	Hsp organizer protein
HRI	heme-regulated inhibitor of protein synthesis

Hsc	heat shock cognate protein
Hsp	heat shock protein
HtpG	high temperature protein G
IKK	IkappaB kinase
KSR	kinase suppressor of Ras
Lck	lymphoid cell kinase
MALDI-TOF	matrix-assisted laser/desorption ionization-time of flight
MAPK	mitogen-activated protein kinase
Met3	deletion mutant of HRI starting at the third methionine
MOK	MAPK/ MAK/ MRK overlapping kinase
Mps1	monopolar spindle gene product
NEM	N-ethylmaleimide
Ni^{2+}-NTA	Ni^{2+}-nitrilotriacetic acid
OA	okadaic acid
PCR	polymerase chain reaction
PERK/PEK	PKR-like ER kinase/pancreatic eIF2α kinase
PIPES	piperazine-1,4-bis(2-ethanesulfonic acid)
PKA	protein kinase A
PKR	double-stranded RNA-activated protein kinase
PMSF	phenylmethanesulfonyl fluoride
pNPP	p-nitrophenyl phosphate
PPIase	peptidyl-prolyl isomerases
PSD	post-source decay
PVDF	polyvinylidene difluoride
Rb	retinoblastoma tumor suppressor protein
RCM-BSA	reduced carboxymethylated bovine serum albumin
RRL	rabbit reticulocyte lysate
SDS-PAGE	sodium dodecyl sulfate-polyacrylamide gel electrophoresis
Src	rous sarcoma virus oncogene
STAT	signal transducers and activators of transcription
Sti1	stress inducible protein-1
TFA	trifluoroacetic acid
TnT	coupled transcription and translation
TPCK	N-p-Tosyl-L-phenylalanine chloromethyl ketone
TPR	tetratricopeptide repeat
TRAP-1	type-1 tumor necrosis factor receptor-associated protein
TRiC	tailless complex polypeptide-1 [TCP-1] ring complex

CHAPTER I

Literature Review

The principle of protein folding has been the subject of intensive studies over the past several decades. Consequently, remarkable progresses have been made in our understanding of the basic principle of such a fundamental and complex biological process that all cellular proteins need to undergo to achieve their native and functional tertiary structures. It is clear that rather than randomly sampling all possible conformations, proteins fold into their native structures through one or more specific pathway(s) in which the conformational space available to the proteins is efficiently restricted (60, 61). The major driving force for the rapid protein folding process appears to be the removal of hydrophobic side chains of amino acids away from the aqueous solution to form the hydrophobic core of the folded proteins (60). According to the widely-accepted Anfinsen theory, all the information necessary to specify the tertiary structure of a protein is contained in its primary amino acid sequence (3). Such a hypothesis was based on the observation that many small denatured proteins are able to fold back to their native conformations spontaneously *in vitro*. As a result, it had been assumed that all cellular proteins fold in the same unassisted fashion *in vivo* as well. However, failure of large multi-domain proteins to refold spontaneously *in vitro* argued strongly against such a simple view (111). Furthermore, even for small single-domain proteins, spontaneous folding *in vitro* could only occur under ideal conditions such as high dilution and low temperature (82). Such an ideal *in vitro* environment differs profoundly from that inside a living cell which is extremely crowded and dynamic with the effective protein concentration estimated to be as high as 300 mg/ml (271). One

could easily predict that proteins, especially nascent or denatured ones with hydrophobic regions exposed, are prone to form aggregations in such a folding unfriendly environment. Nonetheless, studies over the past decade have progressively unveiled the mechanism utilized by the living cells to ensure the correct and efficient folding of many cellular proteins, referred to as assisted protein folding. The secret lies in a number of conserved protein families named molecular chaperones, which as their name implies guide proteins to their correct conformations, but do not remain associated with the final products (reviewed in 24, 82, 96, 200, 202).

Molecular chaperones are ubiquitous cellular proteins many of which are abundantly expressed under both physiological and stressed conditions. They are also often called heat shock proteins (Hsps) based on the fact that their expression level becomes elevated in response to heat shock and other cellular stresses. Unlike folding catalysts, such as protein disulfide isomerases and peptidyl-prolyl isomerases (PPIase), molecular chaperones do not contain steric information specifying correct folding. Instead, they act by preventing incorrect interactions within or between non-native polypeptides, minimizing the number of non-productive folding pathways, thus generally increasing the yield but not the rate of folding reactions. Based primarily on the size and functional mechanism, molecular chaperones can be divided into several distinct families, namely Hsp104/Hsp101, Hsp90, Hsp70, Hsp60/GroEL (chaperonin), and small Hsps (sHsps). Regardless of the differences, the chaperoning activities of most of them are regulated by the dynamic cycles of nucleotide binding, hydrolysis and release except sHsps (reviewed in 24, 82, 96).

Hsp60/GroEL:

As probably the best characterized example of the molecular chaperones, chaperonins exhibit distinct structural and functional features compared to other members of the chaperone family. They are large cylindrical oligomeric protein complexes consisting of two stacked rings of 7 to 9 identical or homologous subunits each depending on the specific sources (reviewed in 25, 82, 96). They can be further classified into two different groups based on the presence or absence of a small cofactor named GroES/Hsp10. In group I chaperonins such as the bacterial GroEL and the Hsp60 complexes from eukaryotic mitochondria and chloroplasts, GroES/Hsp10 forms a ring-shaped lid structure which is essential for the nucleotide-regulated protein folding process of GroEL (73). Such a lid structure appears to be absent in group II chaperonins such as the eukaryotic TRiC (tailless complex polypeptide-1 [TCP-1] ring complex) (100, 134) although recent evidence suggests that a different hetero-oligomeric protein called prefoldin or GimC (genes involved in microtubule biogenesis complex) may be the functional equivalent of GroES/Hsp10 (85, 219, 250). Regardless of these subtle differences in subunit composition and structural architecture, both groups of chaperonins share the same functional mechanism which involves assisted protein folding in the large central cavity formed by the ring-shaped multiple subunits. It is thought that chaperonins function primarily by sequestering their unfolded polypeptide substrates inside the central cavity which mimics an "Anfinsen cage", provides infinite dilution and allows the substrates to fold according to their thermodynamic potentials (68). Extensive studies on the GroEL/GroES complex revealed complicated yet controlled conformational changes of its different subunits during the ATP-driven reaction cycle of the assisted protein

folding process (96, 148). Such studies also suggested the reiterative binding and release of protein substrates by the chaperonins prior to the acquisition of their final native conformations. In addition to its function of preventing unproductive protein aggregation within the central cage, recent evidence suggests another possible mechanism of the GroEL/GroES complex in which it unfolds the trapped intermediates and thus increases the folding rate of some proteins (218).

Hsp90:

Representing 1-2% of the total cytosolic proteins, hsp90 is among the most abundant proteins in eukaryotic cells. Its homologues have been found in the endoplasmic reticulum and mitochondria, namely grp94 (94-kDa glucose-regulated protein) (231) and TRAP-1/hsp75 (type-1 tumor necrosis factor receptor-associated protein), respectively (72, 230). In addition, its counterpart also exists in prokaryotic cells, termed HtpG (high temperature protein G) (7). The eukaryotic cytoplasmic hsp90 has two isoforms, hsp90-α and hsp90-β, which are 76% identical and the consequences of a gene duplication about 500 million years ago. While no major differences have been found between these two isoforms regarding their molecular characteristics and functions, they appear to be differentially expressed with hsp90-α being more inducible by heat shock and other stress conditions than hsp90-β, which is also sometimes referred to as hsc-90 (the constitutively expressed cognate protein of hsp90) (127, 159).

Biochemical and electron microscopic studies indicate that hsp90 contains two conserved domains attached to each other by a highly charged loop which is variable in

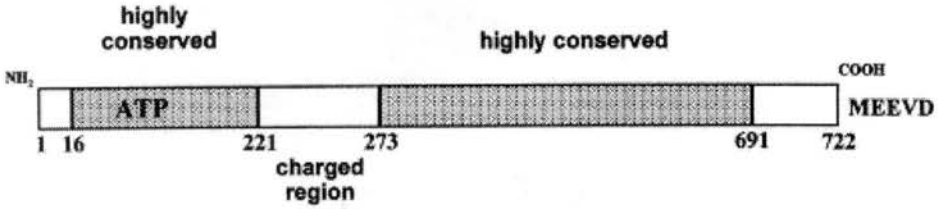

both length and composition among species and homologues (110, 125, 163, 208). Recently, the three-dimensional structures of the isolated N-terminal domains of human and yeast Hsp90s, which were nearly identical, were solved by X-ray crystallography. Remarkably, both contain an unconventional nucleotide binding site which is recognized by ATP, ADP and the Hsp90-specific anti-tumor drug geldanamycin (183, 234). Such an unusual nucleotide-binding site has also been found in DNA gyrase B, MutL and Histidine kinases, and referred to as the Bergerat fold (11, 67). Unlike the conventional nucleotide binding fold, it is a α/β bilayer sandwich consisting of four-stranded antiparallel β-sheet flanked on one side by nine α-helices with the nucleotide bound between the α-helices and β-sheet. In contrast to the extended conformation of the nucleotides bound to Hsp70 and GroEL, those bound to the N-terminal domain of Hsp90 are rather compact and kinked and closely mimicked by geldanamycin (Figure 1) (183, 234). Tertiary structure of the C-terminal part of Hsp90 has not been reported so far. However, functional studies have mapped the docking site for the tetratricopeptide repeat (TPR) domain to its extreme C-terminal 12-kDa fragment (39, 263). TPR domains consist of tandem degenerate repeats of 34 amino acids each of which adopts a basic structure of two anti-parallel α-helices connected by a short turn (53). TPR domains exist in several Hsp90 cohorts, such as p60/Hop, protein phosphatase 5 and immunophilins, and mediate their mutually exclusive interactions with Hsp90 (39). The C-terminal 12-kDa fragment also contains the dimerization site of Hsp90 (156, 162).

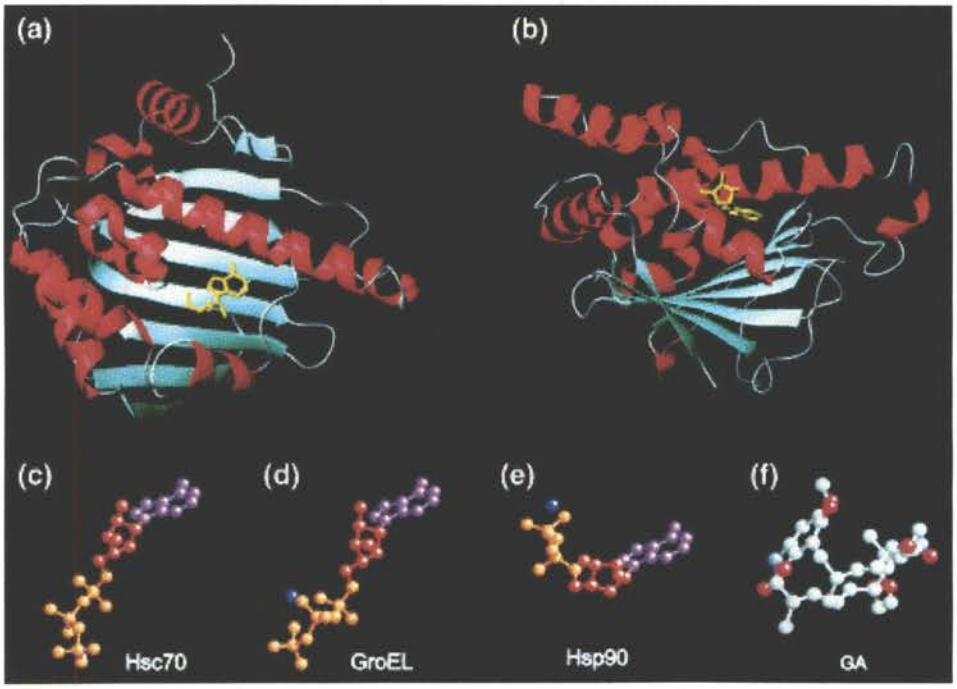

Figure 1. (a) and **(b)** Structure of the N-terminal domain of ATP-bound yeast Hsp90 in two different orientations. **(c-e)** Conformations of ATP bound to Hsc70, GroEL and Hsp90. **(f)** Conformation of geldanamycin (GA), a fungal benzoquinone ansamycin, bound to Hsp90 (adapted from ref 23).

Interestingly, a second ATP-binding site which can be occupied by novobiocin, a coumarin-type antibiotic that antagonizes Hsp90 function both *in vitro* and *in vivo*, has recently been mapped to the C-terminal region of Hsp90 (140) (discussed below).

The charged linker region appears to be unessential for Hsp90 function since it is entirely absent from the prokaryotic HtpG and mammalian mitochondrial TRAP-1/Hsp75 and totally dispensable for the viability and signal transduction functions in yeast (136). However, it contains two major *in vivo* phosphorylation sites of Hsp90 (65, 133) as well as a potential nuclear localization signal (152), indicating its possible involvement in the functional regulation and nucleo-cytoplasmic translocation of eukaryotic Hsp90. Recent evidence implicates that the charged region also mediates the functional communication between the N- and C-terminal domains of Hsp90. It appears to act as a molecular switch between the two domains of Hsp90 in a nucleotide-dependent fashion. According to the model recently proposed by Soti *et al*, in the nucleotide-free conformation of Hsp90 the charged region binds to the C-terminal domain whose ATP-binding ability is concomitantly hindered. The first ATP molecule binds to the N-terminal domain, establishing contacts with the charged region and thus relieving its steric hindrance on the C-terminal domain, which is then able to bind the second ATP molecule (232). Since ATP binding and hydrolysis are directly coupled to the chaperone activity of Hsp90 (discussed below), this charged region is thus an important element for *in vivo* function of eukaryotic Hsp90. Such a model also predicts large conformational changes of Hsp90 accompanying ATP binding, which has been firmly proven by different approaches including circular dichroism spectrum, tryptophan fluorescence and susceptibility to trypsinolysis (46).

Electron microscopy and antibody binding studies suggest that Hsp90 forms a dimer which exhibits an elongated structure. The two monomers are connected at the C-terminal ends whereas their N-terminal ends point to opposite directions. Interestingly, upon ATP binding or heat shock, the linear conformation of the Hsp90 dimer changes into an O-ring-shaped structure in which the N-terminal domains of the two monomers come in contact with each other (142). The existence of a second dimerization site within the N-terminal domain of Hsp90, in addition to the major site in the C-terminal domain, was also supported by the finding that the isolated N-terminal fragments of yeast Hsp90 formed dimers in the crystal structure (184). Recently, the conditional and transient dimerization of the N-terminal domain has been coupled to the ATPase cycle of Hsp90 which is believed to drive the molecular "clamp" of the dimer to open or close as a result of ATP binding and hydrolysis, respectively (182). The similar "clamp" mechanism is also used by DNA gyrase B (120) and MutL (6) both of which share the unusual Bergerat ATP-binding fold with Hsp90. ATPase cycle-regulated opening and closing of the clamp allow these two enzymes to bind and release their DNA substrates accordingly. Although the true functional significance of such a molecular clamp of Hsp90 is currently unclear, its regulated closure and opening may be directly involved in the efficient binding and releasing of the client proteins, which mechanistically resembles its structural relatives (regarding the ATP-binding domain), DNA gyrase B and MutL.

Although it is now firmly established that Hsp90 is an ATP-dependent protein, such an issue has been quite controversial over the past years. The experimental difficulty in solving this question has been mostly due to the weak inherent ATPase activity of Hsp90 (165, 172) which is usually assessed in a high background of noise

from contaminating ATP-binding and hydrolyzing proteins. Recently with a combination of structural, genetic and more stringent biochemical studies it finally became clear that Hsp90 is indeed an "active" molecular chaperone which binds and hydrolyzes ATP, and most importantly such an ATPase activity is essential for its *in vivo* function (165, 172). Hsp90 mutants with compromised activities of ATP binding and hydrolysis (within its N-terminal domain) failed to maintain the viability of yeast cells. Functional regulation of Hsp90 by nucleotides is accompanied by and perhaps a result of its concomitant conformational changes induced by nucleotide binding. According to a simple two-state model, occupation by ATP or its hydrolysis product ADP determines two distinct conformations of Hsp90. In the ATP-bound state, Hsp90 is in a "closed" or "slow on/slow off" form which interacts with the substrates tightly. ADP, on the other hand, changes Hsp90 to an "open" or "fast on/fast off" conformation which displays weaker affinity for the substrates (237). Conformational differences between these two alternating states are also reflected by the preferential binding of its cohorts p23 (91, 117, 237) and p60/Hop (114) to the ATP-bound and ADP-bound forms of Hsp90, respectively. Evidence suggests that nucleotide-free Hsp90 exists in a conformation similar to the ADP-bound form, as judged by the criteria mentioned above (237). The Hsp90 specific inhibitor geldanamycin occupies the N-terminal nucleotide binding pocket of Hsp90, locks it in an ADP-like conformation and destabilizes its normal interaction with the substrates (91, 208, 234, 257). The transition metal oxyanion molybdate, on the other hand, binds to the same nucleotide site and maintains Hsp90 in an ATP-bound state even after ATP hydrolysis, thus stabilizing its interactions with its substrates (90, 99).

Like Hsp70, the inherent ATPase activity of Hsp90 is also regulated by its interaction with the cohorts. Both p60/Hop and $p50^{cdc37}$ have been postulated to inhibit the ATPase activity of yeast Hsp90 (185, 220). The inhibitory effect of p60/Hop, however, is not caused by the simple occupation of the TPR-binding site in the C-terminal domain of Hsp90 *per se* since binding of another TPR-containing cohort Cpr6 to the same site has no effect. Instead, it appears to involve direct interaction of p60/Hop with the N-terminal ATP-binding domain of Hsp90 which causes blockage of nucleotide binding (185). Alternatively, since both p60/Hop and $p50^{cdc37}$ bind to the Hsp90 dimer as dimers themselves, they may exert their inhibitory effects by restricting the conformational flexibility of the Hsp90 dimer which is directly coupled to its ATPase cycle (185, 220). Interestingly, the intrinsic ATPase activity of human Hsp90 is much weaker and seems to be regulated in a somewhat different way than the yeast protein. A recent study reported a 200-fold stimulation of the ATPase activity of human Hsp90 by a client protein, the ligand-binding domain of the glucocorticoid receptor. Whereas p60/Hop inhibits and the immunophilin FKBP59 further enhances the substrate-stimulated ATPase activity of human Hsp90 respectively, they have no effect on its basal ATPase activity. p23, however, inhibits both the basal and substrate-stimulated ATPase activity of human Hsp90 (150).

To make the ATPase cycle of Hsp90 even more complex, a second nucleotide-binding site has recently been identified in its C-terminal region. The investigation started with the finding that novobiocin, a coumarin-type antibiotic which binds adjacent to the ATP-binding site of bacterial DNA gyrase B and interferes with nucleotide binding (147), also interacts with Hsp90 and causes depletion of Hsp90-dependent kinases *in vivo*

(141). Its binding to Hsp90 is readily competed by ATP and such a binding site is mapped to the C-terminal 190 amino acids of Hsp90 which overlaps with the dimerization and TPR-binding sites (140). The two nucleotide binding sites, although separated, seem to function in a cooperative fashion in light of the fact that within the context of the full length Hsp90, occupation of the N-terminal nucleotide pocket is necessary to open up the C-terminal site which is otherwise blocked by the charged region (232). The biological significance of this second nucleotide binding site is also underscored by the observation that novobiocin inhibits the interaction of Hsp90 with two of its co-chaperones p23 and Hsp70 (indirectly bridged by p60/Hop), which are essential components of the Hsp90 chaperone machinery (140). Nonetheless, it is far from clear exactly how these two nucleotide binding sites cooperate to regulate the structure and function of Hsp90.

In vitro folding assays using artificial substrates, such as citrate synthase and rhodanese, have shown that Hsp90 is able to suppress the aggregation of nonnative proteins (112, 258, 264). However, its natural clients *in vivo* seem to be limited to a subset of protein families most of which are involved in cellular signal transduction such as members of the steroid hormone receptors and protein kinases (Table 1) (reviewed in 23, 200). In most cases, the interaction with Hsp90 serves to maintain the client protein in an "inactive" but "activatable" state which is structurally unstable without the chaperone protection. Although this may explain the essentialness of Hsp90 in eukaryotic cells, its high abundance even under unstressed conditions suggests more general functions for this seemingly specialized chaperone. Nonetheless, although Hsp90 is believed to participate in the after-stress recovery of various damaged cellular proteins

along with other molecular chaperones (47), under physiological conditions it does not seem to be important for the general folding of newly synthesized proteins (161). In a recent report Rutherford *et al* hypothesized that Hsp90 plays a pivotal role in evolution by functioning as a "buffer" for protein conformational diversity in the cell. They have found that by inactivating Hsp90 function through conditional mutations or geldanamycin treatment in *Drosophila melanogaster* multiple phenotypic variations were observed due to the unveiling of the preexisting mutations in various regulatory pathways, which are normally kept quiet by the functional Hsp90 (205). Such a buffering capacity of Hsp90 is also conserved in plant kingdom as similar approaches in *Arabidopsis* unveiled a wide array of genetic variations as well (188). Therefore, Hsp90 may serve to preserve protein function in the face of genetic variations by maintaining mutant proteins in their wild-type conformations.

Attempts have been made to map the client binding site on Hsp90. Using different *in vitro* substrates, two chaperone sites have been identified in Hsp90 that differ in both substrate specificity and ATP dependence (209, 264). They are located in the 25-kDa N-terminal nucleotide-binding domain and the 12-kDa C-terminal fragment, respectively. The C-terminal site binds to structured substrates in an ATP-independent fashion whereas the N-terminal site recognizes preferentially unfolded (poly)peptides in an ATP-dependent and geldanamycin-sensitive manner (209). Because the 12-kDa C-terminal fragment also possesses the binding site for the TPR-containing cohorts of Hsp90 (39, 263), chaperone activity at this site may be potentially regulated by these cohorts. More recently, a third substrate binding site has been suggested to reside in the central region of Hsp90 (113). Nonetheless, given the fact that non-native proteins used

Substrate family	Hsp90 substrate
Tyrosine Kinases	Src, Lck, Hck, Fgr Fes, Fgr, Fps, Ros, Yes p75 vV-ErbA p185erbB2 Wee1 Insulin receptor Fak
Serine-threonine Kinases	Raf KSR Gag-Mil Mos MEK Cdk4 Akt eEF 2-kinase eIF 2α-kinases (HRI, PKR, GCN2 and PEK) Casein Kinase II Receptor interacting protein (RIP) Pim-1
Transcription factors	Glucocorticoid receptor Progesterone receptor Estrogen receptor Androgen receptor Mineralcorticoid receptor Dioxin receptor Sim MyoD1 E12 Heat shock factor Tumor promotor-specific binding protein p53
Others	Hepatitis B-reverse transcriptase Cystic fibrosis conductance transmembrane regulator (CFTR) Amino acid tRNA synthetase Cytochrome P450 2E1 $G\alpha_0$-subunit Telomerase Nitric-oxide synthase Apaf-1

Table 1. Examples of identified Hsp90 substrates (adapted from (200).

for these studies are all artificial substrates, the authenticity of these results needs to be further confirmed by future studies using natural substrates of Hsp90. Reciprocally, as to the substrate specificity of Hsp90, it appears that rather than being defined by consensus sequence or motifs as in the case for Hsp70, it may be determined instead by some yet unknown conformational states or folding characteristics that are common to all the substrates of Hsp90 (23). However, despite the uncertainty, the interaction of Hsp90 with its classical substrates protein kinases and steroid hormone receptors have been localized to the kinase domain (223, 233, 236) and ligand binding domain (52), respectively.

In vivo function of Hsp90 is assisted as well as regulated by a host of partner proteins known as cohorts or co-chaperones. Many of them are heat shock proteins and possess chaperone activities themselves (reviewed in 23, 26, 173, 180, 200, 262) (Table 2). Data accumulated from extensive studies on steroid hormone receptors suggest that these cohorts interact with Hsp90 in an ordered and dynamic fashion which defines a cyclic chaperone pathway comprising of distinct heterocomplexes that assist the folding and activation of client proteins sequentially (Figure 2) (178, 200, 208, 226). According to this model, client proteins enter the cycle by associating with the Hsp70 system first. Such a binding reaction involves ATP hydrolysis and is facilitated by sequential actions of the Hsp70 cofactors Hsp40/DnaJ and p48/Hip. Hsp40/DnaJ stimulates ATP hydrolysis by Hsp70 whereas p48/Hip stabilizes the resultant ADP-bound conformation of Hsp70 which binds the nonnative clients with higher affinity (reviewed in 83). Subsequent binding of p60/Hop to this complex leads to the formation of the early complex of the folding pathway. Because the multi-TPR-containing protein p60/Hop is able to interact with Hsp70 and Hsp90 simultaneously (38, 210), Hsp90 is brought into

Hsp90 cohort	Function
Hsp70	chaperone; component of early Hsp90/SHR heterocomplex
Hsp40/DnaJ	Hsp70 cohort (stimulating its ATPase activity); chaperone
Hip	Hsp70 cohort (stabilizing its ADP-bound conformation)
p60/Hop	linker between Hsp90 and Hsp70; inhibitor of Hsp90 ATPase activity
p23	possible substrate release factor of Hsp90; chaperone
FKBP51	prolyl-peptidyl cis/trans isomerase; chaperone
FKBP52	prolyl-peptidyl cis/trans isomerase; chaperone
Cyp40	prolyl-peptidyl cis/trans isomerase; chaperone
$p50^{cdc37}$	kinase-specific cohort of Hsp90; chaperone
protein phosphatase 5	serine-threonine protein phosphatase

Table 2. Hsp90 cohort/cochaperones

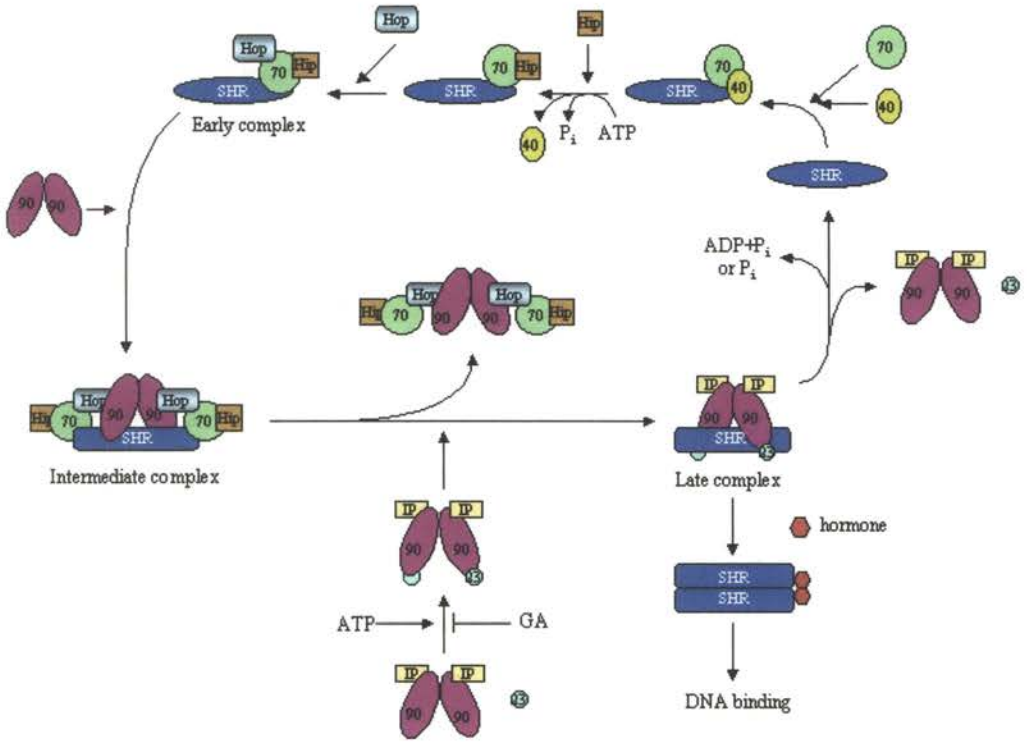

Figure 2. Chaperone cycle for the activation of steroid hormone receptors (SHRs) by Hsp90 machinery (200, 208). Note that it is still an evolving model some steps of which are not well understood and being constantly modified. See text for detailed explanation for each step.

contact with the early complex which thus gives rise to the intermediate complex containing Hsp90, Hsp70, p60/Hop and p48/Hip. This intermediate complex presumably contains Hsp90 in its nucleotide-free or ADP-bound conformation which exhibits a fast-on/fast-off and weaker affinity for the clients. *In vitro* studies have shown that this intermediate complex is sufficient to convert the steroid hormone receptors from the non p23 and one of the TPR-containing immunophilins. In this late complex, Hsp90 is believed to be in its ATP-bound conformation which is preferentially recognized by p23. Geldanamycin, by binding to the ATP pocket of Hsp90 with much greater affinity (200) blocks p23 binding and the functional assembly of the late complex, therefore inhibiting the proper folding and activation of the Hsp90 substrates. Early data have suggested that p23 functions to stabilize the interaction between Hsp90 and its substrates (62), however, an additional or alternative role has been proposed recently where it acts as a substrate release factor for Hsp90 (79, 81, 261). In this role, p23 supposedly couples the conformational change of Hsp90 induced by ATP hydrolysis to the efficient substrate release. This function is consistent with its late appearance in the chaperone pathway where the client proteins are about to dissociate from the Hsp90 heterocomplex. Depending on their folding states, clients are either released in their stable and competent conformations or reenter the chaperone pathway for further rounds of folding.

Hsp70:

70-kDa heat shock proteins (Hsp70s) are a highly conserved family of chaperones that are distributed ubiquitously in both prokaryotic and eukaryotic organisms (reviewed in 82). Hsp70 consists of two structurally and functionally distinct domains, the 44-kDa

N-terminal ATP binding domain (76) and the 18-kDa C-terminal peptide binding domain (269). Like Hsp90, Hsp70 function is also regulated by nucleotide binding and hydrolysis. However, in contrast to Hsp90, the ATP-bound form of Hsp70 represents the "open" and "fast on/fast off" conformation whereas the ADP-bound form exhibits the "closed" and "slow on/slow off" conformation (reviewed in 25, 96). Using approaches such as phage display and synthetic peptide libraries, Hsp70 has been shown to recognize linear polypeptide sequences enriched in hydrophobic amino acids (14, 78, 203). This less selective substrate specificity of Hsp70, in contrast to Hsp90, is consistent with its involvement in general protein folding events. Crystallization experiment shows that peptides are bound in an extended conformation to a cleft in the peptide binding domain of Hsp70 (269).

Several cohort proteins regulate the *in vivo* function of Hsp70 at different stages of its ATPase cycle. In both prokaryotes and eukaryotes, conversion of Hsp70 from the ATP-bound form to the ADP-bound form is facilitated by the Hsp40/DnaJ protein which stimulates ATP hydrolysis by Hsp70 (149, 155, 270). Hsp40/DnaJ proteins possess chaperone activity themselves as demonstrated by their abilities to bind unfolded proteins and prevent their aggregation *in vitro* (130, 238). The conserved J-domain of this protein family binds directly to the ATPase domain of Hsp70 (174, 187). In prokaryotes, conversion of DnaK (Hsp70 homolog) from the ADP-bound state to the ATP-bound state is assisted by GrpE, a 23-kDa protein that acts as a nucleotide exchange factor (95). While a conserved GrpE homolog has not been identified in eukaryotic cytoplasm, a functional analog called Bag-1 has been proposed to carry out such an activity (102, 240). X-ray crystallography studies indicate that, though structurally unrelated, both proteins

bind to the conserved ATPase domain of DnaK and Hsp70, respectively, and induce similar conformational changes within DnaK and Hsp70 that stimulate nucleotide exchange (229). Interestingly, in mammalian cells, a 48-kDa Hsp70-interacting protein (Hip) functions to stabilize the ADP-bound state of Hsp70 (103). Therefore, by switching Hsp70 between its different nucleotide-bound states, these cohorts coordinately regulate the functional interaction of Hsp70 with its clients, helping to fold them correctly.

p60/Hop:

Originally identified as a 60-kDa protein associated with the progesterone receptor (227, 228), p60 was later found to be homologous to the yeast stress-related protein STI1 (164) and a previously characterized TPR-containing human protein that was upregulated in virally transformed cells (106). More than two thirds of p60 is comprised of TPR motifs which are arranged into three tandem TPR domains. Mutagenesis (38) and structural studies (210) revealed that the first TPR domain binds Hsp70 and the central TPR domain interacts with Hsp90. Binding is primarily mediated by electrostatic interactions of the TPR domains with the EEVD motif located at the C-terminus of both Hsp90 and Hsp70, whereas specificities are defined by selective hydrophobic contacts with the upstream residues of each protein. Being able to bind Hsp90 and Hsp70 simultaneously, p60 provides a physical link between these two essential chaperones which do not seem to possess direct binding sites for each other (49). It is thus also called Hop (Hsp organizer protein) and believed to be an essential component of the Hsp90 chaperone machinery at the early stages of the assisted protein folding pathway (38, 63). Such an important function, however, does not seem to arise

entirely from its ability to passively bridge between Hsp90 and Hsp70. Recent evidence indicates that it negatively regulates the intrinsic ATPase activity of yeast Hsp90, which is possibly due to its inhibition of ATP binding to the N-terminal nucleotide binding pocket of Hsp90 (185). It agrees with the fact that p60/Hop preferentially binds to the ADP-bound but not ATP-bound form of Hsp90 (38). In addition, p60/Hop has also been shown to stimulate the ATPase activity of Hsp70 (92), suggesting that it functions to modulate or coordinate the ATP cycle of these proteins while bridging them in a single complex. Nonetheless, unlike other cohorts of Hsp90 such as p23 and immunophilins, p60/Hop has not been found to possess any passive chaperoning activity *in vitro* (17, 80).

p23:

p23 is a highly acidic phosphoprotein that was originally identified as a 23-kDa component of the native steroid hormone receptor heterocomplex (115, 117). It binds selectively to the ATP-bound conformation of Hsp90 (237) although its exact binding site(s) on Hsp90 has (have) not been fully determined yet. Several lines of evidence suggest that rather than recognizing one single region of Hsp90, binding of p23 involves two or more noncontiguous regions of Hsp90 and requires the dimeric structure of Hsp90 (28, 39, 90). p23 possesses passive chaperoning activity as demonstrated by its ability to prevent protein aggregation *in vitro* (17, 80). Nonetheless, its precise function in the Hsp90 chaperone machinery is unclear although it is known to participate in the functional assembly of the Hsp90 heterocomplexes with the steroid hormone receptors and thought to stabilize the mature complexes (62, 108). Recent studies, however suggest that it actually serves as a substrate release factor of Hsp90 which efficiently

couples the ATP hydrolysis of Hsp90 with the acquisition of its substrate releasing conformation (261). Interestingly, it has also been proposed to promote, in conjunction with Hsp90, the functional disassembly of transcriptional regulatory complexes containing the intracellular receptors in response to cellular signal changes such as hormone withdrawal (81).

Immunophilin:

The immunophilins are ubiquitous and conserved proteins that possess peptidyl-prolyl-cis-trans isomerase (PPIase) activity which is inhibitable by immunosuppressive drugs such as FK506 and cyclosporin A. Several high molecular weight immunophilins such as FKBP52, FKBP51 (FK506-binding proteins) and Cyp40 (cyclosporin A-binding protein) have been identified as components of the Hsp90 heterocomplexes containing or free of steroid receptors (reviewed in 180). Besides the conserved PPIase domain, they all contain a C-terminal TPR domain which mediates their mutually exclusive binding to the TPR docking site within the C-terminal domain of Hsp90 (189, 196, 263). Despite the obvious potential for their PPIase catalyzed protein folding activity, their precise functions within the Hsp90 chaperone machinery are not well understood. In fact, inhibition of the PPIase activity either by drugs or mutations does not seem to alter the integrity and function of the Hsp90 heterocomplexes containing the immunophilins (66, 107, 198). Similar to Hsp90, they possess passive chaperone activity *in vitro* (17, 80), and such an activity of FKBP52 was recently mapped to its C-terminal domain which also contains its TPR motifs (177). In addition, a role has been proposed for these large immunophilins, in the context of Hsp90 complexes, in the cytoplasmic-nuclear

trafficking of the steroid hormone receptors by functioning as a physical connector between the receptors and the cellular movement machine (179). Such a model is supported by several lines of evidence including the co-localization of FKBP52 with the microtubules (50) and its direct interaction with both the steroid receptors and the molecular motor dynein (84, 222). Consistent with the hypothesis that FKBP52 is involved in the intracellular trafficking of steroid receptors, Davies *et al* recently reported a hormone-dependent switching of FKBP51 to FKBP52 in the Hsp90/GR heterocomplex and the concomitant recruiting of dynein to the same complex prior to the hormone-induced GR transport to the nucleus (54).

Other Hsp90 cochaperones: Literature relevant to $p50^{cdc37}$, Hsp90's so-called "kinase-specific co-chaperone" will be reviewed in Chapter II and IV. Literature relevant to the TPR-containing co-chaperone, protein phosphatase 5 (PP5) will be reviewed in Chapter III and V.

CHAPTER II

Hsp90 Regulates p50^{cdc37} Function during the Biogenesis of the Active Conformation of the Heme-regulated eIF2α Kinase

Introduction:

The heme-regulated inhibitor (HRI) of protein synthesis is a protein-serine kinase which coordinates the synthesis of globin chains with the availability of heme in reticulocytes (31, 32). Under heme-deficient conditions, HRI phosphorylates the α-subunit of eukaryotic translational initiation factor eIF2. Phosphorylation of eIF2α causes an inhibition of polypeptide chain initiation and the arrest of protein synthesis, preventing the synthesis of apo-globin chains in the absence of heme. HRI is also activated under heme-replete conditions in response to a host of other adverse environmental stimuli, such as heat shock, agents that generate oxidative stress, and the presence of denatured proteins (31, 32).

The biogenesis and activation of HRI into an active heme-regulatable eIF2α kinase requires its functional interaction with the chaperone machinery containing the 90-kDa heat shock protein (Hsp90) and the 70-kDa heat shock cognate protein (Hsc70) (246, 248). During HRI biogenesis and its subsequent transformation and activation, several discrete HRI intermediates are generated; these intermediates can be distinguished on the basis of their competence to become an active kinase in response to heme deficiency or upon treatment with sulfhydryl reactive compounds, such as *N*-ethylmaleimide. Immediately after their synthesis, HRI molecules are not active in heme-replete or heme-deficient rabbit reticulocyte lysate (RRL) and cannot be activated by *N*-ethylmaleimide treatment. This immature population interacts with Hsp90 and Hsc70 (144, 146, 246, 248,

259). Subsequent to this immature phase, a "mature-competent" HRI population appears. The mature-competent population can be activated by heme-deficiency or treatment with *N*-ethylmaleimide, but remains quiescent in the absence of such "stimuli." The mature-competent HRI population continues to interact with Hsp90 machinery, and this interaction is required to maintain HRI's ability to respond to heme deficiency (246).

Under heme-deficient conditions, however, a portion of the population of HRI molecules "transform" to produce kinase populations with enhanced auto-kinase and eIF2α kinase activities. Transformation of HRI requires Hsp90 function and autophosphorylation of HRI, and correlates with the production of a population of HRI molecules which exhibit retarded electrophoretic mobility on SDS-PAGE (246). This transformation frees HRI from its functional requirements for Hsp90 and terminates its physical association with Hsp90 machinery (246).

Hsp90 binds numerous other protein kinases, primarily when they are in relatively inactive conformations (reviewed in Refs (15, 206)). However, Hsp90's association with inactive kinases reflects its essential positive role in facilitating kinase folding, maturation, and activation rather than a recognition of repressed kinase molecules *per se*. Consistent with this model for Hsp90 function, the Hsp90 chaperone machine does not interact with previously transformed HRI molecules when their kinase activity is subsequently inhibited by hemin addition, nor do such "repressed" HRI molecules require Hsp90 support to maintain their ability to reactivate in response to heme-deficiency or stress (246). Consistent with the specific role of Hsp90 in kinase biogenesis, both repressed HRI and transformed HRI exhibit the same slow electrophoretic mobility on SDS-PAGE,

indicating that repressed HRI retains the hsp90-independent "transformed" conformation (246).

Hsp90 functions in concert with a number of co-chaperones and cohorts to facilitate their clients' acquisition of functional conformations (reviewed in 181). Early studies detected a 50-kDa protein present in heterocomplexes formed between Hsp90 and viral members of the Src family of protein tyrosine kinases (reviewed in 20). This 50-kDa protein has recently been identified as a product of the vertebrate homolog of the yeast cell division cycle gene *CDC37* (51, 74, 88, 175, 235). *In vitro*, the yeast $p50^{cdc37}$ homolog exhibits chaperone activity (122). Genetic (48, 59, 71, 122) and biochemical (89, 235) studies indicate that $p50^{cdc37}$ plays an essential positive role in supporting a number of protein kinases. Therefore, we examined whether $p50^{cdc37}$ is a component of the Hsp90 chaperone complex which is required for the maturation and transformation of HRI. In this report, we present evidence that $p50^{cdc37}$ acts in concert with Hsp90 and facilitates the transformation and activation of HRI. We further demonstrate that nucleotide-mediated conformational switching of Hsp90 regulates the kinase binding activity of $p50^{cdc37}$.

Materials and Methods:

Construction of Plasmids for Expression of Wild Type and Mutant $p50^{cdc37}$ Proteins-Two cDNA clones were obtained from Genome Systems, Inc.: one lacking sequences encoding the N-terminal 8 amino acids (MVDYSVWD) of human $p50^{cdc37}$ (dbEST number 810394, GenBank™ accession number AA172101 (designated here as $p50^{cdc37}$/N8aa)); and another containing sequence encoding the full-length human Cdc37 gene product (dbEST number 321710, GenBank™ accession number R87892

(designated here $p50^{cdc37}$)). The coding sequence for $p50^{cdc37}$/N8aa was ligated into the bacterial expression vector pET-30a(+). Recombinant His-tagged $p50^{cdc37}$/N8aa was purified on Ni^{2+}-NTA resin (Ni^{2+}-nitrilotriacetic acid coupled to agarose, Qiagen), and used as antigen to produce polyclonal mouse ascites anti-$p50^{cdc37}$ antibody. For expression of full-length recombinant $p50^{cdc37}$ in *Escherichia coli*, the sequence encoding full-length $p50^{cdc37}$ was cloned into the pQE-32 expression vector (Qiagen). (His_6)-$p50^{cdc37}$ was expressed in M15[pREP4] cells and purified on Ni^{2+}-NTA-agarose (Qiagen). Coomassie Blue staining of the purified proteins separated by SDS-PAGE indicated that the proteins were greater than 90% pure.

For *in vitro* translation, sequences encoding $p50^{cdc37}$/N8aa or full-length $p50^{cdc37}$ were cloned into a modified version of pSP64T (126), and translated by coupled transcription/translation in RRL (97). The mutant $p50^{cdc37}$/N8aa protein produced includes 11 N-terminal amino acids (MADIGSEFGST) encoded by sequences carried over from the pET-30a(+) vector, followed by the coding sequence of the human Cdc37 gene product from His^9 to Val^{378}. The previously described N-terminal deletion mutant of human $p50^{cdc37}$ lacking 163 amino acids from its N terminus (89) (designated here as $p50^{cdc37}/\Delta N$) was similarly cloned into and expressed from pSP64T. Tryptic fingerprints were generated from wild type [^{35}S]$p50^{cdc37}$ and [^{35}S]$p50^{cdc37}$/N8aa proteins as described previously for *de novo* synthesized [^{35}S]$p56^{lck}$ kinase (98).

For *in vitro* expression, individual domains of HRI were constructed in pSP64T and pSP64TL (97) (encoding a (His_6)-tag preceding a unique NcoI site) vectors using standard PCR cloning techniques. Pairs of oligonucleotide primers corresponding to N- and C-terminal sequences of each HRI domain were synthesized to include convenient

built-in restriction sites, NcoI in the 5' primers and EcoRI (for N- and C-terminal kinase lobes), StyI (for heme-binding domain) or HindIII (for kinase insertion sequence) in the 3' primers which were followed by an engineered stop codon. They were coupled in PCR reactions using the full-length HRI-pSP64T as the template. The resulting PCR products were digested with NcoI/EcoRI (N- and C-terminal kinase lobes), NcoI/StyI (heme-binding domain) or NcoI/HindIII (HindIII end was then filled in to generate a blunt end) and inserted into the corresponding sites of the pSP64T or pSP64TL vectors.

Expression and Purification of $p50^{cdc37}$ Protein Constructs from Eukaryotic Cells-Human FLAG-tagged $p50^{cdc37}$ and FLAG-tagged $p50^{cdc37}/\Delta C$ were expressed in and purified from Sf9 cells as described previously (89). FLAG-$p50^{cdc37}/\Delta C$ lacks 214 amino acids from the C terminus of $p50^{cdc37}$. GST-tagged $p50^{cdc37}$ was also expressed in and purified from COS-1 cells as described previously (89). Proteins were provided by Dr. Nicholas Grammatikakis.

Analysis of the Association of $p50^{cdc37}$ with HRI in Cultured Mammalian Cells-Human K562 erythroleukemia cells were cultured for 48 h at 37 °C and 5% CO_2 in RPMI medium supplemented with 10% fetal bovine serum (Life Technologies, Inc.). Approximately 1×10^7 geldanamycin-treated (1 μg/ml for 2 h) or untreated (equivalent volume of Me_2SO for 2 h) cells were lysed in buffer containing 20 mM HEPES, pH 7.5, 100 mM NaCl, 0.1% Nonidet P-40, 1% Triton X-100, 10% glycerol, 1 mM Na_3VO_4, 2 mM EGTA, 1 mM dithiothreitol, 50 mM glycerophosphate, 1 mM NaF, 0.4 mM phenylmethylsulfonyl fluoride, and 10 μg/ml each of leupeptin and aprotinin, and cell

extracts were clarified. Endogenous $p50^{cdc37}$ was immunoadsorbed from cell extracts via a mixture of rabbit, and mouse anti-$p50^{cdc37}$ (Transduction Laboratories) antibodies bound to GammaBind-Plus Sepharose (Amersham Pharmacia Biotech), and the immunopellets were washed as described previously (89). Half of the recovered $p50^{cdc37}$ immunocomplexes were analyzed by Western/ECL (Amersham Pharmacia Biotech) for the presence of associated HRI, using guinea pig antibody raised against the N-terminal 154 amino acids of rabbit HRI. Blots were then stripped, and rabbit anti-$p50^{cdc37}$ antibody was used to verify that equivalent amounts of $p50^{cdc37}$ were adsorbed from each extract. The second half of the anti-$p50^{cdc37}$ immunocomplexes were analyzed by Western blotting with rat anti-Hsp90 monoclonal antibody (SPA-830 from Stressgen). This work was done in collaboration with Dr. Nicholas Grammatikakis (Department of Microbiology and Immunology, Queen's University, Kingston, Ontario K7L 3N6, Canada).

De Novo Synthesis and Maturation of HRI in Rabbit Reticulocyte Lysate-Coupled transcription/translation (TnT) of plasmids encoding HRI or (His_7)-HRI in rabbit reticulocyte lysate (TnT RRL) and the subsequent maturation of the expressed HRI or (His_7)-HRI in hemin-supplemented or heme-deficient RRL was carried out as described previously (246, 248).

Co-translational Interaction of Hsp90 and $p50^{cdc37}$ with HRI-HRI and luciferase were synthesized with concomitant [^{35}S]-radiolabeling in separate TnT RRL for 15 min at 30 °C. TnT RRL was either treated, or not treated with 1 mM puromycin for 5 min at

30 °C to release the nascent polypeptide chains from polyribosome. The polyribosomes were then isolated by centrifugation and analyzed by Western blotting for Hsp90 and $p50^{cdc37}$ as described previously (246, 248).

Immunoadsorption of Protein Complexes-Chaperone/cochaperone and chaperone/kinase heterocomplexes were analyzed by reciprocal immunoadsorptions utilizing resin-bound anti-$p50^{cdc37}$ and anti-His-tag antibodies as described previously (97). Nonimmune mouse IgG (MOPC 21 from Sigma) was used as a control for nonspecific binding. As an additional control for nonspecific binding, [^{35}S]HRI lacking the histidine tag was assessed in parallel with reactions containing (His_7)-[^{35}S]HRI. Relative amounts of immunoadsorbed proteins were quantified by scanning densitometry of autoradiograms or Western blots. Comparisons of changes in the relative protein levels made in the text reflect corrections made for levels of nonspecific binding.

Assay of the Effect of $p50^{cdc37}$ and $p50^{cdc37}$/ΔC on HRI Transformation-[^{35}S]HRI or (His_7)-[^{35}S]HRI was synthesized in TnT RRL (246, 248). Subsequently, 4 μl of the TnT RRL was transferred to heme-deficient RRL (30 μl) which contained 10 μl of immunoresin (M2 anti-FLAG-agarose) that had been previously saturated with FLAG-peptide, FLAG-$p50^{cdc37}$, or FLAG-$p50^{cdc37}$/ΔC. The reaction mixtures were incubated at 30 °C for 1 h. After washing of the immunoresins, the immunoresins were analyzed for bound [^{35}S]HRI, HRI kinase activity, and/or associated chaperones, as specified in the figure legends.

Alternatively, [^{35}S]HRI or (His_7)-[^{35}S]HRI were chased into 7 volumes of heme-deficient protein synthesizing RRL containing purified (His_6)-$p50^{cdc37}$ (~1.5 μg/μl), GST-$p50^{cdc37}$ (~1 μg/μl), or an equivalent volume of the appropriate control buffer. After 1 h of maturation at 30 °C, samples were adsorbed to Ni^{2+}-NTA resin (Fig. 10*B*) or GaG-agarose containing bound mouse monoclonal anti-(His_5)-IgG (Fig. 11). Resins were subsequently washed and analyzed for kinase activity (246, 248).

Assay of the Kinase Activity of (His_7)-[^{35}S]HRI-To quantify HRI kinase activity, (His_7)-[^{35}S]HRI or [^{35}S]HRI (control for nonspecific binding) was captured from RRL reaction mixtures on Ni^{2+}-NTA-agarose (Qiagen) that had been pre-equilibrated with 10 mM Tris-HCl, pH 7.4, 10 mM imidazole, and 50 mM NaF, or by immunoadsorption with anti-(His_5) monoclonal antibody. Assays for eIF2α kinase activity were performed as described (246, 248). The kinase activity of HRI was quantified by scanning densitometry of the [^{32}P]-labeled eIF2α band visualized by autoradiography and expressed as optical density (O.D.) × mm^2.

Results:

$p50^{cdc37}$ Interacts with HRI in Concert with Hsp90-To determine whether $p50^{cdc37}$ was a component of the chaperone complex that Hsp90 forms with HRI, we examined the ability of anti-His-tag antibodies to co-adsorb Hsp90 and $p50^{cdc37}$ upon immunoadsorption of newly synthesized (His_7)-[^{35}S]HRI from RRL (Fig. 3*A*). As previously shown (246), immunoadsorption of (His_7)-[^{35}S]HRI folding intermediates immediately after their synthesis (8 min post-translation) specifically co-adsorbed Hsp90.

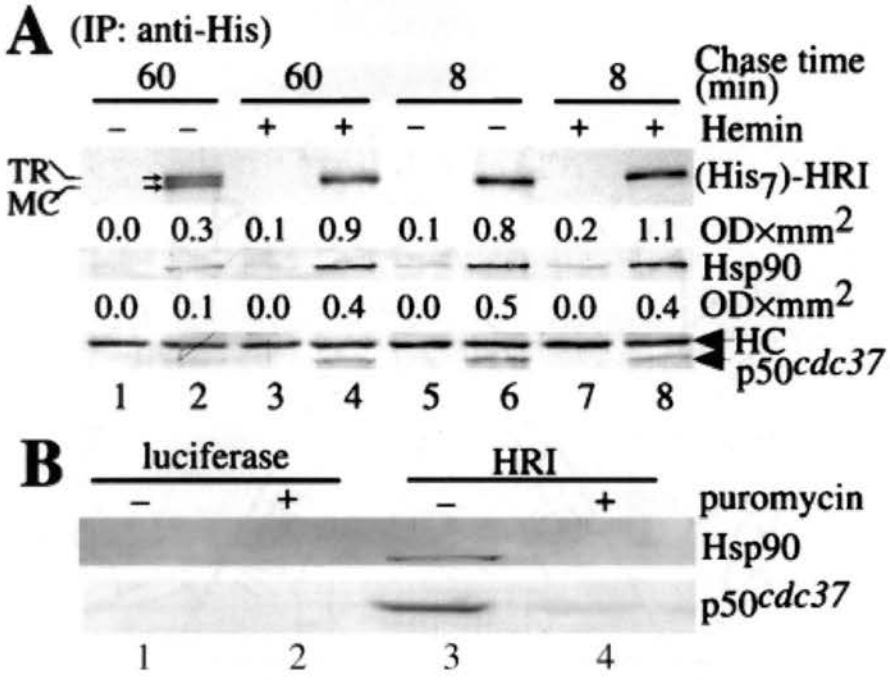

Figure 3. Interaction of endogenous p50^{cdc37} and Hsp90 with newly synthesized (His$_7$)-[^{35}S]HRI in RRL. A) (His$_7$)-[^{35}S]HRI (*lanes 2, 4, 6,* and *8*) and [^{35}S]HRI lacking the (His$_7$)-tag (*lanes 1, 3, 5,* and *7*) were synthesized and then matured in normal heme-deficient (*lanes 1, 2, 5,* and *6*) or hemin-supplemented (*lanes 3, 4, 7,* and *8*) RRL as described under "Materials and Methods." Aliquots (30 µl) of the reaction mixtures were taken after 8-min (*lanes 5-8*) or 60-min (*lanes 1-4*) of maturation and mixed with GaG-agarose pre-coupled with anti-(His$_5$) monoclonal antibody as described under "Materials and Methods." After washing the immune pellets, samples were analyzed by SDS-PAGE, followed by transfer to polyvinylidene difluoride membrane. (His$_7$)-[^{35}S]HRI was visualized by autoradiography (*upper panel*: *TR*, transformed HRI with slower electrophoretic mobility; *MC*, mature competent form of HRI with faster electrophoretic mobility). Endogenous RRL Hsp90 and p50^{cdc37} that was specifically co-adsorbed with (His$_7$)-[^{35}S]HRI were detected by Western blotting membranes with anti-Hsp90 (*middle panel*) or anti-p50^{cdc37} (*lower panel*) antibodies. *HC*: antibody heavy chain. Band densities were quantified by scanning densitometry and expressed as optical density × mm^2 (*numbers above* each panel). Densitometry indicated that equivalent amounts of total (His$_7$)-[^{35}S]HRI were specifically immunoadsorbed (*even lanes*). **B)** Co-translational interaction of HRI with Hsp90 and p50^{cdc37} in RRL: TnT RRLs were programmed with HRI (*lanes 3* and *4*) or luciferase template (*lanes 1* and *2*) for 15 min at 30 °C. Translation mixes were then either treated (*lanes 2* and *4*) or not treated (*lanes 1* and *3*) with 1 mM puromycin for 5 min at 30 °C to release the nascent chains, followed by separation on 15 to 40% sucrose gradients as described under "Materials and Methods." Isolated polyribosomes were analyzed by SDS-PAGE, followed by Western blot detection for Hsp90 and p50^{cdc37}.

Immunoadsorption of newly synthesized HRI also co-adsorbed $p50^{cdc37}$, demonstrating the existence of a heterocomplex containing $p50^{cdc37}$ and these newly synthesized HRI molecules. The amount of Hsp90 and $p50^{cdc37}$ co-adsorbed with HRI was similar whether the newly synthesized HRI was immunoadsorbed from heme-replete or heme-deficient RRL. Thus, heme did not directly regulate the polypeptide binding activity of Hsp90 (246, 259) or $p50^{cdc37}$.

Previously, we have demonstrated that Hsp90 interacts with nascent HRI co-translationally (246). To determine whether $p50^{cdc37}$ similarly binds to HRI during its synthesis on ribosomes, polyribosomes were isolated from RRL that was programmed with HRI template. For a negative control, ribosomes were also prepared from RRL that was programmed with luciferase template. Western blotting indicated that both Hsp90 and $p50^{cdc37}$ were present in the ribosome pellet containing bound nascent HRI polypeptide chains (Fig. 3*B*), but were absent when the nascent polypeptide chains had been released by incubation with puromycin prior to isolation of the polyribosomes. Thus, $p50^{cdc37}$, like Hsp90, becomes specifically associated with HRI prior to the completion of kinase synthesis and the release of newly synthesized HRI from the ribosome.

The interaction of Hsp90 with HRI persists after release of newly synthesized HRI from polyribosomes in heme-replete RRL (246). To assess if the interaction between $p50^{cdc37}$ and HRI was similarly maintained, the newly synthesized (His_7)-[^{35}S]HRI population was subjected to maturational incubations in hemin-supplemented RRL where the transformation of HRI into an active kinase is suppressed. After a 60-min incubation in the presence of hemin, neither the level of Hsp90 nor $p50^{cdc37}$ associated with HRI declined significantly relative to the level observed immediately after translation (Fig. 3*A*,

lane 4 versus 6 and *8*). Thus, in heme-replete RRL, HRI continued to interact with $p50^{cdc37}$ for prolonged periods after its synthesis.

In heme-deficient RRL, HRI autophosphorylates and transforms into an active kinase that no longer interacts with Hsp90 (246). To determine whether transformation of HRI similarly terminated its interaction with $p50^{cdc37}$, the newly synthesized HRI kinase population was incubated in hemin-deficient RRL for 60 min. Under these conditions, ~50% of the pulse-labeled (His_7)-[^{35}S]HRI exhibited the slower electrophoretic mobility associated with "transformation" (246). The amount of Hsp90 and $p50^{cdc37}$ that was co-adsorbed with (His_7)-HRI from heme-deficient RRL decrease by ~67 and 75%, respectively, relative to that co-adsorbed with the "mature-competent/untransformed" HRI population present in RRL held under heme-replete conditions (Fig. 3*A, lane 2 versus 4*). Thus, the transformation of HRI that was induced by hemin deficiency correlated with a reduction in the interaction of HRI with Hsp90 and $p50^{cdc37}$.

Previously, the interaction between Hsp90 and HRI was demonstrated to be specific to the "untransformed" (fast electrophoretic mobility) form of HRI (246). To determine whether $p50^{cdc37}$, like Hsp90, recognized a specific component of the HRI population, the kinase populations associated with $p50^{cdc37}$ were captured by immunoadsorption with anti-$p50^{cdc37}$ antibodies after incubation of newly synthesized HRI in heme-replete or heme-deficient RRL for 8 or 60 min (Fig. 4). Only untransformed forms of [^{35}S]HRI, consisting of early folding intermediates (8 min chase) or mature-competent HRI (60 min chase), were specifically coimmunoadsorbed with $p50^{cdc37}$ from either heme-replete or heme-deficient RRL (Fig. 4*A, PEL*). The 65% decrease in the amount of untransformed HRI that was co-adsorbed with $p50^{cdc37}$ from heme-deficient

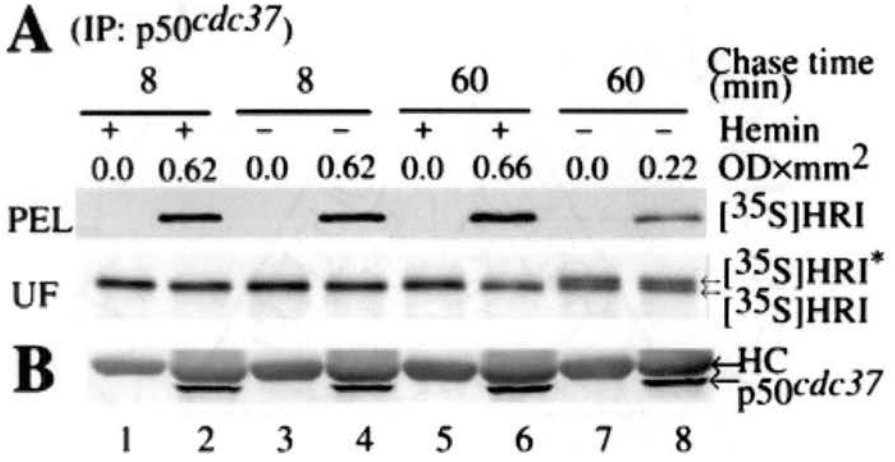

Figure 4. Interaction of newly synthesized HRI with endogenous p50^{cdc37} in RRL. [^{35}S]HRI was synthesized in TnT RRL and subsequently matured in normal hemin-supplemented (10 μM hemin) (*lanes 1, 2, 5,* and *6*) or heme-deficient (*lanes 3, 4, 7,* and *8*) RRL protein synthesis mixtures as described under "Materials and Methods." Aliquots (30 μl) of the reaction mixtures were taken after 8 (*lanes 1-4*) or 60 min (*lanes 5-8*) of maturation and mixed with GaG-agarose pre-coupled with anti-p50^{cdc37} polyclonal antibodies (*lanes 2, 4, 6,* and *8*) or nonimmune control mouse IgG (*lanes 1, 3, 5,* and *7*) as described under "Materials and Methods." A 2-μl aliquot of each reaction was also taken at 8 or 60 min for analysis of the forms of [^{35}S]HRI which were present in the RRL maturation mixtures prior to immunoadsorption. After washing the immune pellets, samples were analyzed by SDS-PAGE, followed by transfer to polyvinylidene difluoride membrane and autoradiography. **A)** [^{35}S]HRI co-adsorbed with p50^{cdc37} (*A, PEL*); [^{35}S]HRI present in the RRL maturation mixes prior to immunoadsorption (*A, UF*) [^{35}S]HRI*: transformed HRI with slower electrophoretic mobility. Band densities were quantified by scanning densitometry and expressed as optical density × mm^2 (*numbers above* each panel). **B)** p50^{cdc37} that was specifically immunoadsorbed was detected by probing the polyvinylidene difluoride membrane of PEL panel with anti-p50^{cdc37} polyclonal antibodies. *HC*: antibody heavy chain. Densitometry indicated that equivalent amounts of total [^{35}S]HRI were present during the immunoadsorption (*UF*), and that equivalent amounts of p50^{cdc37} were specifically immunoadsorbed.

RRL correlated with the approximate 50% transformation of the [^{35}S]HRI population after 60 min of incubation in heme-deficient RRL. The observation that transformed (slow electrophoretic mobility form) HRI was not coimmunoadsorbed by anti-p50^{cdc37} antibodies is consistent with the data presented in Fig. 3, and supports the conclusion that p50^{cdc37}, like Hsp90, does not interact with transformed HRI.

Previously, we have demonstrated that the kinase activity of transformed HRI is inhibited upon addition of hemin to heme-deficient maturation mixes, and that this population of "repressed HRI" molecules does not interact with Hsp90 (246). Similarly, we have observed that repressed HRI did not co-adsorb with p50^{cdc37} from RRL (not shown). Thus, p50^{cdc37} did not bind to transformed HRI regardless of whether the kinase was active or repressed.

The N-terminal Domain of p50^{cdc37} Binds HRI Independent of Hsp90-Hsp90 and p50^{cdc37} both recognize untransformed populations of HRI molecules (Fig. 3 and 4). To differentiate between p50^{cdc37} associating with HRI directly or binding HRI indirectly via its interaction with Hsp90, we compared the kinase binding activity of affinity purified FLAG-tagged p50^{cdc37} with that of a C-terminal truncated FLAG-tagged Cdc37 gene product (p50^{cdc37}/ΔC). p50^{cdc37}/ΔC had previously been shown to bind the Raf-1 kinase, but not Hsp90 (89). HRI was readily captured by resins containing the full-length wild-type Cdc37 gene product and by resins containing the truncated Cdc37 gene product p50^{cdc37}/ΔC, but was not captured by anti-FLAG control resins (Fig. 5*A, upper panel*). In contrast, Hsp90 was adsorbed by resins containing the wild-type Cdc37 gene product, but only barely detectable amounts of Hsp90 were bound to resins containing p50^{cdc37}/ΔC

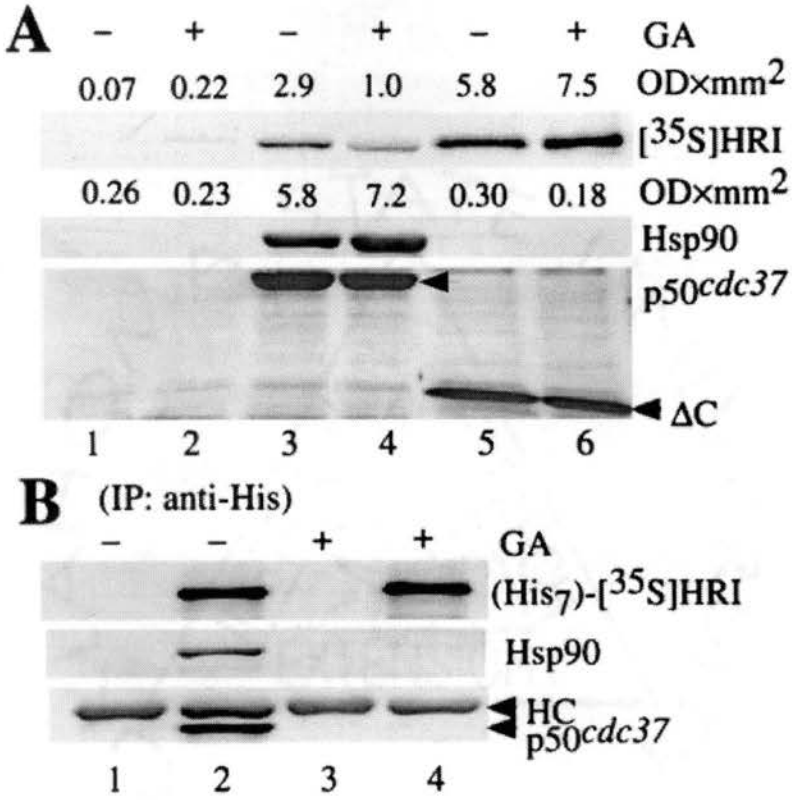

Figure 5. Effect of geldanamycin on the association of HRI with p50^{cdc37} and the p50^{cdc37}/ΔC mutant. A) [^{35}S]HRI was synthesized in TnT RRL in the presence of 10 μg/ml geldanamycin (*lanes 2, 4*, and *6*) or an equivalent amount of Me_2SO (*lanes 1, 3*, and *5*), followed by maturation in normal heme-deficient RRL containing M2-agarose pre-saturated with control FLAG-peptide (*lanes 1* and *2*), or Sf9 cell-expressed FLAG-tagged p50^{cdc37} (*lanes 3* and *4*), or FLAG-tagged p50^{cdc37}/ΔC (*lanes 5* and *6*) for 60 min at 30 °C as described under "Materials and Methods," followed by the addition of 20 mM sodium molybdate. After washing the M2-agarose pellets with buffer containing 20 mM sodium molybdate, samples were analyzed by SDS-PAGE, followed by transfer to polyvinylidene difluoride membrane. Co-adsorbed [^{35}S]HRI was detected by autoradiography (*upper panel*). Co-adsorbed Hsp90 was visualized by Western blot with anti-Hsp90 antibodies (*middle panel*). Band densities were quantified by scanning densitometry and expressed as optical density × mm^2 (*numbers above* each panel). M2 resin-immobilized FLAG-tagged proteins were visualized by Coomassie Blue staining (*lower panel,* ΔC: p50^{cdc37}/ΔC). **B)** (His_7)-[^{35}S]HRI (*lanes 2* and *4*) and [^{35}S]HRI lacking (His_7)-tag (*lanes 1* and *3*) were synthesized for 25 min in TnT RRL in the presence of 10 μg/ml geldanamycin (*lanes 3* and *4*) or an equivalent amount of Me_2SO (*lanes 1* and *2*). 20-μl aliquots were immunoadsorbed with GaG-agarose containing bound anti-(His_5) monoclonal antibody as described under "Materials and Methods." After washing the immune pellets, samples were analyzed by SDS-PAGE, followed by transfer to polyvinylidene difluoride membrane. (His_7)-[^{35}S]HRI was visualized by autoradiography (*upper panel*). Hsp90 (*middle panel*) and p50^{cdc37} (*lower panel*) were detected by Western blot with anti-Hsp90 and anti-p50^{cdc37} antibodies, respectively. *HC*: antibody heavy chain.

truncated Cdc37 gene product (Fig. 5*A, middle panel*). These findings suggested that Cdc37 gene products did not bind to kinase folding intermediates indirectly via an interaction with kinase-bound Hsp90.

The above result implied that the C-terminal truncated Cdc37 gene products could bind kinase folding intermediates independent of Hsp90 function. To test this, the effects of poisoning RRL with the Hsp90-specific antagonist geldanamycin (234, 257) were assessed. Consistent with previous reports (89, 235), the ability of full-length FLAG-p50^{cdc37} gene product to bind untransformed kinase molecules was markedly reduced (67%) in the presence of geldanamycin (Fig. 5*A, upper panel*), but the presence of geldanamycin had no inhibitory effect on the interaction of FLAG-p50^{cdc37} with Hsp90 (Fig. 5*A, middle panel*). In contrast, inhibition of Hsp90 function by geldanamycin did not abrogate the ability of the truncated Cdc37 gene product p50^{cdc37}/ΔC to bind untransformed HRI. In fact, geldanamycin treatment appeared to potentiate the kinase binding activity of truncated Cdc37 gene products. Thus, the resistance of the interaction between p50^{cdc37}/ΔC and HRI to inhibition by geldanamycin indicated that the N-terminal half of the Cdc37 gene product was capable of binding kinase folding intermediates independent of Hsp90.

The effects of geldanamycin on chaperone binding to untransformed HRI intermediates was confirmed by the reciprocal co-adsorption assays (Fig. 5*B*). (His_7)-HRI was immunoadsorbed from control or geldanamycin-treated RRL and analyzed for the presence of co-adsorbed Hsp90 and p50^{cdc37}. While the association of Hsp90 and p50^{cdc37} with (His_7)-HRI in control RRL was readily detected, treatment of RRL with geldanamycin resulted in the near quantitative disruption of the association of Hsp90 and

$p50^{cdc37}$ with (His_7)-HRI (Fig. 5*B*), thus confirming that inhibition of Hsp90 disrupted the direct recognition of kinase molecules by $p50^{cdc37}$.

The failure of C-terminal deleted $p50^{cdc37}$ to bind Hsp90 (89) suggested that the elements of $p50^{cdc37}$ which mediated its interaction with Hsp90 resided in the C-terminal domain of $p50^{cdc37}$. To further differentiate whether the C-terminal region of $p50^{cdc37}$ contained the Hsp90-binding site or whether it was simply required to maintain the structure of an Hsp90-binding site elsewhere in the protein, we constructed the corresponding N-terminal deletion mutant of $p50^{cdc37}$ lacking the first 163 amino acids from its N terminus ($p50^{cdc37}/\Delta N$). $p50^{cdc37}/\Delta N$ was synthesized in TnT RRL and assayed for Hsp90 binding. Anti-Hsp90 antibody specifically co-adsorbed [^{35}S]$p50^{cdc37}/\Delta N$ in conjunction with Hsp90 (Fig. 6*A*). Furthermore, anti-His antibodies specifically co-adsorbed Hsp90 with His-tagged $p50^{cdc37}/\Delta N$ (Fig. 6*B*). These findings indicated that the C-terminal domain of $p50^{cdc37}$ contained elements adequate for Hsp90 binding, independent of the presence of $p50^{cdc37}$'s N-terminal domain.

$p50^{cdc37}$ interacts with the N-terminal lobe of the kinase domain of HRI in an Hsp90-dependent manner-In an attempt to locate the binding site of $p50^{cdc37}$ in HRI, four major domains of HRI, the heme-binding domain (HBD), the N-terminal kinase lobe (NL), the kinase insertion sequence (KIS) and the C-terminal kinase lobe (CL) were constructed in the RRL expression vector pSP64TL, which was designed to automatically add an N-terminal (His_6)-tag to the inserted coding sequences (32, 192, 247) (Fig. 7*A*). Four different His-tagged domains of HRI were synthesized in separate RRL reactions with concomitant radiolabeling with [^{35}S]Met, followed by immunoadsorption with anti-(His_5)

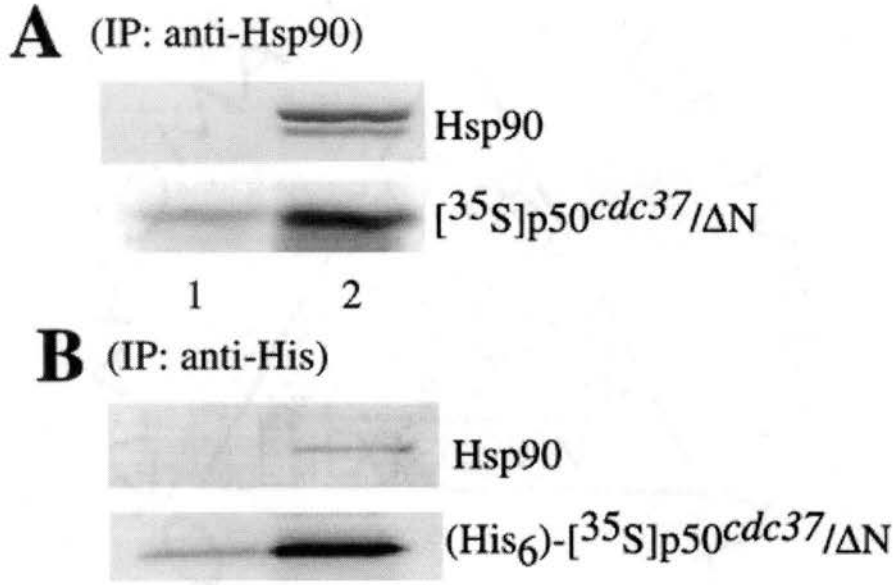

Figure 6. Interaction of the N-terminal domain deletion mutant of p50^{cdc37}, p50^{cdc37}/ΔN, with endogenous Hsp90 in RRL. **A**) [^{35}S]p50^{cdc37}/ΔN was synthesized in TnT RRL at 30 °C for 25 min. Aliquots of (20 µl) TnT RRL containing [^{35}S]p50^{cdc37}/ΔN were then immunoadsorbed with goat anti-mouse IgM cross-linked to agarose pre-coupled with mouse monoclonal anti-Hsp90 IgM, 8D3 (*lane 2*), or equivalent amount of nonimmune mouse IgM (*lane 1*). Samples were analyzed by SDS-PAGE, followed by transfer to polyvinylidene difluoride membrane. Immunoadsorbed Hsp90 was visualized by Western blot with anti-Hsp90 antibody (*upper panel*), and co-adsorbed [^{35}S]p50^{cdc37}/ΔN was detected by autoradiography (*lower panel*). **B)** (His_6)-[^{35}S]p50^{cdc37}/ΔN was synthesized in TnT RRL at 30 °C for 25 min. Aliquots of (20 µl) TnT RRL containing (His_6)-[^{35}S]p50^{cdc37}/ΔN were then immunoadsorbed with GaG-agarose containing bound anti-(His_5)-antibody (*lane 2*) or an equivalent amount of nonimmune mouse IgG (*lane 1*). Samples were analyzed by SDS-PAGE, followed by transfer to polyvinylidene difluoride membrane. Immunoprecipitated (His_6)-[^{35}S]p50^{cdc37}/ΔN was visualized by autoradiography (*lower panel*) and co-adsorbed Hsp90 was detected by Western blot with anti-Hsp90 antibody (*upper panel*).

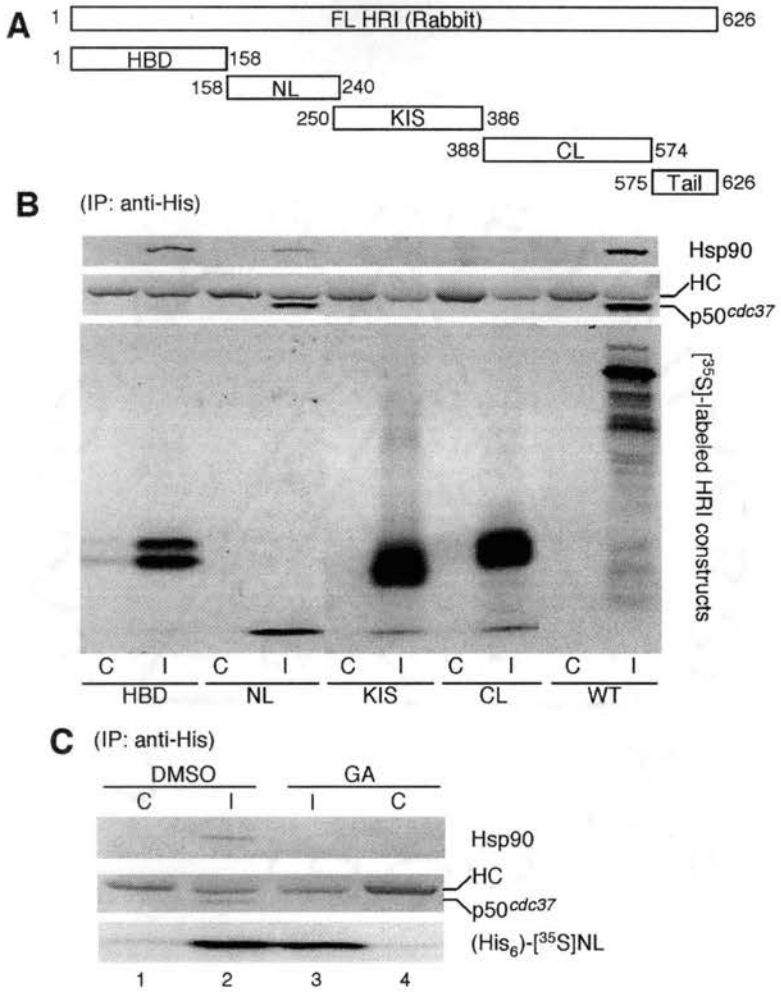

Figure 7. Interactions of HRI domains with Hsp90 and p50^{cdc37}. A) Domain structure of HRI. **B)** Four different His-tagged domains of HRI, the heme-binding domain (HBD), the N-terminal lobe (NL), the kinase insertion sequence (KIS) and the C-terminal lobe (CL) along with the wild type HRI (WT) were synthesized with concomitant radiolabeling with [^{35}S]Met in separate TnT RRL at 30 °C for 30 min. They were subsequently immunoadsorbed to the anti-(His_5) antibody (*even lanes*) or an equal amount of nonimmune control mouse IgG antibody (*odd lanes*), separated on an 8% SDS-PAGE and transferred to PVDF membrane. Immunoadsorbed [^{35}S]-labeled HRI constructs and the coadsorbed endogenous Hsp90 and p50^{cdc37} were detected by autoradiography (*lower panel*) and Western blotting analyses (*upper and middle panels*), respectively. **C)** His-tagged N-terminal lobe of HRI kinase domain was synthesized and labeled with [^{35}S]Met in TnT RRL containing 10 µg/ml geldanamycin (*Lanes 3 and 4*) or an equal volume of DMSO (*Lanes 1 and 2*) at 30 °C for 30 min. RRL reactions were subsequently immunoadsorbed to the anti-(His_5) antibody (*Lanes 2 and 3*) or an equivalent amount of nonimmune control mouse IgG antibody (*Lanes 1 and 4*), separated on an 8% SDS-PAGE and transferred to PVDF membrane. Immunoadsorbed [^{35}S]-NL of HRI (*lower panel*) and the coadsorbed endogenous Hsp90 (*upper panel*) and p50^{cdc37} (*middle panel*) were detected by autoradiography and Western blotting analyses, respectively. HC: antibody heavy chain.

antibody. The coadsorption of endogenous Hsp90 and p50^{cdc37} from RRL was subsequently assessed by Western blotting analysis (Fig. 7*B*). While all four domains of HRI were synthesized at comparable levels and immunoprecipitated, only the N-terminal lobe of the HRI kinase domain pulled down the endogenous p50^{cdc37} (Fig. 7*B*, *lane 3*). The N-terminal kinase lobe also specifically pulled down Hsp90, an observation that is consistent with the concerted interactions of Hsp90 and p50^{cdc37} with the full-length HRI. However, the Hsp90-binding was not simply limited to the N-terminal kinase lobe as it specifically interacted with the heme-binding domain of HRI as well (Fig. 7*B*, *lane 2*).

Since p50^{cdc37} interacts with the full-length HRI in a geldanamycin-sensitive fashion, we then examined whether its interaction with the N-terminal kinase lobe of HRI is also inhibitable by geldanamycin. In doing so, His-tagged N-terminal kinase lobe of HRI was synthesized in RRL mixtures containing (Fig. 7*C*, *lane 3*) or lacking (Fig. 7*C*, *lane 2*) geldanamycin, and subsequently immunoadsorbed to anti-His resin. Coadsorption of the endogenous Hsp90 and p50^{cdc37} was then analyzed by Western blot. As anticipated, like its interaction with the full-length HRI, p50^{cdc37} bound to the N-terminal kinase lobe in the same geldanamycin-sensitive fashion, confirming the notion that the geldanamycin-inhibitable function of Hsp90 is required for the direct binding of p50^{cdc37} to the client protein HRI.

Mutation of the N Terminus of p50^{cdc37} Inhibits Its Binding to HRI-To further characterize the domains and motifs of p50^{cdc37} required for kinase binding, we utilized a p50^{cdc37} mutant whose first 8 N-terminal amino acids were replaced by 11 residues encoded by irrelevant plasmid sequence (p50^{cdc37}/N8aa). Two observations indicated that replacement

of the first 8 residues of p50^{cdc37} did not cause global disruption of p50^{cdc37} structure. (i) This mutation did not compromise the ability of [^{35}S]p50^{cdc37}/N8aa to associate with Hsp90 (Fig. 8*A*). (ii) This mutation did not compromise the structural integrity of p50^{cdc37}/N8aa as determined by mild proteolytic nicking: the sensitivity to protease digestion and the pattern of proteolytic fragments generated were essentially the same for the p50^{cdc37}/N8aa and the wild type p50^{cdc37} proteins (Fig. 8*B*). However, p50^{cdc37}/N8aa was not co-adsorbed with epitope-tagged (His_7)-HRI despite the efficient co-adsorption of HRI by wild-type p50^{cdc37} and the equivalent amounts of each Cdc37 gene product present in these assays (Fig. 8*C*). These observations demonstrated that the N-terminal 8 amino acids of p50^{cdc37} were essential for its interaction with HRI.

p50^{cdc37} Enhances HRI Activity in Heme-deficient RRL in an Hsp90-dependent Fashion- To further characterize the role of p50^{cdc37} in the biogenesis of HRI, we examined the effect of affinity purified (His_6)-p50^{cdc37} on the transformation and activation of newly synthesized [^{35}S]HRI in heme-deficient RRL (Fig. 9). Aliquots of the HRI transformation reactions were also taken at the indicated times and analyzed by SDS-PAGE for transformation-specific shifts in HRI's electrophoretic mobility (Fig. 9*A*). Maturation of HRI in heme-deficient RRL containing (His_6)-p50^{cdc37} produced transformed HRI molecules equivalent to the storage buffer control. However, inclusion of (His_6)-p50^{cdc37} in HRI activation reactions increased the proportion of transformed HRI that became hyperphosphorylated at all time points examined relative to the control. Results similar to those presented in Fig. 9 were also obtained upon supplementing RRL with GST-tagged p50^{cdc37} (not shown: *e.g.* see Fig. 9).

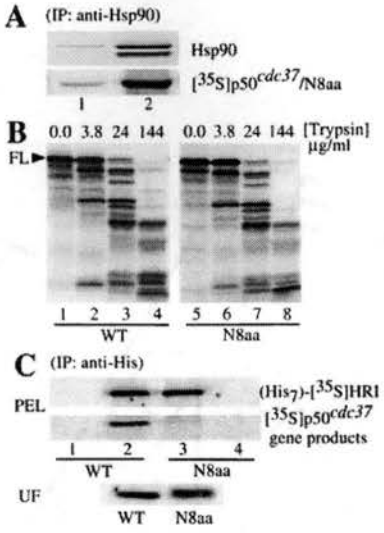

Figure 8. Effect of mutation of the N-terminal amino acids of p50^{cdc37} on the interaction of p50^{cdc37} with HRI and Hsp90. A) Co-adsorption of p50^{cdc37}/N8aa with endogenous Hsp90: [^{35}S]p50^{cdc37}/N8aa was synthesized in TnT RRL at 30 °C for 40 min, followed by a 40-min maturation in the presence of ATA (60 µM). An aliquot of the TnT RRL mixture (30 µl) was then immunoadsorbed with GaG-agarose containing bound mouse polyclonal anti-Hsp90 antibodies (*lane 2*) or nonimmune mouse IgG (*lane 1*) as described under "Materials and Methods." Samples were separated by SDS-PAGE, transferred to polyvinylidene difluoride membrane, and co-adsorbed [^{35}S]p50^{cdc37}/N8aa was detected by autoradiography (*lower panel*) whereas the immunoprecipitated Hsp90 was visualized by Western blot analysis with anti-Hsp90 antibody (*upper panel*). **B)** Comparison of proteolytic peptide mapping between wild type p50^{cdc37} and p50^{cdc37}/N8aa mutant: wild type p50^{cdc37} (*WT*) and p50^{cdc37}/N8aa (N8aa) were synthesized with concomitant ^{35}S-radiolabeling in separate TnT RRL at 30 °C for 40 min, followed by a 1-h maturation in the presence of ATA (60 µM). TnT RRL containing [^{35}S]p50^{cdc37} or [^{35}S]p50^{cdc37}/N8aa were then diluted into 3 volumes of proteolysis assay buffer (98) containing four different concentrations of trypsin as specified in the figure, followed by a 6-min digestion on ice. Reaction was terminated by adding boiling SDS sample buffer to the samples. Proteolytic peptide fragments were separated by 12% SDS-PAGE, followed by autoradiography analysis. *FL* denotes full-length p50^{cdc37}. **C)** (His$_7$)-[^{35}S]HRI was pulse-labeled in TnT RRL. Aliquots (10 µl) of TnT RRL containing (His$_7$)-[^{35}S]HRI were then chased by incubation in hemin-supplemented RRL containing previously synthesized [^{35}S]p50^{cdc37} (*PEL: lanes 1* and *2*) or [^{35}S]p50^{cdc37}/N8aa (*PEL: lanes 3* and *4*) for 8 min at 30 °C as described under "Materials and Methods." (His$_7$)-[^{35}S]HRI was immunoadsorbed from the reaction mixtures with anti-(His$_5$) antibody (*lanes 2* and *3*) or equivalent amount of nonimmune mouse IgG (*lanes 1* and *4*). Samples were analyzed by SDS-PAGE, followed by transfer to polyvinylidene difluoride membrane. Immunoadsorbed (His$_7$)-[^{35}S]HRI (*upper panel* of *PEL*) and co-adsorbed [^{35}S]p50^{cdc37} or [^{35}S]p50^{cdc37}/N8aa (*lower panel* of PEL) were visualized by autoradiography. A 2-µl aliquot of each reaction was also taken prior to immunoadsorption to verify that equivalent amounts of [^{35}S]p50^{cdc37} or [^{35}S]p50^{cdc37}/N8aa were synthesized and present in each reaction mixture (*UF panel*).

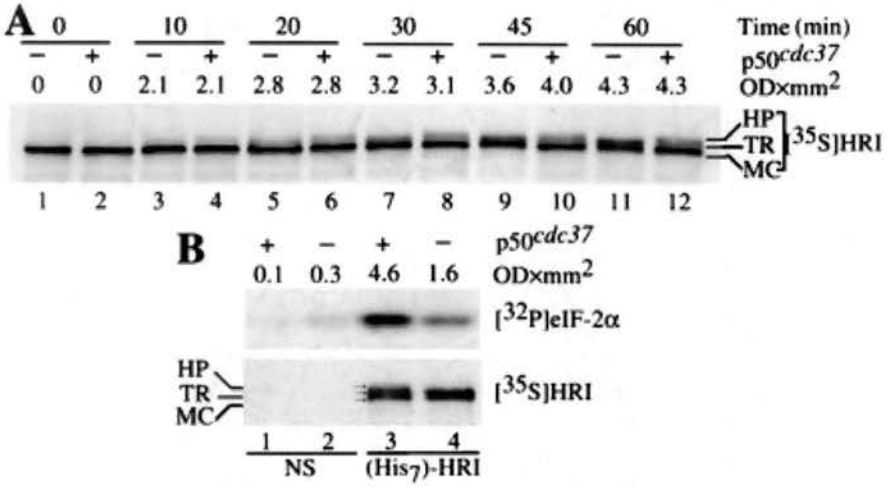

Figure 9. Effect of purified (His$_6$)-p50^{cdc37} on HRI transformation (*A*) and activity (*B*) in heme-deficient RRL. A) [^{35}S]HRI was pulse-labeled in TnT RRL. TnT RRL containing [^{35}S]HRI (3 µl) was then chased into heme-deficient RRL mixture (22 µl) which was supplemented with 12 µg of (His$_6$)-p50^{cdc37} (*even lanes*) or an equivalent amount of buffer (*odd lanes*) in which the (His$_6$)-p50^{cdc37} was stored as described under "Materials and Methods." Aliquots of maturation RRL mixtures were taken after 0, 10, 20, 30, 45, and 60 min of incubation at 30 °C for direct analysis of HRI transformation. Samples were separated by SDS-PAGE, transferred to polyvinylidene difluoride membrane, and visualized by autoradiography. The amount of transformed (*TR*) plus hyperphosphorylated (*HP*) [^{35}S]HRI was quantified by scanning densitometry and expressed as optical density × mm^2 (*numbers above* lanes in panel). **B)** For analysis of HRI activity, aliquots (50 µl) of the RRL reaction mixtures containing (His$_7$)-[^{35}S]HRI ((His$_7$)-HRI: *lanes 3* and *4*) or [^{35}S]HRI (*NS: lanes 1* and *2*) matured in the presence of 25 µg of (His$_6$)-p50^{cdc37} (*lanes 1* and *3*), or an equivalent volume of storage buffer (*lanes 2* and *4*) were taken after 60 min of incubation at 30 °C and adsorbed to Ni^{2+}-NTA-agarose as described under "Materials and Methods." After washing away unbound materials, the eIF2α kinase activity of the adsorbed HRI was assayed as described under "Materials and Methods." Samples were separated by SDS-PAGE, transferred to polyvinylidene difluoride membrane, and [^{35}S]HRI (**B**, *lower panel*) and [^{32}P]eIF2α (**B**, *upper panel*) were detected by autoradiography. The amount of [^{32}P]eIF2α was quantified by scanning densitometry and expressed as optical density × mm^2 (numbers above the eIF2α panel). Densitometry indicated that equivalent amounts of total [^{35}S]HRI were specifically immunoadsorbed (*lanes 3* and *4*). *HP*: hyperphosphorylated form of HRI; *TR*: transformed form of HRI; *MC*: mature competent form of HRI.

The effect of p50^{cdc37} on the eIF2α kinase activity of HRI was also assessed (Fig. 9*B*). After 60 min of incubation, the eIF2α kinase activity of HRI matured in p50^{cdc37}-supplemented heme-deficient RRL was nearly 3-fold higher relative to HRI matured in control RRL supplemented with buffer alone. Thus, the physical association of p50^{cdc37} with untransformed intermediates of HRI appeared to reflect a positive role for this co-chaperone in HRI maturation/activation pathway, as supplementation of RRL with p50^{cdc37} promoted the acquisition of an active conformation.

The data presented in Fig. 5 indicated that p50^{cdc37} required geldanamycin-inhibitable Hsp90 function for it to form a stable complex with untransformed HRI intermediates. To determine whether endogenous Hsp90 function was also required for the stimulatory effects of recombinant p50^{cdc37} on HRI transformation and activity, the effect of including geldanamycin in the transformation-activation assays was assessed (Fig. 10). Similar to the results obtained with (His$_6$)-p50^{cdc37}, supplementation of RRL with recombinant GST-p50^{cdc37} enhanced the eIF2α kinase activity of HRI 3-fold over the control, and this enhancement of activity correlated with the generation of a [^{35}S]HRI species with a slower electrophoretic mobility (*lower panel*, denoted *HP*). Addition of geldanamycin inhibited the activation of HRI in both buffer-supplemented control and p50^{cdc37}-supplemented heme-deficient RRL (Fig. 10, *upper panel*). Consistent with this finding, the slow electrophoretic form of HRI representing transformed HRI molecules was not produced in geldanamycin-poisoned reactions (Fig. 10, *lower panel*). These results indicated that geldanamycin inhibitable Hsp90 function was essential for the observed stimulatory effects of p50^{cdc37} on HRI transformation-activation.

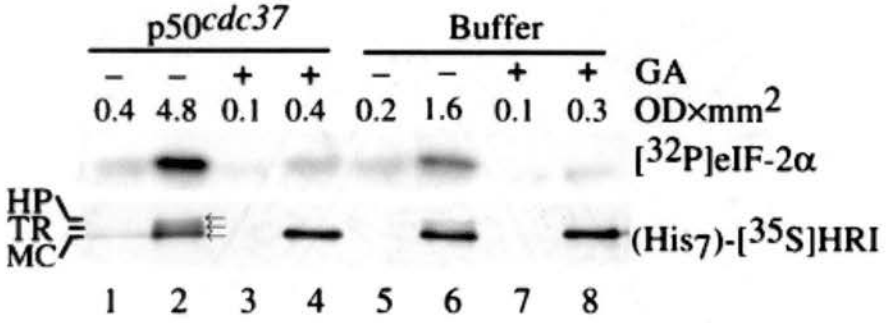

Figure 10. The effect of geldanamycin on the ability of GST-p50^{cdc37} to enhance HRI transformation and activation in heme-deficient RRL. (His_7)-[^{35}S]HRI (*lanes 2, 4, 6,* and *8*) and [^{35}S]HRI lacking the (His_7)-tag (*lanes 1, 3, 5,* and *7*) were pulse-labeled in TnT RRL and then chased and matured at 30 °C for 1 h in heme-deficient RRL containing GST-p50^{cdc37} (*lanes 1-4*) or GST-p50^{cdc37} purification buffer (*lanes 5-8*) in the presence of 10 μg/ml geldanamycin (*lanes 3, 4, 7,* and *8*) or Me_2SO (*lanes 1, 2, 5,* and *6*) as described under "Materials and Methods." RRL maturation mixtures were adjusted to 20 mM sodium molybdate and immunoadsorbed with GaG-agarose containing bound anti-(His_5) monoclonal antibody. After washing away unbound material, the eIF2α kinase activity of adsorbed HRI was assayed as described under "Materials and Methods." Samples were separated by SDS-PAGE, followed by transfer to polyvinylidene difluoride membrane. (His_7)-[^{35}S]HRI that was specifically immunoadsorbed (*lower panel*) and [^{32}P]eIF2α (*upper panel*) were detected by autoradiography. The amount of [^{32}P]eIF2α was quantified by scanning densitometry and expressed as optical density × mm^2 (*numbers above* the eIF2α panel). Densitometry indicated that equivalent amounts of total (His_7)-[^{35}S]HRI were specifically immunoadsorbed (*even lanes*). *HP*: hyperphosphorylated form of HRI; *TR*: transformed form of HRI; *MC*: mature competent form of HRI.

To further test the hypothesis that the positive effect which $p50^{cdc37}$ has on HRI activity is modulated through its interaction with Hsp90, we examined the effect of the $p50^{cdc37}$/ΔC mutant on the transformation and activation of HRI in heme-deficient RRL (Fig. 11). The data presented in Fig. 5 indicate that complexes formed between HRI and the $p50^{cdc37}$/ΔC mutant lacked bound Hsp90. Thus, the $p50^{cdc37}$/ΔC mutant was predicted to retard HRI transformation and activation when added to heme-deficient RRL. (His_7)-HRI (Fig. 11, *even lanes*) or non-His-tagged HRI (Fig. 11, *odd lanes*) was synthesized and then matured in heme-deficient RRL in the presence of control M2 anti-FLAG tag-agarose presaturated with FLAG-peptide, FLAG-tagged-$p50^{cdc37}$, or FLAG-tagged $p50^{cdc37}$/ΔC. The electrophoretic mobility of the non-His-tagged [^{35}S]HRI that was specifically associated with $p50^{cdc37}$ or $p50^{cdc37}$/ΔC indicated that the HRI was not transformed, and the eIF2α kinase activity of non-His-tagged [^{35}S]HRI bound to $p50^{cdc37}$ and $p50^{cdc37}$/ΔC were the same as the activity present in the control pellet for nonspecifically bound activity (Fig. 11, *lanes 1, 3,* and *5*).

The effects of the $p50^{cdc37}$ and $p50^{cdc37}$/ΔC mutant on the eIF2α kinase activity and electrophoretic properties of the total (His_7)-[^{35}S]HRI population matured in these RRLs and subsequently adsorbed to anti-His resin were also examined (Fig. 11, *lanes 2, 4,* and *6*). The eIF2α kinase activity of the (His_7)-[^{35}S]HRI that was matured in heme-deficient RRL in the presence of wild type $p50^{cdc37}$ was almost twice as high as the eIF2α kinase activity present in the control RRL containing M2 anti-FLAG tag-agarose with bound FLAG-peptide. In contrast, the eIF2α kinase activity of the (His_7)-HRI that was matured in the presence of the $p50^{cdc37}$/ΔC mutant was decreased by 60% relative to the kinase activity adsorbed from control RRL. A portion of the (His_7)-[^{35}S]HRI that was

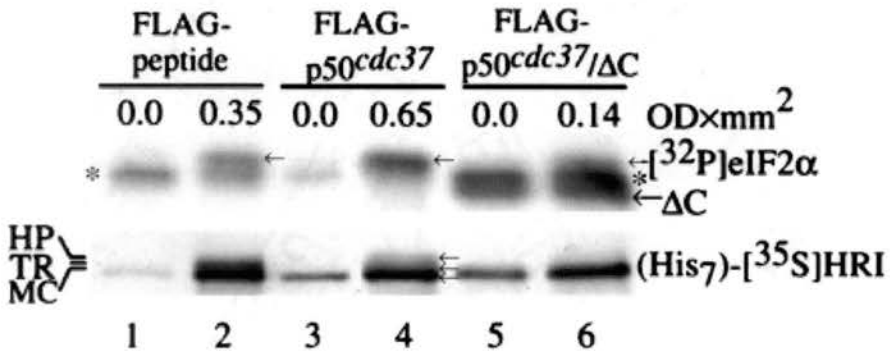

Figure 11. Effect of removal of the C-terminal region of p50^{cdc37} on HRI transformation and activation in heme-deficient RRL. (His_7)-[^{35}S]HRI (*lanes 2, 4,* and *6*) and [^{35}S]HRI lacking the (His_7)-tag (*lanes 1, 3,* and *5*) were pulse-labeled in TnT RRL and then chased and matured at 30 °C for 1 h in normal heme-deficient RRL containing M2-agarose that had been pre-saturated with FLAG peptide (Eastman Kodak Co.) (*lanes 1* and *2*), FLAG-tagged p50^{cdc37} (*lanes 3* and *4*), or FLAG-tagged p50^{cdc37}/ΔC (*lanes 5* and *6*) as described under "Materials and Methods." The RRL maturation mixtures were then immunoadsorbed with GaG-agarose containing bound anti-(His_5) monoclonal antibody. After washing away unbound material, the eIF2α kinase activity of adsorbed (His_7)-HRI was assayed as described under "Materials and Methods." Samples were separated by SDS-PAGE, followed by transfer to polyvinylidene difluoride membrane. (His_7)-[^{35}S]HRI that was specifically immunoadsorbed (*lower panel*) and [^{32}P]eIF2α (*upper panel*) were detected by autoradiography. The amount of [^{32}P]eIF2α was quantified by scanning densitometry and expressed as O.D. × mm^2 (*numbers above* the eIF2α panel). Densitometry indicated that equivalent amounts of total (His_7)-[^{35}S]HRI were specifically immunoadsorbed (*even lanes*). *ΔC*, p50^{cdc37}/ΔC that was also highly phosphorylated and labeled by [γ-^{32}P]ATP during the kinase assay. "*": an unknown protein contaminant present in the purified eIF2 preparation, which became phosphorylated and labeled by [γ-^{32}P]ATP during kinase assay.

matured in the presence of wild type $p50^{cdc37}$ exhibited a slower electrophoretic mobility than the (His_7)-[^{35}S]HRI that was matured in control RRL, indicating it had become hyperphosphorylated (Fig. 11, *lower panel, lane 4 versus 2 (HP)*). This shift in electrophoretic mobility caused the band to appear more diffuse. However, quantification of the total amount of (His_7)-[^{35}S]HRI molecules exhibiting slower electrophoretic mobilities indicated that nearly the same amount of (His_7)-[^{35}S]HRI became transformed in RRL supplemented with wild type $p50^{cdc37}$ (O.D. × mm^2 = 4.14) compared with control RRL (O.D. × mm^2 = 4.11). This observation is consistent with the enhanced eIF2α kinase activity displayed by the (His_7)-[^{35}S]HRI that was matured in the presence of wild type $p50^{cdc37}$. In addition, the fast electrophoretic mobility of the (His_7)-[^{35}S]HRI that was matured in the presence of $p50^{cdc37}$/ΔC indicated that it remained mostly untransformed, consistent with its suppressed kinase activity (Fig. 11, *lane 6*). These results indicate that Cdc37 gene products which do not interact with Hsp90 may act as dominant negative inhibitors of $p50^{cdc37}$ function: a conclusion consistent with the observation that Hsp90 is required for $p50^{cdc37}$ to exert its positive effect on HRI activity upon transformation.

$p50^{cdc37}$ Does Not Enhance HRI Activity after Its Transformation-HRI can become further activated in RRL after its transformation and release from Hsp90. This further activation of transformed HRI is negatively attenuated by the interaction of Hsc70 with HRI, and is also accompanied by HRI's hyperphosphorylation (248). To verify that $p50^{cdc37}$ functions are specific to untransformed HRI, HRI was transformed in hemin-deficient RRL prior to the addition of recombinant $p50^{cdc37}$ (Fig. 12). As an additional

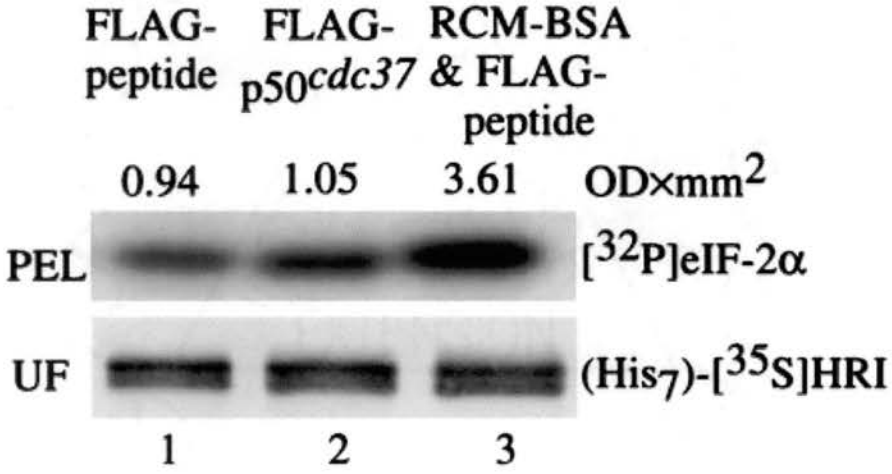

Figure 12. Effect of recombinant FLAG-p50^{cdc37} on HRI kinase activity upon addition subsequent to HRI transformation. (His_7)-[^{35}S]HRI was pulse-labeled in TnT RRL and chased and matured at 30 °C for 1 h in normal heme-deficient RRL as described under "Materials and Methods." The effect of FLAG-peptide alone (*lane 1*), FLAG-tagged p50^{cdc37} (*lane 2*), or FLAG-peptide plus soluble reduced carboxymethylated bovine serum albumin (*lane 3*) was evaluated by incubating the RRL maturation mixtures for an additional 20 min at 30 °C. The RRL mixtures were then immunoadsorbed with GaG-agarose containing bound anti-(His_5) monoclonal antibody. A 2-μl aliquot of each maturation mixture was taken prior to immunoprecipitation to detect different forms of [^{35}S]HRI generated (*UF panel*). After washing away the unbound material, the eIF2α kinase activity of adsorbed (His_7)-HRI was assayed as described under "Materials and Methods." Samples were separated by SDS-PAGE, followed by transfer to polyvinylidene difluoride membrane, and autoradiography detection of [^{32}P]eIF2α (*PEL panel*). The amount of [^{32}P]eIF2α was quantified by scanning densitometry and expressed as O.D. × mm^2 (*numbers above* the PEL panel).

control, denatured (reduced carboxymethylated) bovine serum albumin was similarly added to heme-deficient RRL after the completion of HRI's transformation to block the ability of Hsc70 to negatively attenuate HRI's activation (145, 243, 248). Addition of reduced carboxymethylated bovine serum albumin to heme-deficient RRL stimulated the eIF2α kinase activity of HRI 4-fold compared with the activity observed in control RRL. In contrast, the addition of an equivalent amount of recombinant $p50^{cdc37}$ to heme-deficient RRL subsequent to HRI transformation caused little further stimulation of HRI's eIF2α kinase activity (approximately 10%) compared with the control. Therefore, the stimulatory effects of $p50^{cdc37}$ were specific to that HRI population whose transformation had been previously documented to be functionally dependent upon geldanamycin-inhibitable Hsp90 function.

Interaction of $p50^{cdc37}$ with HRI in Vivo-Interactions between endogenously expressed $p50^{cdc37}$ and HRI were examined in the chronic myelogenous leukemic K562 cell line to determine whether $p50^{cdc37}$ also interacted with HRI *in vivo*. K562 cells, cultured in the presence or absence of geldanamycin for 2 h, were lysed and endogenous $p50^{cdc37}$ was immunoadsorbed (Fig. 13). Immunoblotting with HRI-specific antibodies indicated that HRI was co-adsorbed with $p50^{cdc37}$ from extracts of control cells (Fig. 13, *upper panel*). However, treatment of K562 cells with geldanamycin abolished the interaction of $p50^{cdc37}$ with HRI. In contrast, geldanamycin treatment of K562 cells had no effect on the avid interaction between $p50^{cdc37}$ and Hsp90 *in vivo* (Fig. 13, *middle panel*). Stripping and reprobing with anti-$p50^{cdc37}$ antisera verified that equivalent amounts of $p50^{cdc37}$ were immunoprecipitated from the extracts of the untreated and geldanamycin-treated cells

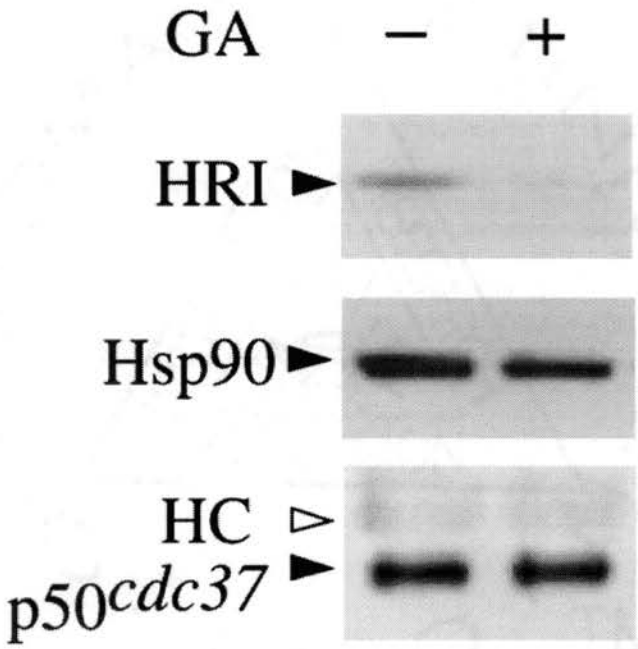

Figure 13. Endogenous p50^{cdc37} associates with HRI *in vivo*. Cultured human erythroleukemia K562 cells were treated with Me_2SO (*lane 1*) or with 1 μg/ml geldanamycin (*lane 2*) for 2 h. Endogenous p50^{cdc37} was immunoprecipitated as described under "Materials and Methods." Immunocomplexes were separated by SDS-PAGE, transferred to polyvinylidene difluoride membrane, and analyzed for the presence of p50^{cdc37} (*lower panel*) and associated HRI (*upper panel*). An equivalent aliquot of the immunopellet was similarly analyzed for the presence of Hsp90 (*middle panel*). Proteins that were specifically detected when membranes were probed with anti-HRI, anti-p50^{cdc37}, or anti-Hsp90 antibodies are indicated by *solid arrowheads*. The detected proteins were of the expected molecular weight. *Open arrowheads* denote the position of the heavy chain of the immunoprecipitating anti-p50^{cdc37} antibodies. Analysis of anti-p50^{cdc37} immunoadsorptions from two additional sets K562 cell extracts gave similar results.

(Fig. 13, *lower panel*). These results indicated that HRI existed in geldanamycin-sensitive native complexes with $p50^{cdc37}$ in cultured K562 cells.

Discussion:

$p50^{cdc37}$ plays a positive role in facilitating activation of HRI in response to heme-deficiency. Supplementation of heme-deficient RRL with recombinant $p50^{cdc37}$ during the HRI activation process stimulates the production of HRI populations with enhanced kinase activity and stimulates the production of HRI populations with retarded electrophoretic mobilities which are diagnostic of HRI activation/transformation. While our present work is the first to directly address the role of $p50^{cdc37}$ in kinase biogenesis in an *in vitro* model system, these observations are consistent with biochemical and genetic data which indicate that $p50^{cdc37}$ plays an essential positive role in supporting the function of numerous protein kinases (59, 71, 89, 122, 143, 166, 235). This positive function is consistent with a primary role for $p50^{cdc37}$ in a striking partnership with Hsp90 as a kinase-specific cohort.

The stimulatory effect of $p50^{cdc37}$ is specific to the HRI activation process: $p50^{cdc37}$ has no effect on the kinase activity or electrophoretic mobility of HRI when added subsequent to HRI's transformation. Consistent with this specificity, $p50^{cdc37}$ interacts with newly synthesized HRI and with the inactive HRI population maintained in the presence of hemin, but does not interact with HRI that has been transformed in response to heme deficiency or with transformed HRI whose activity has been repressed by hemin. Therefore, like Hsp90's association with inactive kinases, the interaction of $p50^{cdc37}$ with HRI appears to reflect its role in facilitating kinase folding, maturation, and

activation, and not its association with kinase molecules whose activity is repressed *per se*. Similarly, the fast electrophoretic form of Raf-1 has been found to be preferentially co-adsorbed with $p50^{cdc37}$ from cultured cells. The observed specificity of $p50^{cdc37}$ for untransformed HRI intermediates is also consistent with other studies demonstrating that $p50^{cdc37}$ and Hsp90 recognize kinase molecules which represent specific maturation or activation intermediates (20, 71, 166, 235).

Data presented here allowed us to locate the $p50^{cdc37}$-binding site to the N-terminal lobe of the conserved kinase domain of HRI, but not to any other domains. This region of HRI is also recognized by Hsp90, an observation that is consistent with reports on the interactions of Hsp90 and $p50^{cdc37}$ with the catalytic domains of other client kinases, including Raf-1 and KSR (223, 233, 236). The "coincident" bindings of these two chaperones to the same HRI domain further implies their functional cooperation in terms of regulating client proteins, a notion that has already been suggested by various other studies (8, 20, 29, 51, 89, 122, 158, 175, 211, 235, 236). Moreover, since Hsp90 and $p50^{cdc37}$ interact with the client kinases through direct physical contacts (223, 235) and in a non-overlapping fashion, it thus indicates that subtle but significant differences must exist in their specific binding sites within the kinase domains of the client proteins. Interestingly, besides the N-terminal kinase lobe Hsp90 binds to the unique regulatory heme-binding domain (HBD) of HRI as well, a region that is not recognized by $p50^{cdc37}$. In constrast to the interaction between Hsp90 and the N-terminal kinase lobe of HRI, the interaction between Hsp90 and the HBD was not affected by the Hsp90 specific inhibitor geldanamycin (data not shown). This observation suggests that the interaction of Hsp90 with the HBD represents its passive (non-ATP-dependent) chaperone function:

interacting with partially denatured polypeptides to prevent aggregation. It is in agreement with the recent identification of an ATP-independent chaperone site in the C-terminal region of Hsp90 (209, 264). Taken together, the difference in the recognition sites of Hsp90 and p50^{cdc37} for HRI is consistent with the notion that these two chaperones may regulate their common clients differentially *in vivo* although their functions may be cooperative or interdependent in some regards (122).

p50^{cdc37} has at least two semi-independent units that mediate its biological activity. The N-terminal half of p50^{cdc37} contains an autonomous kinase-binding unit, since it binds HRI (Fig. 5) and Raf-1 (89) when its C-terminal half was deleted. Consistent with this localization, the first 8 amino acids at the N terminus of p50^{cdc37} were found to be essential to its kinase binding activity (Fig. 8). Thus, these residues either participate directly in kinase binding or provide essential support to the structure of an N-terminal kinase-binding domain. Additionally, complexes formed between p50^{cdc37}/ΔC and HRI (Fig. 5) or Raf-1 (89) lack bound Hsp90. Furthermore, the interaction between p50^{cdc37}/ΔC and HRI was enhanced by geldanamycin (Fig. 5), apparently due to lack of competition from endogenous Hsp90/p50^{cdc37} in the presence of geldanamycin. Thus, the N-terminal domain of p50^{cdc37} binds to HRI directly rather than associating with HRI via Hsp90. This finding is consistent with similar conclusions reached previously regarding the association of p50^{cdc37} with Raf-1 or Cdk4 (89, 223, 235).

In contrast to the N-terminal region, the C-terminal half of p50^{cdc37} contains one or more motifs or domains which mediate its interaction with Hsp90. Deletion of the C-terminal half of p50^{cdc37} abolishes its interaction with Hsp90 (Fig. 5), a finding consistent with previous *in vivo* characterizations of the truncated Cdc37 gene product (89).

However, it was not previously clear if such truncations directly deleted a discrete Hsp90-binding domain or motif, or if they indirectly compromised Hsp90 binding by disrupting essential support of other protein structures present within the N-terminal half of $p50^{cdc37}$. We demonstrate here that the C-terminal half of $p50^{cdc37}$ contains semi-autonomous Hsp90 binding activity (Fig. 6). Thus, sequences or structures present in the C-terminal region of $p50^{cdc37}$ directly mediate its binding to Hsp90. However, despite the observation that the N-terminal domain of $p50^{cdc37}$ does not stably interact with Hsp90, we cannot rule out the possibility that motifs in regions outside of the C terminus of $p50^{cdc37}$ may also contribute directly or indirectly to the interaction of $p50^{cdc37}$ with Hsp90.

Our data indicate that $p50^{cdc37}$ exerts its biochemical effects in cooperation with Hsp90. This conclusion is indicated by the observation that the Hsp90-specific inhibitor geldanamycin inhibits the ability of recombinant $p50^{cdc37}$ to stimulate HRI transformation (Fig. 10). Geldanamycin similarly inhibits the ability of $p50^{cdc37}$ overexpression to stimulate Raf activation in cultured cells (89), indicating that Hsp90 is required for $p50^{cdc37}$ to exert its positive effect on Raf-1 activation *in vivo*. Furthermore, these results do not reflect a direct disruption of the Hsp90-$p50^{cdc37}$ interaction (Figs. 5 and 13) (89). Instead, geldanamycin disrupts the normal association of $p50^{cdc37}$ with HRI in RRL and in cultured K562 cells (Figs. 5 and 13). This finding is consistent with previous characterization of the effects of geldanamycin on $p50^{cdc37}$ interactions with CDK4, Raf-1, and KSR *in vivo* (89, 235, 236).

In contrast, geldanamycin does not inhibit the ability of C-terminal truncated Cdc37 gene products to bind kinase folding intermediates; inhibition of Hsp90 actually increases the availability of HRI molecules for binding to truncated cdc37 proteins (Fig.

5). This observation has 3 important implications. 1) Geldanamycin's disruption of $p50^{cdc37}$-kinase heterocomplexes does not result from sequestration or masking of kinase-folding intermediates by geldanamycin-poisoned Hsp90 machinery. 2) The physical interaction of full-length $p50^{cdc37}$ with Hsp90 determines geldanamycin's ability to inhibit the binding of $p50^{cdc37}$ to kinase molecules. 3) Geldanamycin-inhibitable Hsp90 function is necessary to assemble heterocomplexes formed directly between kinase molecules and full-length $p50^{cdc37}$ and to chaperone the kinase substrate toward its activation-specific conformation.

Geldanamycin is known to act as a specific inhibitor of Hsp90 through its ability to bind avidly within Hsp90's nucleotide-binding pocket, thus blocking the binding of ATP (91, 183, 234). This binding prevents nucleotide-mediated switching between alternative Hsp90 conformations (91, 99, 116, 237) and abolishes Hsp90's ability to establish high affinity interactions with its substrates (97, 243), thus inhibiting Hsp90-supported kinase function. Therefore, geldanamycin's ability to inhibit the binding of wild type $p50^{cdc37}$ to kinase-folding intermediates demonstrates that Hsp90's nucleotide-mediated conformational switching regulates the direct binding of $p50^{cdc37}$ to Hsp90's kinase clients. Additionally, our data illuminate potential mechanisms underlying the chemotherapeutic potential of benzoquinonoid ansamycins.

CHAPTER III

Evidence That Protein Phosphatase 5 Functions To Negatively Modulate the Maturation of the Hsp90-Dependent Heme-Regulated eIF2α Kinase

Introduction:

The *h*eme-*r*egulated *i*nhibitor (HRI) of protein synthesis is a protein kinase that acts in reticulocytes and reticulocyte lysates to coordinate the synthesis of globin chains with the availability of heme (32). Under heme-deficient conditions, HRI becomes activated and phosphorylates the α-subunit of the eukaryotic translational initiation factor eIF2 at Ser51. Phosphorylation of eIF2α causes the sequestration of eIF2B, the guanine nucleotide exchange factor responsible for the recycling of eIF2, in complexes with phosphorylated eIF2. The subsequent accumulation of nonfunctional GDP-bound eIF2 ultimately shuts off initiation of protein synthesis. In addition to heme deficiency, HRI is also activated by other environmental or chemical stimuli including heat shock, oxidative stress, denatured proteins, and sulfhydryl-reactive reagents (32).

The activation of HRI under physiological and nonphysiological conditions is accompanied by phosphorylation events. While a preponderance of evidence supports the notion that the phosphorylation of HRI is autocatalytic (9, 32, 70, 246), heterophosphorylation by casein kinase II has also been proposed to regulate HRI activation (151). Despite characterizations performed to date, the specific phosphorylation/dephosphorylation events regulating HRI function are poorly understood.

In addition to governing HRI activation, evidence indicates that phosphorylation of HRI also regulates its posttranslational maturation and that the pathways for HRI maturation and activation overlap (215, 246, 248). Newly synthesized HRI is inactive and

cannot be activated by heme deficiency or treatment with *N*-ethylmaleimide. This "immature" population of HRI is physically associated with chaperone machinery containing the 90 kDa heat-inducible phosphoprotein Hsp90 (215, 246, 248). HRI molecules subsequently mature such that they become competent to activate in response to heme deficiency or treatment with *N*-ethylmaleimide. However, this "mature-competent" form of HRI continues to require physical and functional interactions with Hsp90 to maintain the kinase's competence to respond to activating stimuli (246). When mature-competent HRI is exposed to activating conditions (e.g., heme deficiency), HRI molecules become "transformed". Transformation is characterized by activation of HRI's kinase activity and the cessation of physical and functional interactions with Hsp90. Transformation of HRI appears to occur through its autophosphorylation, as it requires the presence of a conserved lysine in HRI's catalytic pocket (246). Additionally, transformed HRI shows retarded electrophoretic mobility on SDS-PAGE (215, 246). The altered electrophoretic mobility of transformed and hyperphosphorylated HRI on SDS-PAGE is reversed by pretreatment of samples with alkaline phosphatase (9, 137), indicating that the altered electrophoretic mobility of HRI is diagnostic of its altered phosphorylation status. While studies to date indicate that autophosphorylation governs HRI's Hsp90-dependent activation and transformation (246), HRI is multiply phosphorylated *in vitro* and *in vivo* (9, 32, 70, 137, 215, 246, 248), and the importance of individual phosphorylated residues has yet to be defined.

The composition of the Hsp90 chaperone machine associated with untransformed HRI has been partially characterized in previous studies (97, 144-146, 215, 246, 248). In addition to Hsp90, HRI-chaperone complexes can also contain Hsc70, $p50^{cdc37}$, the

immunophilin FKBP52, and the nucleotide-responsive cohort p23. Several Hsp90 cochaperones, such as FKBP52 and p60/Hop, contain tetratricopeptide repeat (TPR) motifs (reviewed in 13) that mediate their interaction with Hsp90 (27, 101, 153, 170, 189, 196). Regarding the $p50^{cdc37}$- and TPR-containing components of Hsp90 heterocomplexes, *in vitro* competition studies have suggested that these Hsp90 cohorts might represent mutually exclusive subunits that compete for binding to the Hsp90 chaperone "machine" (170, 171, 223). More recently, however, $p50^{cdc37}$ and FKBP52 have been found to bind to Hsp90 simultaneously both in the basal (no kinase client) chaperone machine and in client-chaperone heterocomplexes (97). This co-occurrence suggests that the poorly characterized role(s) of these proteins is (are) exercised in concert during Hsp90-mediated protein folding.

Protein phosphatase 5 (PP5) is a novel component of the Hsp90 chaperone machine (35). PP5 has been found in all eukaryotic cells so far examined from yeast to humans (41) and has a cytoplasmic/nuclear localization (5, 19, 37, 160, 167, 204). PP5 contains an N-terminal TPR domain that mediates its interaction with Hsp90 (35, 194, 204) and a C-terminal catalytic phosphatase domain (10, 37, 42). Limited proteolysis of PP5 has indicated that its phosphatase activity is negatively modulated by its TPR domain and a region at its C-terminus (36, 224). Polyunsaturated fatty acids, such as arachidonic or linoleic acid, stimulate the phosphatase activity of purified PP5 substantially and are thought to relieve the autoinhibition of PP5 by binding to its TPR domain (36, 225). Like the immunophilin FKBP52, competition studies performed *in vitro* suggest that the association of PP5 with Hsp90 can be mutually exclusive with regard to $p50^{cdc37}$ and immunophilins (223).

The apparent ubiquitous expression of PP5 has prompted the conjecture that PP5 plays an as yet underappreciated role in the regulation of signal transduction within cells (41). This hypothesis is supported by the observations that, besides being present in heterocomplexes formed between Hsp90 and steroid hormone receptors (35, 221), PP5 has been found to be associated with the atrial natriuretic peptide (ANP) receptor (42), the CDC16/CDC27 subunits of the anaphase-promoting complex (APC) (167), the apoptosis signal-regulating kinase 1 (ASK1) (160), the A-subunit of phosphatase 2A (138), the GANG-MCM3 complex involved in B cell transition (124), and the blue light photoreceptor hCRY2 (267). The potential physiological significance of these interactions is supported by the observations that PP5 overexpression appears to negatively regulate glucocorticoid-mediated growth arrest *in vivo* (272) and PP5 appears to act as a negative feedback inhibitor of ASK1 activation (160).

In this report, the physical and functional association of PP5 with HRI maturation/activation intermediates was characterized by biochemical and pharmacological approaches in rabbit reticulocyte lysate, lysates of cells in which HRI is naturally expressed. Data indicate that PP5 is a nonexclusive Hsp90 partner protein that associates with HRI during overlapping pathways of HRI maturation and regulation. Pharmacological characterizations indicate that this association is functionally relevant. The coexistence of PP5 and $p50^{cdc37}$ within Hsp90 heterocomplexes suggests that physiological signals that regulate HRI transformation and activation may be modulated by the opposing actions of these two Hsp90 cochaperones on HRI.

Materials and Methods:

Reagents-For *in vitro* translation in rabbit reticulocyte lysate, the *Eco*RI fragment of pCMV6 encoding rat FLAG-tagged PP5 (provided by Dr. Michael Chinkers) (35) was ligated into the corresponding site of a modified version of the *in vitro* transcription vector pSP64T (126). For expression in *Escherichia coli,* the same *Eco*RI fragment was cloned into the corresponding site of the bacterial expression vector pET-30a(+). The resulting construct encoded a recombinant PP5 with a relatively large leading sequence of approximately 50 amino acids containing a (His_6)-tag followed by vector-encoded sequence. For expression of the isolated TPR domain, the pET-30a(+)-PP5 plasmid was digested with HindIII which separates the C-terminal phosphatase domain from the N-terminal TPR domain of PP5, and the resulting large HindIII fragment encoding the TPR domain only was self-annealed. Due to the removal of the original stop codon immediately following the phosphatase domain of PP5, the resulting TPR domain used the one in the pET-30a(+) vector and this had a short C-terminal tail containing a second (His_6)-tag (AAALEHHHHHH). Recombinant His-tagged FLAG-PP5 or His-tagged PP5/K97A or PP5/R101A in the pET-15b expression vector (provided by Dr. Michael Chinkers) (204) was expressed in BL21(DE3) cells and purified under native conditions as described previously for His-tagged recombinant $p50^{cdc37}$ (215) for addition into reaction mixtures. Rabbit Hsp90 was purified as described previously (242) and used for immunization of mice to produce polyclonal ascites anti-Hsp90 antibodies. Other antibodies utilized include mouse anti-PP5 (P75520, BD Transduction Laboratories), antigen affinity-purified mouse antibodies recognizing the His_5 epitope (anti-His-tag) (Qiagen), polyclonal ascites antibodies directed against $p50^{cdc37}$ (97), and M2 anti-FLAG-tag antibody (Sigma). Rabbit reticulocyte lysate reaction mixtures were assembled, and

proteins were synthesized de novo and radiolabeled via coupled transcription and translation as previously described (215, 246, 248).

Assays of the Effects of Pharmacological Agents on HRI Transformation-His-tagged HRI [(His_7)-HRI] was synthesized by coupled transcription and translation in rabbit reticulocyte lysate for 15 min followed by a 4 min pulse labeling with [^{35}S]Met (215, 246, 248). Aliquots (6 μL) of the reticulocyte lysate were subsequently transferred to heme-supplemented or heme-deficient reticulocyte lysate mixtures (44 μL) containing the initiation inhibitor aurintricarboxylic acid (ATA, 60 μM final) for HRI maturation/activation. These maturation/activation reactions contained or lacked 500 nM okadaic acid or nodularin (Calbiochem), 34 μM fostriecin (Calbiochem), or various concentrations of arachidonic acid (Cayman) or linoleic acid (Sigma) (50-600 μM) individually, as indicated in the figure legends. Control maturation/activation reactions contained equal amounts of okadaic acid-7,10,24,28-tetraacetate (Calbiochem) in DMSO as the negative control for okadaic acid, DMSO as the vehicle control for geldanamycin, water as the vehicle control for nodularin and linoleic acid, 95% ethanol as the vehicle control for arachidonic acid, and stearic acid (Sigma) in 100% methanol as the negative control for arachidonic acid. After addition of HRI to the drug-treated lysates, the reaction mixtures were incubated at 30° C for 1 h to allow for HRI maturation/activation.

To assay for the postmaturational effect of drug additions, (His_7)-[^{35}S]HRI was synthesized by coupled transcription and translation in reticulocyte lysate and matured/activated in heme-deficient reticulocyte lysate for 45 min as described above.

The drugs were then added, and the reaction mixtures were incubated for an additional 20 min at 30 °C. Negative controls were as described above.

After maturation/activation in reticulocyte lysate, (His_7)-[^{35}S]HRI was immunoadsorbed from reaction mixtures with mouse anti-(His_5) monoclonal antibody prebound to agarose containing cross-linked anti-mouse IgG (anti-His-tag antibody resin). To assess the interaction of [^{35}S]HRI with Hsp90 and p50^{cdc37}, Hsp90 and p50^{cdc37} were immunoadsorbed with 8D3 anti-Hsp90 or anti-p50^{cdc37} antibodies as previously described (215, 246). Reaction mixtures incubated with reticulocyte lysate containing no template were used as controls for nonspecific binding. Resins were washed with PIPES buffer (10 mM, pH 7.2) containing 150 mM NaCl and 50 mM NaF. Immunoadsorbed HRI was assayed for its eIF2α kinase activity as previously described (215, 246, 248), and gel mobility shifts on SDS-PAGE were used to monitor HRI transformation as previously described (215, 246, 248). Samples were analyzed by SDS-PAGE, electrotransfer to PVDF membranes, and autoradiography.

Protein-Protein Interaction Assays-To assay for the interaction of HRI with the endogenous PP5 in reticulocyte lysate, (His_7)-[^{35}S]HRI was synthesized by coupled transcription and translation in reticulocyte lysate for 30 min at 30 °C, after which lysate reactions were immunoadsorbed with anti-His-tag antibody resin. Immunoadsorptions were washed with PIPES buffer (10 mM, pH 7.2) containing 150 mM NaCl and 0.5% Tween-20. As negative controls, blank reticulocyte lysate reactions lacking DNA templates were assessed in parallel adsorptions. Proteins adsorbed or coadsorbed from control and experimental reticulocyte lysate were separated on 8% SDS-PAGE gels,

transferred to PVDF membranes, and analyzed by autoradiography or by Western blotting with antibodies directed against PP5 or other chaperones as indicated.

In an alternative assay with enhanced sensitivity for the detection of the interaction of PP5 with HRI, FLAG-tagged PP5 and HRI were synthesized de novo by coupled transcription and translation and radiolabeled in separate reticulocyte lysate reactions for 30 min at 30 °C. Synthesis and labeling were arrested via addition of ATA (60 μM final) for 10 min, and equal volumes of these individual reactions were then mixed. Subsequently, the mixed reactions were incubated for 20 min at 30 °C with or without addition of pharmacological agents, followed by immunoadsorption of FLAG-tagged PP5 with M2 anti-FLAG-tag antibody resin. In the reciprocal experiment, (His_7)-HRI and FLAG-PP5 were synthesized and mixed as described above, followed by immunoadsorption of (His_7)-HRI with anti-His-tag antibody resin. Immunoadsorptions were washed with PIPES buffer (10 mM, pH 7.2) containing 0.5% Tween-20 and NaCl at concentrations indicated in the figure legends. Radiolabeled coadsorbing proteins were assessed by SDS-PAGE and autoradiography. The presence of other coadsorbed chaperones was assessed by Western blotting. Relative amounts of proteins were quantified by scanning densitometry.

To assess the interaction between HRI and PP5 mutants, aliquots of reticulocyte lysate containing [^{35}S]HRI generated by coupled transcription and translation were mixed with hemin-supplemented lysate that had been supplemented with purified recombinant His-tagged PP5, PP5K97A, or PP5/R101A. Reaction mixtures were incubated for 20 min at 30 °C, followed by immunoadsorption with anti-His-tag antibody resin. Samples were

then analyzed by SDS-PAGE, Coomassie Blue staining, autoradiography, and Western blotting.

Results:

PP5 Is a Nonexclusive Component of HRI-Chaperone Heterocomplexes-Since PP5 has been reported to interact with Hsp90, we tested the hypothesis that PP5 occurred on heterocomplexes with the Hsp90-dependent kinase HRI. (His_7)-[^{35}S]HRI was synthesized de novo by coupled transcription and translation in heme-replete rabbit reticulocyte lysate, yielding a mixture of immature and mature-competent Hsp90-dependent molecules due to the presence of heme in translation reactions (246). After immunoadsorption of HRI with anti-His-tag antibody resin, coadsorbing proteins were detected by SDS-PAGE and Western blotting. As we have reported previously, Hsp90 was coadsorbed with newly synthesized (His_7)-[^{35}S]HRI (Figure 14A). In contrast, no similar (nonspecific) recovery of Hsp90 was observed in anti-His-tag immunoadsorptions from reactions lacking (His_7)-[^{35}S]HRI. Like Hsp90, PP5 was coadsorbed with (His_7)-[^{35}S]HRI, and this adsorption was specific for reactions programmed to synthesize (His_7)-[^{35}S]HRI. These results indicated that PP5 endogenous to reticulocyte lysate occurred in heterocomplexes with HRI molecules.

To further study the interaction of HRI with PP5 in reticulcyte lysate, untagged [^{35}S]HRI or (His_7)-[^{35}S]HRI and FLAG-tagged [^{35}S]PP5 were generated in separate reticulocyte lysate reactions. The reactions were then mixed and incubated for 20 min. After incubation, PP5 (Figure 14B) or HRI (Figure 14C) was immunoadsorbed with anti-FLAG-tag or anti-His-tag antibody resin, respectively, and assayed for coabsorbing

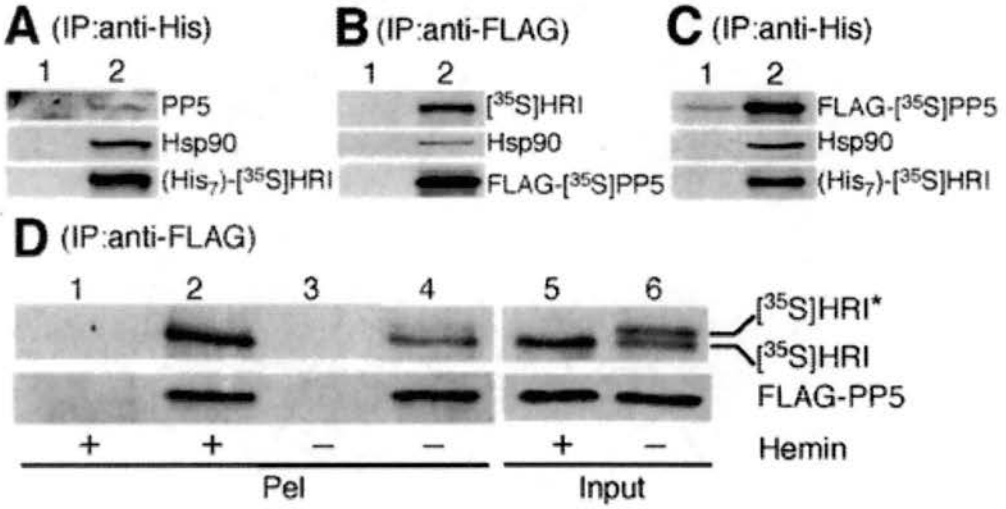

Figure 14. Interaction of HRI with PP5 in reticulocyte lysate. **A)** Reticulocyte lysate containing (*lane 2*) or lacking (*lane 1*) plasmid encoding for (His_7)-[^{35}S]HRI was incubated for 30 min, HRI was adsorbed with anti-His-tag antibody and samples were analyzed as described under "Materials and Methods". (His_7)-[^{35}S]HRI and coadsorbed endogenous PP5 were visualized by autoradiography and Western blotting, respectively. [^{35}S]HRI (**B**) or (His_7)-[^{35}S]HRI (**C**) and FLAG-tagged [^{35}S]PP5 were synthesized in separate reticulocyte lysate reaction mixtures for 30 min as described under "Materials and Methods". Reticulocyte lysate containing [^{35}S]HRI (**B**) or FLAG-tagged [^{35}S]PP5 (**C**) was mixed at a 1:1 ratio with lysate containing (*lane 2*) or lacking (*lane 1*) FLAG-tagged [^{35}S]PP5 (**B**) or (His_7)-[^{35}S]HRI (**C**), respectively. After 20 min of incubation, PP5 (**B**) and HRI (**C**) were immunoadsorbed with anti-FLAG-tag and anti-His-tag antibody resin, respectively, and analyzed as described under "Materials and Methods". [^{35}S]HRI or FLAG-[^{35}S]PP5 and Hsp90 were visualized by autoradiography and Western blotting. ***D***) HRI was synthesized in reticulocyte lysate for 15 min as described under "Materials and Methods". Aliquots of the reactions were then diluted into 7 volumes of heme-supplemented (*lanes 1, 2, and 5*) or heme-deficient rabbit reticulocyte lysate (*lanes 3, 4, and 6*) containing (*lanes 2 and 4*) or lacking (*lanes 1 and 3*) 17 μg/mL purified recombinant FLAG-PP5. After 1 h PP5 was immunoadsorbed with M2 anti-FLAG-tag antibody resin, and samples were analyzed as described under "Materials and Methods". FLAG-PP5 and coadsorbing [^{35}S]HRI (Pel) were detected by Western blotting and autoradiography, respectively. Portions of the maturation mixtures containing the purified FLAG-PP5 were analyzed in parallel (Input). [^{35}S]HRI*: transformed form of HRI with slower electrophoretic mobility; [^{35}S]HRI: mature-competent form of HRI with faster electrophoretic mobility.

proteins. Hsp90 was specifically coadsorbed with FLAG-tagged [^{35}S]PP5 (Figure 14B, lane 2), a finding consistent with the previously described interaction of these proteins. In addition to Hsp90, [^{35}S]HRI was also coadsorbed with FLAG-tagged [^{35}S]PP5, confirming the occurrence of PP5 in heterocomplexes with HRI molecules. While a low level of nonspecific binding of PP5 to the anti-His-tag resin was noted in the reciprocal experiment (Figure 14C, lane 1), both PP5 and Hsp90 were clearly found to be coadsorbed specifically with (His_7)-[^{35}S]HRI from the reactions (Figure 14C, lane 2).

To determine whether PP5 was associated with a specific population of HRI maturation intermediates, newly synthesized [^{35}S]HRI was matured in hemin-supplemented or heme-deficient reticulocyte lysate that had been supplemented with purified recombinant FLAG-PP5. After maturational incubations, FLAG-PP5 was adsorbed with anti-FLAG antibody resin in the presence of NaF to inhibit phosphatase activity. Adsorbing/coadsorbing PP5 and HRI were detected by Western blotting and autoradiography, respectively. Incubation of HRI in heme-deficient reticulocyte lysate resulted in the transformation of approximately 55% of the HRI, as indicated by the presence of a band with retarded electrophoretic mobility relative to immature and mature-competent forms of HRI (Figure 14D, lanes 5 and 6). The fast electrophoretic mobility form (representing immature and/or mature-competent HRI molecules) was the primary form of HRI coadsorbed with PP5 from hemin-supplemented and heme-deficient lysates (Figure 14D, lanes 2 and 4). However, a proportion of HRI with retarded electrophoretic mobility (~10% of the total) was also observed to coadsorb with PP5. Previous results suggesting that Hsp90 and p50^{cdc37} interacted exclusively with immature and mature-competent (untransformed) forms of HRI (215, 246) were obtained in the

absence of NaF. Inclusion of NaF in buffers during anti-Hsp90 and anti-p50^{cdc37} immunoadsorptions confirmed that a small percentage of HRI with retarded electrophoretic mobility was also coadsorbed with these chaperone hetercomplexes (data not shown). These results suggest that HRI becomes phosphorylated while associated with Hsp90 heterocomplexes and that chaperone-associated phosphorylated HRI is a target for one or more phosphatases present in reticulocyte lysate.

Although *in vitro* competition assays have suggested that p50^{cdc37} is an exclusive Hsp90 cohort that does not coexist in heterocomplexes with FKBP52 and PP5 (170, 171, 223), our recent findings are inconsistent with this model: p50^{cdc37} and FKBP52 occur simultaneously in Hsp90 complexes (97). Since PP5 had similarly been postulated to be mutually exclusive with regard to p50^{cdc37} (223), we examined PP5-Hsp90 complexes to determine if p50^{cdc37} occurred in Hsp90 heterocomplexes with PP5. For these assays, FLAG-tagged PP5 and/or HRI were (was) synthesized, and the reactions were mixed as described above. Proteins coadsorbing with PP5 were detected by autoradiography or Western blotting. Anti-FLAG immunoadsorptions of control reactions that were not programmed to synthesize FLAG-tagged PP5 retained no detectable Hsp90, p50^{cdc37}, or [^{35}S]HRI, indicating that these adsorptions were not compromised by nonspecific binding (Figure 15B, lanes 1, 4, 7, and 10). In contrast, immunoadsorptions of reactions programmed to synthesize FLAG-tagged [^{35}S]PP5 specifically coadsorbed endogenous Hsp90 and p50^{cdc37} (Figure 15B, lanes 2 and 8). This result confirmed the previously described association of Hsp90 with PP5 and provided novel evidence for the occurrence of p50^{cdc37} in heterocomplexes containing PP5. Consistent with this finding, the occurrence of p50^{cdc37} in PP5 complexes was dramatically enriched in the presence of

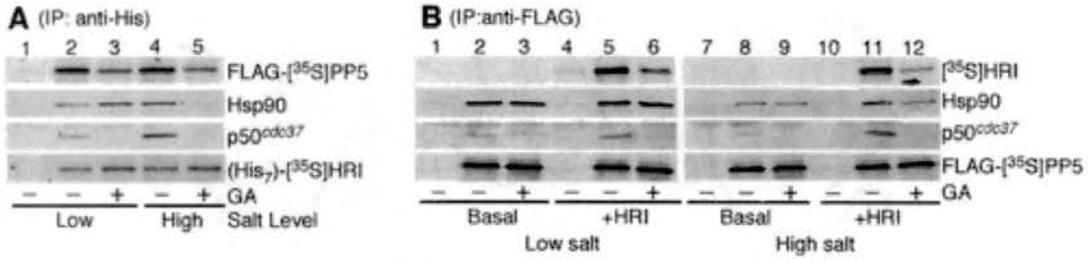

Figure 15. Effect of geldanamycin (GA) on the interaction of HRI with PP5 in reticulocyte lysate. (His_7)-[^{35}S]HRI was synthesized in reticulocyte lysate mixtures in the presence (+) or absence (-) of 10 μg/mL geldanamycin, and FLAG-[^{35}S]PP5 was synthesized in a separate lysate mixture for 30 min as described under "Materials and Methods". The reactions were then mixed in a 1:1 ratio with each other or with lysate lacking (His_7)-[^{35}S]HRI (**A**, *lane 1*) or lysate lacking FLAG-[^{35}S]PP5 (**B**, *lanes 1, 4, 7, and 10*) and incubated for another 20 min. Reaction mixtures were subsequently immunoabsorbed using anti-His-tag antibody resin (**A**) or M2 anti-FLAG-tag resin (**B**), followed by washing with PIPES buffers (10 mM, pH 7.2) containing no salt (***A***, *lanes 1-3*; **B**, *lanes 1-6*) or 500 mM NaCl (**A**, *lanes 4 and 5*; **B**, *lanes 7-12*), and analyzed as described under "Materials and Methods". (His_7)-[^{35}S]HRI and FLAG-[^{35}S]PP5, and endogenous Hsp90 and p50^{cdc37}, were visualized by autoradiography and Western blotting, respectively. The basal interactions of FLAG-[^{35}S]PP5 with Hsp90 and p50^{cdc37} in the absence of newly synthesized HRI are shown in panel **B**, *lanes 2, 3, 8, and 9*.

Hsp90-dependent HRI client (Figure 15B, lanes 5 and 11), indicating that Hsp90, PP5, and $p50^{cdc37}$ can bind to HRI molecules concomitantly.

The PP5/HRI Interaction Is Only Partially Sensitive to Hsp90 Inhibition by Geldanamycin-Geldanamycin is a well-characterized inhibitor of Hsp90 function that acts by binding within the ATP-binding pocket of Hsp90 (183, 234). This binding enforces an alternative Hsp90 conformation (99) that does not support the formation of high-affinity interactions between Hsp90-$p50^{cdc37}$ and Hsp90-dependent kinases, but has no effect on the basal interaction of $p50^{cdc37}$ with Hsp90 (97, 215). This binding also prevents the Hsp90-dependent recruitment of $p50^{cdc37}$ to kinase-Hsp90 heterocomplexes, indicating that $p50^{cdc37}$ binding to client kinases is regulated by Hsp90's ATP-dependent conformational switching (97, 215).

To test the hypothesis that PP5 binding to HRI was similarly regulated by Hsp90, reactions containing Hsp90-dependent (His_7)-[^{35}S]HRI molecules, which were generated in the presence or absence of geldanamycin, were mixed with reactions containing FLAG-[^{35}S]PP5. These reactions were incubated for 20 min, and HRI was then immunoadsorbed with anti-His-tag antibody resin. Immunoresins were washed with buffers lacking salt or with buffers containing 0.5 M NaCl, and the proteins that coadsorbed with HRI were then assessed by SDS-PAGE, autoradiography, and Western blotting.

As previously described (97, 215), geldanamycin inhibited the recruitment of $p50^{cdc37}$ to kinase-chaperone heterocomplexes and compromised the typical salt-resistant interaction of Hsp90 with its client kinase (Figure 15A). In contrast, geldanamycin only

partially inhibited (~50% loss relative to untreated reactions) the association of PP5 with client HRI molecules. Furthermore, the binding of PP5 to HRI that did occur in both geldanamycin-treated and untreated reticulocyte lysate was not sensitive to high-salt washing. Importantly, PP5 remained associated with HRI after high-salt washing of immunocomplexes isolated from geldanamycin-treated reticulocyte lysate, conditions which quantitatively remove Hsp90 from complexes with client HRI molecules. Thus, PP5's association with client kinases was quite different from that observed for the $p50^{cdc37}$: PP5's association with HRI was not quantitatively dependent upon geldanamycin-inhibitable Hsp90 function, and PP5 remained tightly bound to HRI independent of this function. However, similar to the interaction of $p50^{cdc37}$ with Hsp90 (97, 215), geldanamycin had no impact on the magnitude of the basal chaperone-chaperone interaction of PP5 with Hsp90 (Figure 15B, lanes 2 and 8 versus lanes 3 and 9).

This novel finding was reexamined using the reciprocal approach: anti-FLAG antibody resin was used to immunoadsorb PP5 from reticulocyte lysate reactions containing or lacking FLAG-tagged PP5 (Figure 15B, +HRI). Again, PP5's association with HRI was decreased by approximately 50% in geldanamycin-treated reticulocyte lysate, but HRI remained bound to PP5 when immunocomplexes were washed with high salt (Figure 15B, lane 12), a condition which strips Hsp90 from HRI complexes (Figure 15A, lane 5). Furthermore, the presence of geldanamycin blocked the association of $p50^{cdc37}$ with kinase-chaperone heterocomplexes (Figure 15B, lanes 6 and 12). The observation that PP5 remains bound to HRI under conditions that strip Hsp90 from immunocomplexes indicates that their interaction is not mediated solely through their common association with Hsp90.

The HRI binding site is located in the TPR domain of PP5-Studies by different groups have already shown that the TPR domain of PP5 is sufficient to mediate its interactions with multiple proteins (35, 42, 124, 138, 167). To test whether it similarly mediates the interaction between PP5 and HRI, we constructed the isolated TPR domain in the bacterial expression vector and compared the HRI-binding activity of the purified recombinant TPR domain with that of the full-length PP5. Recombinant FLAG-tagged TPR domain was mixed with RRL containing newly synthesized [^{35}S]HRI in the presence (Figure 16, lane 3) or absence (Lane 2) of geldanamycin. In parallel, full-length recombinant FLAG-PP5 was assayed in the same fashion (Lanes 4 and 5). In addition, nonspecific binding of [^{35}S]HRI was monitored by mixing the FLAG-protein-free buffer with the [^{35}S]HRI-containing RRL (Lane 1). Reaction mixtures were subsequently immunoadsorbed to anti-FLAG resin and the coadsorption of [^{35}S]HRI along with the endogenous Hsp90 were examined by autoradiography and Western blotting analyses. Consistent with its ability to bind to various proteins, the TPR domain of PP5 was also sufficient to interact with HRI at a comparative level to that with the full-length PP5, indicating that the HRI-binding motif is located in the TPR domain of PP5. Supporting this hypothesis, we detected no HRI-binding activity in the catalytic domain of PP5 which was obtained from the limited trypsinolysis (data not shown). Also, the TPR domain interacted with HRI in the same partial GA-sensitive fashion as did the full-length PP5, further strengthening the hypothesis that the HRI-binding activity, possibly a combination of both Hsp90-dependent and independent events, exists solely in the TPR domain of PP5. Furthermore, similar to the interaction between PP5 and Hsp90, GA had

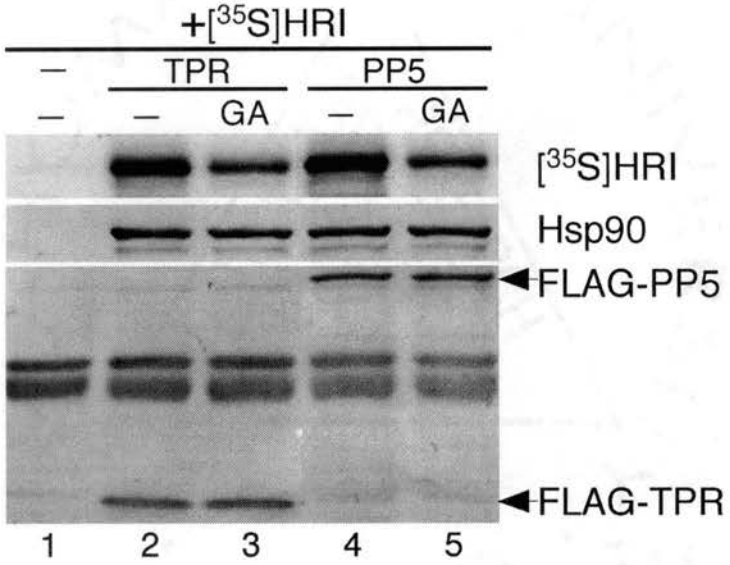

Figure 16. Interaction of the TPR domain of PP5 with HRI in reticulocyte lysate. [^{35}S]HRI was synthesized in reticulocyte lysate in the presence (*lanes 3 and 5*) or absence (*lanes 2 and 4*) of 10 μg/mL geldanamycin for 30 min as described under "Materials and Methods". Reaction mixtures containing [^{35}S]HRI were then mixed at a 1:1 ratio with normal heme-supplemented rabbit reticulocyte lysate containing (*lanes 3 and 5*) or lacking (*lanes 2 and 4*) 10 μg/mL geldanamycin with no additions (*lane 1*) or with the addition of 50 μg/mL purified recombinant wild type (His_6)-FLAG-PP5 (*lanes 4 and 5*) or (His_6)-FLAG-TPR of PP5 (*lanes 2 and 3*). After a 20-min incubation, reactions were absorbed to anti-FLAG-tag antibody resin and analyzed as described under "Materials and Methods". (His_6)-FLAG-tagged PP5 or TPR, [^{35}S]HRI, and Hsp90 were visualized by Coomassie blue staining, autoradiography, and Western blotting, respectively.

no effect on the basal interaction of the TPR domain with Hsp90. Therefore, the TPR domain of PP5 appears to mediate its interactions with both the partner Hsp90 and the putative client HRI.

The Geldanamycin-resistant binding site of PP5 resides in the N-terminal heme-binding domain of HRI-Besides the two conserved kinase subdomains (N-terminal and C-terminal kinase lobes) HRI contains three additional unique regulatory domains/regions, an N-terminal heme-binding domain (HBD), a kinase-insertion sequence (KIS) located between the two kinase lobes, and a short tail sequence at the C-terminus (Chapter II, Figure 7A) (32, 192, 247). We have previously located the Hsp90 binding sites to the HBD and N-lobe of HRI and that of $p50^{cdc37}$ to the N-lobe only (Chapter II, Figure 7B and C). Considering the different behavior of PP5 from $p50^{cdc37}$ with regard to the GA-sensitivity of their interactions with HRI, we hypothesize that they recognize topologically different regions of HRI. To test such a hypothesis, four different His-tagged HRI domains (except the C-terminal tail) were synthesized separately in RRL with concomitant radiolabeling with [^{35}S]Met, which were then mixed with RRL containing [^{35}S]-labeled FLAG-PP5. Reaction mixtures were subsequently immunoadorbed to anti-His resin, and the coadsorption of FLAG-[^{35}S]PP5 as well as the endogenous Hsp90 and $p50^{cdc37}$ were examined through autoradiography and Western blotting analyses, respectively (Figure 17A). To assess the nonspecific binding of FLAG-[^{35}S]PP5, blank RRL lacking TnT expression vector was mixed with the FLAG-[^{35}S]PP5-containing RRL, followed by the same immunoadsorption procedures. Consistent with our hypothesis, PP5 interacted specifically with the HBD of HRI,

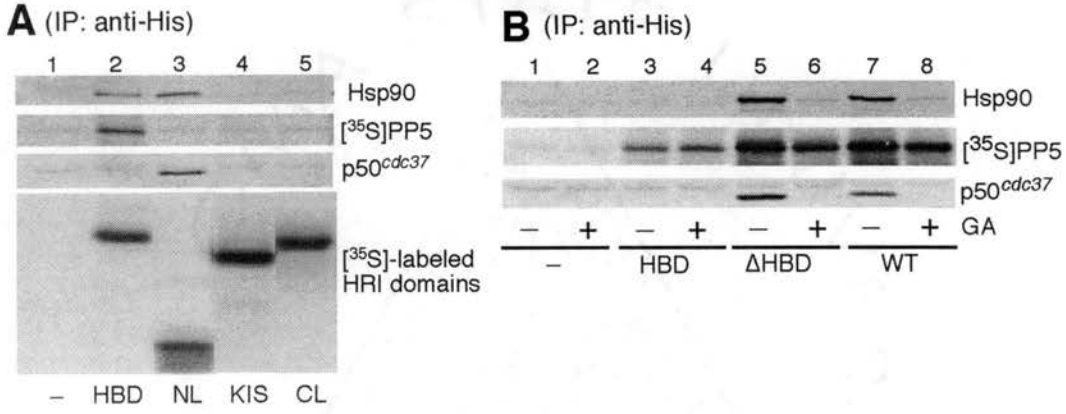

Figure 17. Interaction of the HRI domains with PP5 in reticulocyte lysate. **A**) Individual His-tagged HRI domains (HBD, the heme-binding domain; NL, the N-terminal kinase lobe; KIS, the kinase insertion sequence; CL, the C-terminal kinase lobe) were synthesized and radiolabeled with [^{35}S]-Met in separate TnT reticulocyte lysate reaction mixtures for 30 min as described under "Materials and Methods". They were then mixed at a 1:1 ratio with TnT reticulocyte lysate containing newly synthesized FLAG-[^{35}S]PP5 and incubated for 20 min. A mock reticulocyte lysate reaction lacking the His-tagged HRI domain was similarly assembled and mixed with an equal volume of FLAG-[^{35}S]PP5-containing lysate to assess the nonspecific binding of coadsorbed proteins (*lane 1*). Resulting lysate mixtures were subsequently immunoadsorbed to anti-His-tag antibody resin and analyzed as described under "Materials and Methods". [^{35}S]-labeled His-tagged HRI domains and FLAG-PP5, coadsorbed endogenous Hsp90 and p50^{cdc37} were visualized by autoradiography and Western blotting analyses, respectively. **B**) Wild type HRI, ΔHBD (HRI lacking the N-terminal heme-binding domain) and HBD of HRI were synthesized and radiolabeled with [^{35}S]-Met in separate TnT reticulocyte lysate reactions in the presence (*even-numbered lanes*) or absence (*odd-numbered lanes*) of 10 μg/mL geldanamycin for 30 min as described under "Materials and Methods". Two mock reactions (without cDNA template) containing (*lane 2*) or lacking (*lane 1*) geldanamycin were also similarly assembled. They were then mixed at a 1:1 ratio with TnT reticulocyte lysate synthesizing FLAG-[^{35}S]PP5 which contained (*even-number lanes*) or lacked (*odd-numbered lanes*) 10 μg/mL geldanamycin and incubated for 20 min. Resulting mixtures were subsequently immunoadsorbed to anti-His-tag antibody resin and analyzed as described under "Materials and Methods". Coadsorption of FLAG-[^{35}S]PP5 and endogenous Hsp90 and p50^{cdc37} was analyzed by autoradiography and Western blot, respectively.

but not with the N-lobe of HRI which is recognized by $p50^{cdc37}$, or KIS or C-lobe of HRI.

Because Hsp90 binds to HBD (Chapter II, Figure 7), it is possible that the interaction between PP5 and HBD is mediated indirectly through their common associations with Hsp90. To test this possibility, we treated the RRL reaction mixture containing (His_6)-HBD and FLAG-[^{35}S]PP5 with geldanamycin, immunoadsorbed it to anti-His resin in the presence of high salt, and examined the coadsorption of FLAG-[^{35}S]PP5 and endogenous Hsp90 through autoradiography and Western blotting analyses, respectively (Figure 17B, lanes 3 and 4). As the controls, wild type HRI (Lanes 7 and 8) and a deletion mutant lacking the HBD (ΔHBD) (Lanes 5 and 6) were also analyzed for their abilities to bind FLAG-[^{35}S]PP5 under the same conditions. Nonspecific binding of FLAG-[^{35}S]PP5 was similarly assessed as described in the previous experiments. Consistent with our early observations (97, 99), geldanamycin treatment in conjunction with high salt washing of the immunopellet almost completely stripped Hsp90 from the wild type HRI and the ΔHBD mutant (Lanes 6 and 8 versus 5 and 7, respectively). Again, the same partial disruption of the interaction of PP5 with HRI by geldanamycin was also observed. However, surprisingly, we also detected specific interactions between PP5 and the ΔHBD mutant of HRI, which, lacking the HBD, was predicted to be incapable of binding PP5. Moreover, its interaction with PP5 exhibited the same partial sensitiveness to geldanamycin treatment. Therefore, contrary to our hypothesis, additional PP5-binding site(s) exist(s) in HRI outside the HBD. However, based on our failure to identify such binding site(s) in any of the remaining individual domains of HRI, it seems likely that it (they) is (are) formed between adjacent domains, none of which alone is sufficient to mediate the interaction. As to HBD, high salt wash alone seemed to be able

to remove all the Hsp90 molecules from it irrespective of geldanamycin treatment. However, although no detectable Hsp90 was observed in association with HBD under high salt wash, a specific interaction of PP5 with the HBD was still detected and, most importantly geldanamycin treatment had no effect on the magnitude of such an interaction. Therefore, our data suggested that HRI is recognized by PP5 at multiple sites with the HBD being the one that is resistant to geldanamycin and thus the nucleotide-regulated conformational switching of Hsp90. This observation helps to explain the partial disruption of the interaction between HRI and PP5 by geldanamycin as opposed to the complete abolishment of that between $p50^{cdc37}$ and HRI (Lanes 6 and 8 versus 5 and 7, respectively). However, the fact that geldanamycin failed to completely disrupt the interaction between PP5 and ΔHBD also brought up the possibility that more than one type of interactions exist between PP5 and its additional binding sites in HRI, those modulated, and not modulated, by the nucleotide-regulated conformational switching of Hsp90.

The Interaction of PP5 with HRI Requires the Association of PP5 with Hsp90-The interaction of PP5 with Hsp90 is modulated through the interaction of conserved positively charged amino acid side chains with the conserved EEVD motif at the C-terminus of Hsp90 (Chapter V, Figure 36) (194, 204). To determine whether the interaction of PP5 with HRI is mediated through its association with Hsp90, we examined whether PP5 containing mutations of these positively charged amino acid residues, PP5/K97A or PP5/R101A, that do not bind Hsp90 could interact with newly synthesized HRI. Purified recombinant His-tagged wild-type PP5 or PP5 mutants were added to

hemin-supplemented reticulocyte lysate and mixed with lysate containing newly synthesized HRI in the presence or absence of geldanamycin. While HRI was specifically coadsorbed from reticulocyte lysate containing wild-type PP5, little HRI was coadsorbed above the nonspecific binding control from lysate containing the PP5/K97A or PP5/R101A mutants (Figure 18). Again geldanamycin reduced the amount of HRI coadsorbing with PP5 by approximately 50%. In the presence of geldanamycin, the binding of HRI to the PP5 mutants was reduced to the level of the nonspecific background. The lack of interaction of the PP5 mutants with HRI further indicates that the binding of PP5 to HRI is specific and supports the notion that Hsp90 is responsible for targeting PP5 to maturing populations of HRI molecules.

Impact of PP5 Inhibitors: Okadaic Acid and Nodularin Induce Hyperphosphorylation of Transformed HRI-To examine the potential significance of the association of PP5 with immature/inactive HRI molecules in reticulocyte lysate, the effects of a number of phosphatase inhibitors on the Hsp90-dependent maturation, transformation, and activation of HRI were examined. (His_7)-[^{35}S]HRI was synthesized in reticulocyte lysate and subsequently matured in hemin-supplemented or heme-deficient lysate containing okadaic acid [PP5, IC_{50} = 7 nM (16)]. Okadaic acid had no effect on the electrophoretic mobility or kinase activity of HRI matured in hemin-supplemented lysate [wherein HRI does not undergo Hsp90-dependent transformation (not shown)]. As described previously (215, 246, 248), transfer of newly synthesized (His_7)-[^{35}S]HRI to heme-deficient reiculocyte lysate led to the generation of active HRI kinase molecules (TR), which

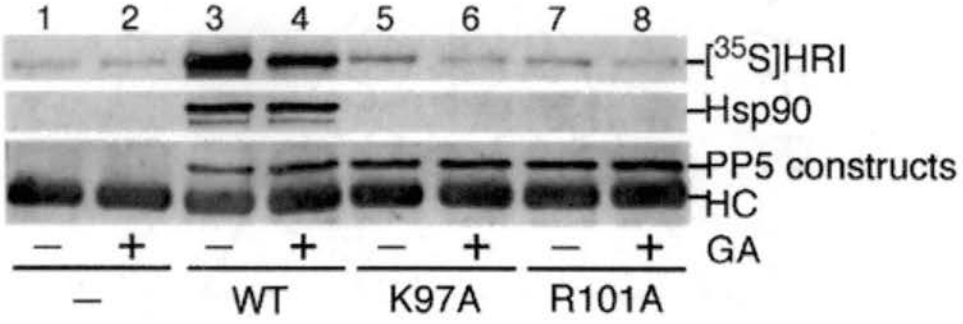

Figure 18. Effect of mutations that block the binding of PP5 to Hsp90 on the interaction of PP5 with HRI. [^{35}S]HRI was synthesized in reticulocyte lysate in the presence (*lanes 2, 4, 6, and 8*) or absence (*lanes 1, 3, 5, and 7*) of 10 μg/mL geldanamycin for 30 min, as described under "Materials and Methods". Reaction mixtures containing [^{35}S]HRI were then mixed at a 1:1 ratio with normal heme-supplemented rabbit reticulocyte lysate containing (*even-numbered lanes*) or lacking (*odd-numbered lanes*) 10 μg/mL geldanamycin with no additions (*lanes 1 and 2*) or with the addition of 50 μg/mL purified recombinant wild-type (His_6)-PP5 (*lanes 3 and 4*), (His_6)-PP5/K97A mutant (*lanes 5 and 6*), or (His_6)-PP5/R101A mutant (*lanes 7 and 8*). After a 20 min incubation, reactions were absorbed to anti-His-tag antibody resin and analyzed as described under "Materials and Methods". (His_6)-PP5 proteins, [^{35}S]HRI, and Hsp90 were visualized by Coomassie blue staining, autoradiography, and Western blotting, respectively. HC: antibody heavy chain.

exhibited retarded electrophoretic mobility relative to mature-competent HRI molecules (MC; Figure 19A, lane 2).

When compared to the activity of HRI that was matured and activated in control reactions, maturation and activation of HRI in reticulocyte lysate containing 500 nM okadaic acid led to the generation of HRI populations with increased kinase activity (2-fold more active than the control) (Figure 19A, lane 3). Incubation in the presence of okadaic acid also resulted in the production of HRI molecules with electrophoretic mobilities even slower than those typical of the transformation process, suggesting that the transformed HRI had become hyperphosphorylated (HP). Consistent with previous reports indicating that these mobility shifts are due to phosphorylation events (9, 137), treatment of samples with purified alkaline phosphatase generated HRI populations with fast electrophoretic mobilities similar to mature-competent HRI (not shown). Quantification of the amount of [^{35}S]HRI present in each lane confirmed that equivalent amounts of HRI were recovered from each reaction mixture. Thus, the observed increase in the phosphorylation of eIF2α represented an increase in the specific kinase activity of HRI.

Since HRI's dependence on Hsp90 chaperone machinery is conditional with respect to HRI's activation status, we next examined the impact of okadaic acid when applied to HRI populations 45 min *after* their Hsp90-dependent maturation and activation. In contrast to its application concomitant with maturation/activation, addition of okadaic acid after HRI maturation/activation did not lead to the enhanced activation of HRI's eIF2α kinase activity (Figure 19A, lane 4). In fact, addition of okadaic acid had a slight inhibitory effect on the kinase activity of preactivated HRI populations. In addition,

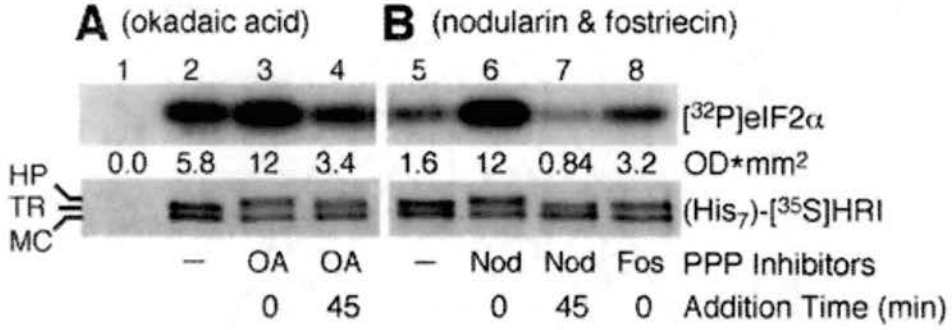

Figure 19. Effect of serine-threonine protein phosphatase inhibitors, okadaic acid, nodularin, and fostriecin, on HRI transformation and activation in heme-deficient reticulocyte lysate. (His_7)-[^{35}S]HRI was synthesized in reticulocyte lysate as described under "Materials and Methods". Reactions were then transferred to 7 volumes of heme-deficient normal rabbit reticulocyte lysate mixtures supplemented with (**A**) 500 nM okadaic acid-7,10,24,28-tetraacetate (inactive control for okadaic acid) (-, *lane 2*), 500 nM okadiac acid (OA, *lane 3*), or no drug (*lane 4*) or with (**B**) 500 nM nodularin (Nod, *lane 6*), 34 μM fostriecin (Fos, *lane 8*), or equivalent amounts of H_2O as their vehicle controls (*lanes 5 and 7*). The same volume of reticulocyte lysate containing no cDNA template was similarly transferred to heme-deficient lysate as the control for any nonspecific binding of lysate protein kinase activities (**A**, *lane 1*). After 45 min of incubation, 500 nM okadaic acid (**A**, OA, *lane 4*) or 500 nM nodularin (**B**, Nod, *lane 7*) was added to the maturation mixture lacking the initial supplementation of drugs, and the incubation was continued for an additional 20 min. (His_7)-[^{35}S]HRI was immunoadsorbed with anti-His-tag antibody resin, assayed for eIF2α kinase activity, and analyzed as described under "Materials and Methods". The amount of [^{32}P]eIF2α was quantified by scanning densitometry and expressed as optical density OD*mm^2 (numbers below the eIF2α panel). HP: hyperphosphorylated form of HRI; TR: transformed form of HRI; MC: mature-competent form of HRI.

almost no HRI with the very slow electrophoretic mobility diagnostic of HRI's hyperphosphorylation was observed when okadaic acid was added to reticulocyte lysate after most of the HRI had undergone its Hsp90-dependent transformation process. Nodularin (104, 105), a water-soluble phosphatase inhibitor with a structure similar to microcystin [IC_{50} for PP5 of 2.5 nm (16)], had effects comparable to those of okadaic acid on HRI's maturation/transformation and activity (Figure 19B, lanes 5-7).

The effect of a third phosphatase inhibitor, fostriecin, was also examined. Maturational reaction mixes were incubated in the presence of 34 μM fostriecin, a concentration which is inhibitory to PP2A (IC_{50} = 3.2 nM) but is well below its IC_{50} for PP1 (130 μM) and PP5 (700 μM) (16, 253). Addition of fostriecin caused only a slight stimulation of HRI's kinase activity and had little effect on HRI's electrophoretic mobility (Figure 19B, lane 8). This result suggested that PP2A did not mediate the effects of phosphatase inhibitors on HRI maturation/activation; nonetheless, PP1, as well as PP5, remained as a candidate phosphatase.

Taken together, the experiments described in Figure 19 indicated that the specific activity of HRI was enhanced only when phosphatase inhibitors were applied concomitant with Hsp90-dependent activation/maturation events. This concomitance implied that the compounds were acting at, or upon, this stage of HRI maturation/activation. To support this conclusion, we examined the impact of preventing HRI maturation/activation by the concurrent addition of the Hsp90 inhibitor geldanamycin with okadaic acid. Consistent with the results seen in Figure 19, HRI matured/activated in the presence of okadaic acid was 5-fold more active than HRI matured in the presence of okadaic acid-7,10,24,28-tetraacetate, an inactive analogue of

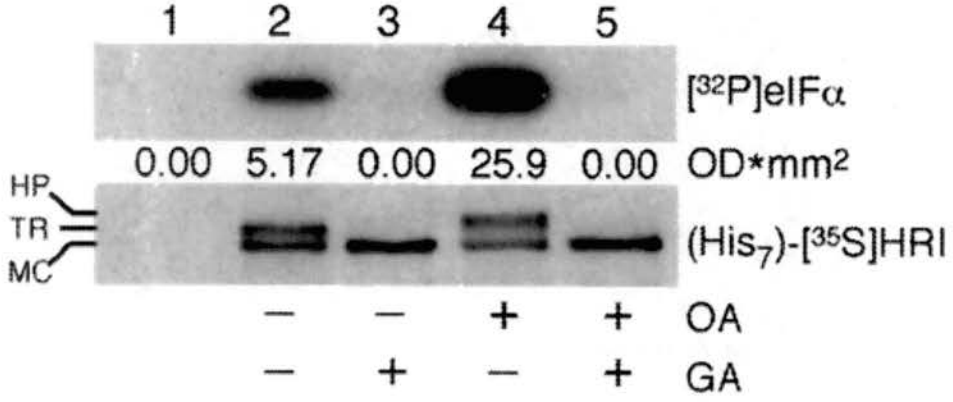

Figure 20. Effect of geldanamycin on the stimulation of HRI activation by okadaic acid. (His_7)-[^{35}S]HRI was synthesized in rabbit reticulocyte lysate as described under "Materials and Methods". (His_7)-[^{35}S]HRI was then transferred to 7 volumes of heme-deficient normal rabbit reticulocyte lysate mixtures supplemented with DMSO (vehicle control, *lane 2*), 10 μg/mL geldanamycin (GA, *lane 3*), 500 nM okadaic acid (OA, *lane 4*), or 10 μg/mL GA in combination with 500 nM okadaic acid (OA, GA, *lane 5*). An equivalent amount of reticulocyte lysate containing no cDNA template was similarly transferred to a heme-deficient lysate mixture containing no drug as the control for nonspecific binding of any reticulocyte lysate kinase activities (*lane 1*). After 60 min of incubation, (His_7)-[^{35}S]HRI was immunoadsorbed with anti-His-tag antibody resin, assayed for eIF2α kinase activity, and analyzed as described under "Materials and Methods". The amount of [^{32}P]eIF2α was quantified by scanning densitometry of autoradiograms and expressed as optical density OD*mm^2 (numbers below the eIF2α panel). HP: hyperphosphorylated form of HRI; TR: transformed form of HRI; MC: mature-competent form of HRI.

okadaic acid (Figure 20). However, HRI synthesized in the presence of geldanamycin was inactive irrespective of okadaic acid application. Thus, Hsp90 function was a prerequisite for the coincident stimulation of HRI kinase activity induced by okadaic acid.

Polyunsaturated Fatty Acids Inhibit HRI Transformation and Activation in a Dose-Dependent Fashion-To further test the hypothesis that PP5 function impacted the Hsp90-dependent maturation/activation of HRI, we examined the effect of arachidonic acid on this process. Arachidonic acid is a polyunsaturated fatty acid that stimulates the phosphatase activity of PP5 *in vitro* (36, 225). Application of this compound during HRI maturation/activation led to the generation of HRI molecules that were deficient in kinase activity (Figure 21A, lanes 3-7) relative to those produced in control reactions (Figure 21A, lane 2). This inhibition was dose-dependent: increasingly higher levels of arachidonic acid led to increasingly greater degrees of HRI inhibition. Like the effects seen for phosphatase inhibitors (Figure 19), the effects of the phosphatase activator arachidonic acid depended on HRI maturation/activation status: application of arachidonic acid after 45 min of HRI maturation/activation had only minor effects on the activity of HRI (Figure 21A, lanes 9-13). Additionally, the electrophoretic gel shift diagnostic of HRI transformation was inhibited by arachidonic acid, an effect consistent with its effect on kinase activity. Equivalent results were seen with linoleic acid, another polyunsaturated fatty acid activator of PP5 (not shown). In contrast, stearic acid, a saturated fatty acid that has little capacity to stimulate PP5's activity *in vitro* (36, 225), had little inhibitory effect on HRI's transformation and activation compared to similar concentrations of arachidonic or linoleic acid (Figure 21B). Thus, the impact of these

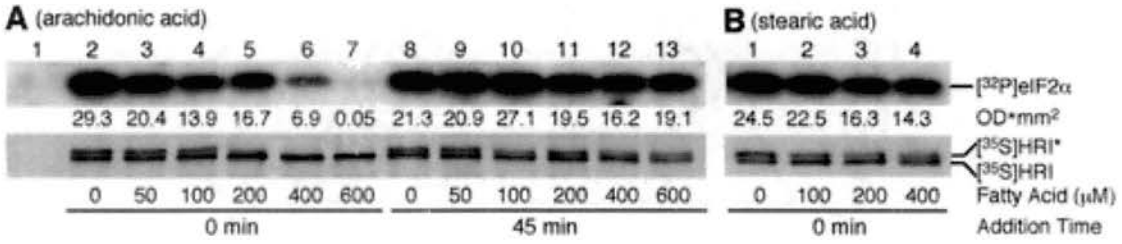

Figure 21. Effect of arachidonic acid (**A**) and stearic acid (**B**) on HRI transformation and activation in heme-deficient reticulocyte lysate. (His_7)-[^{35}S]HRI was synthesized in reticulocyte lysate as described under "Materials and Methods" and then transferred to 7 volumes of heme-deficient normal rabbit reticulocyte lysate mixtures supplemented with 50, 100, 200, 400, or 600 μM arachidonic acid (**A**, *lanes 3-7*), an equivalent amount of 95% ethanol as the vehicle control (**A**, *lane 2*), 100, 200, or 400 μM stearic acid (**B**, *lanes 2 to 4*), or an equivalent amount of methanol as the vehicle control (**B**, *lane 1*). (His_7)-[^{35}S]HRI was also incubated in a duplicate set of heme-deficient reticulocyte lysate mixtures lacking the initial supplementation of fatty acids (**A**, *lanes 8-13*), to which 50, 100, 200, 400, or 600 μM arachidonic acid (*lanes 9-13*) or 95% ethanol (*lane 8*) was added after 45 min of maturation, followed by incubation for another 20 min. An equivalent amount of reticulocyte lysate containing no cDNA template was similarly transferred to the heme-deficient reticulocyte lysate mixture containing no drug as the control for nonspecific binding of any protein kinase activities (**A**, *lane 1*). (His_7)-[^{35}S]HRI was immunoadsorbed with anti-His-tag antibody resin, assayed for eIF2α kinase activity, and analyzed as described under "Materials and Methods". The amount of [^{32}P]eIF2α was quantified by scanning densitometry and expressed as optical density OD*mm^2 (numbers below the eIF2α panel). [^{35}S]HRI*: transformed form of HRI; [^{35}S]HRI: mature-competent form of HRI.

fatty acid compounds was specific to the compound's structures rather than representing a nonspecific property of fatty acids *per se*.

Polyunsaturated Fatty Acids Disrupt the HRI/Hsp90/p50^{cdc37} Heterocomplex in a Dose-Dependent Fashion-Since polyunsaturated fatty acids inhibited the transformation and activation of HRI, we examined their effect on the composition of Hsp90-kinase heterocomplexes. (His_7)-[^{35}S]HRI and FLAG-[^{35}S]PP5 were synthesized in separate heme-replete reticulocyte lysate, after which they were mixed and various concentrations of fatty acids were added. The reaction mixtures were incubated for an additional 20 min, and the composition of chaperone-HRI complexes was subsequently characterized in coadsorption assays (Figure 22).

Addition of arachidonic or linoleic acid to lysate did not result in disruption of the basal (no client) interaction of p50^{cdc37} with Hsp90 (not shown). However, HRI heterocomplexes isolated from reticulocyte lysate treated with arachidonic or linoleic acid showed compromised association of Hsp90 and p50^{cdc37} with immature/mature-competent HRI molecules (Figure 22A, B). This effect was dose-dependent: increasingly higher levels of arachidonic or linoleic acid caused increasingly greater deficiencies in chaperone association (Figure 22A, B). In contrast, arachidonic and linoleic acid treatments had little effect on the interaction of PP5 with HRI. We noted, however, that high concentrations of both arachidonic and linoleic acid resulted in reproducible decreases in levels of (His_7)-[^{35}S]HRI recovered from rabbit reticulocyte lysate. To quantify chaperone losses in a manner that was compensatory for this loss of HRI, protein levels were quantified by densitometry, and the amounts of (His_7)-[^{35}S]HRI,

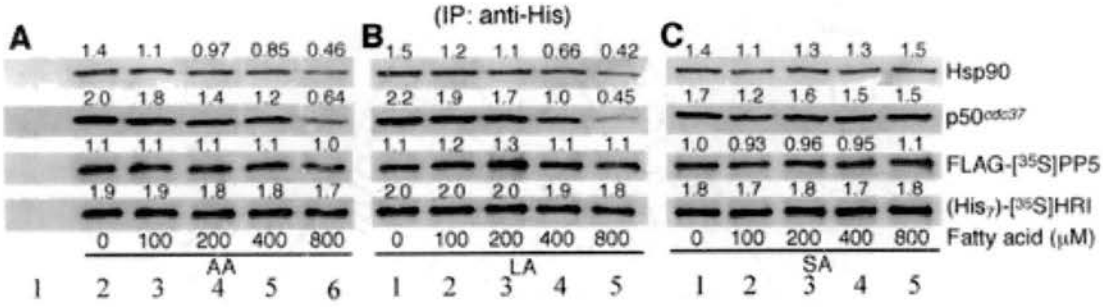

Figure 22. Effect of polyunsaturated fatty acids on the integrity of the HRI/Hsp90/p50^{cdc37}/PP5 heterocomplex. (His_7)-[^{35}S]HRI and FLAG-tagged [^{35}S]PP5 were synthesized in reticulocyte lysate mixtures as described under "Materials and Methods". The reactions were then mixed in a 1:1 ratio and incubated in the presence of 100, 200, 400, or 800 μM arachidonic acid (**A**, AA, *lanes 3-6*), linoleic acid (**B**, LA, *lanes 2-5*), stearic acid (**C**, SA, *lanes 2-5*), or their respective vehicle controls [**A**, 95% ethanol (*lane 2*); **B**, H_2O (*lane 1*); **C**, methanol (*lane 1*)]. The reticulocyte lysate mixture lacking the (His_7)-HRI template was similarly incubated with FLAG-[^{35}S]PP5-containing lysate as the control for nonspecific binding (**A**, *lane 1*). Reaction mixtures were immunoadsorbed with anti-His-tag antibody resin and analyzed as described under "Materials and Methods". (His_7)-[^{35}S]HRI and coadsorbed FLAG-[^{35}S]PP5, and coadsorbed Hsp90 and p50^{cdc37}, were visualized by autoradiography and Western blotting, respectively. The amount of each protein was quantified by scanning densitometry and expressed as OD*mm^2 (numbers above each panel).

Hsp90, p50^{cdc37}, and PP5 are presented in Figure 22. The data indicate that the relative levels of Hsp90 and p50^{cdc37}, but not PP5, associated with HRI were compromised and declined in concert in arachidonic or linoleic acid treated reticulocyte lysate. Finally, control experiments using stearic acid confirmed the specificity of the effect: this saturated fatty acid did not disrupt the association of Hsp90 and p50^{cdc37} with HRI (Figure 22C).

Discussion:

Work done in numerous laboratories over the past 2 decades has firmly established that phosphorylation plays an essential role in regulating the function of HRI. Nevertheless, the question of whether the function of HRI might be regulated by reversible phosphorylation has remained unclear. In this report, we present for the first time biochemical and pharmacological evidence that the Hsp90-dependent transformation and activation of HRI in response to heme-deficiency are regulated by the activity of a phosphatase, and the data indicate that the phosphatase is likely PP5.

In support of this hypothesis, we find that PP5 is an Hsp90 cohort that occurs in complexes with the Hsp90-dependent kinase HRI. The interaction of PP5 with HRI is mediated by its TPR domain and dependent upon Hsp90, as mutations in PP5 that inhibit its ability to bind Hsp90 (194, 204) also block the interaction of PP5 with HRI (Figure 18). This effect suggests that Hsp90 plays a direct role in recruiting PP5 to HRI heterocomplexes and would be consistent with PP5's direct association with Hsp90 in the absence of the Hsp90 client.

The interaction of PP5 with HRI occurs in a manner that is distinct from that described previously for other Hsp90 cochaperones (97, 215), as the binding of PP5 molecules to HRI is only partially (50%) inhibited by geldanamycin. The observation that PP5 coadsorbs with HRI in the presence of geldanamycin, despite the quantitative high-salt washing of Hsp90 from HRI/PP5 complexes, indicates that PP5 can interact directly with HRI. Such a direct binding site seems to be located in the unique regulatory heme-binding domain of HRI as it remains stably bound to PP5 even when its associated Hsp90 is completely removed by high salt wash (Fig. 17B). Geldanamycin has no effect on the magnitude of such an interaction, indicating that the binding affinity of PP5 for the heme-binding domain of HRI is not modulated by the nucleotide-regulated conformational switching of Hsp90. However, additional binding site(s) of PP5 in HRI seem(s) to exist as indicated by the observation that the deletion mutant of HRI (ΔHBD) which lacks the entire heme-binding domain still interacts with PP5. Like its interaction with the full-length HRI, PP5 binds to the ΔHBD mutant in the same partial geldanamycin-sensitive fashion, indicating that even within regions outside the heme-binding domain both direct and indirect binding sites for PP5 exist in HRI. Interestingly, these binding sites do not seem to be localized in any of the remaining single domains of HRI as no specific interactions were observed between them and PP5. Thus, it strongly indicates that they are formed instead topologically by adjacent domains of HRI. Nevertheless, the ability of mutations that inhibit the interaction of PP5 with Hsp90 to block the binding of PP5 to HRI indicates that the binding of PP5 to HRI is still modulated by Hsp90. Taken together, these results suggest that the interaction of Hsp90 with PP5 is required for the HRI binding site of PP5 to become accessible and that the binding of PP5 to HRI can be

initiated through the weak salt-labile interaction that occurs between Hsp90 and HRI in the presence of geldanamycin. However, it is clear that the interaction of PP5 with HRI maturation intermediates differs from that of the Hsp90-regulated cohorts p50^{cdc37} and p23: unlike the binding of p50^{cdc37} and p23 to Hsp90-dependent kinases (97, 215), the binding of PP5 to HRI is not quantitatively dependent upon Hsp90's nucleotide-dependent conformational switching, and it is likely to result from the multi-site recognition and interactions of PP5 with HRI.

Data presented in this paper indicate that PP5 and p50^{cdc37} can occur on the same Hsp90 chaperone machinery and that they can coexist in chaperone-client heterocomplexes. This conclusion derives from the observation that these Hsp90 cohorts co-immunoadsorb under various experimental conditions (Figure 15). Furthermore, expression of the Hsp90-client HRI enhances the association of p50^{cdc37} with PP5 immunocomplexes (Figure 15). The description here of concomitant binding of PP5 and p50^{cdc37} to Hsp90 and Hsp90-client heterocomplexes is consistent with our recent demonstration that p50^{cdc37} and the immunophilin FKBP52 form a novel four-component chaperone machine (97). However, the coincident occurrence of p50^{cdc37} on Hsp90 complexes with the TPR-containing cohorts FKBP52 and PP5 is inconsistent with studies that suggest that these components compete for adjacent docking sites on Hsp90 (170, 171, 223). As we have discussed previously for the four-component Hsp90-p50^{cdc37}-FKBP52-p23 machine (97), the discrepancy between our findings and *in vitro* competition assays may reflect the existence of a dimeric Hsp90 machine (28, 142, 156, 176, 182) in which each Hsp90 subunit binds a different Hsp90 cohort.

Data presented here indicate that one (or more) protein phosphatase(s) has (have) the potential to act upon HRI's Hsp90-dependent activation process. This conclusion derives from the finding that application of the phosphatase inhibitors okadaic acid and nodularin to HRI maturation/activation reactions leads to the generation of *hyperactive* HRI populations (Figure 19). Consistent with this finding, application of compounds that activate PP5 *in vitro* (arachidonic and linoleic acid) leads to the generation of *hypoactive* HRI populations (Figure 21A). The identities of these agents and their effective concentrations are consistent with the pharmacological profile of PP5 (16, 36, 225). While the concentration of free arachidonate has been reported to reach 180 μM during brain ischemia (168), we feel that it would be premature to propose that the supraphysiological concentrations of unsaturated fatty acids used in this study act similarly *in vivo*. In fact, it has been postulated that the high micromolar concentration of polyunsaturated fatty acids required to activate PP5 *in vitro* is due to their poor solubility in aqueous solution, and the inability of saturated long chain fatty acids to do so is a result of their even lower solubility under the same condition. This speculation has recently been confirmed by Ramsey *et al* as the more water-soluble derivatives of the long chain fatty acids, their CoA-esters, were able to activate PP5 at physiological concentrations. More importantly, both saturated and unsaturated fatty acyl-CoA esters were able to activate PP5 at similar concentrations (193). Therefore, the inability of the control stearic acid to have the same effect on HRI phosphorylation level and kinase activity as arachidonic and linoleic acid may simply result from the extremely low concentration of soluble stearic acid in rabbit reticulocyte lysate. Future experiments employing the putative physiological activators of PP5, the fatty acyl-CoA esters, as well

as the appropriate controls should confirm our data presented here. Nonetheless, utilization of these agents enables us to manipulate PP5 activity in reticulocyte lysate-based assays, and overcomes many of the limitations inherent to the study of PP5, notably, PP5's autoinhibition (36, 121, 225) and the potential requisite roles of trans-acting PP5 modulators, partners, or competitors. In addition, supporting our hypothesis on the functional regulation of HRI by PP5, we do note that addition of the recombinant PP5 catalytic domain to HRI transformation reactions has effects qualitatively similar to those of fatty acid stimulators: resultant HRI populations have decreased kinase activity.

The phosphatase(s) responsible for these effects can only impact HRI function concomitant with HRI maturation/transformation processes: the pharmacological response of HRI to phosphatase inhibition/activation is wholly dependent upon the timing drug application (Figures 19 and 21). Thus, we propose two models for the action of PP5 on HRI maturation.

In the first model, PP5 may dephosphorylate HRI during its maturation/activation. This interpretation is supported by the finding that HRI with retarded electrophoretic mobility can be detected in Hsp90 heterocomplexes when the phophatase inhibitor NaF was present during the immunoadsorption protocol. Furthermore, this interpretation is consistent with our recent demonstration that phosphorylation of Hsp90-dependent kinases is one possible mechanism for generating Hsp90-independent kinase populations. For the Src-family kinases, Lck and Hck, point mutations of their C-terminal regulatory tyrosines generate kinase populations which show continuous requirements for Hsp90 function (12, 98, 213); however, their wild-type counterparts do not show such a continuous requirement and, instead, flow vectorially from Hsp90-dependent to Hsp90-

independent forms. Similarly, HRI is released from its continuous requirement for Hsp90 function by conditions that activate its kinase activity, and release correlates with kinase autophosphorylation (215, 246). Furthermore, Hsp90 function is required for activation and phosphorylation of Mos, but once activated, Mos no longer requires Hsp90 to support its function (75). However, while circumstantial evidence suggests that kinase phosphorylation may represent an important determinant of kinase maturity and Hsp90 independence, direct correlations between Hsp90 dependence and specific kinase phosphorylation sites have not yet been documented. Nonetheless, these evolving models describing Hsp90's support of protein structure suggest that phosphorylation is an important determinant of Hsp90 dependence, and the physical and functional involvement of PP5 in these processes is consistent with these models. In this model of HRI dephosphorylation coincident with the maturation/activation process, PP5 might modulate HRI's response to activating stimuli. Such modulation could be postulated to be an important tuning of translational repression given HRI's action on eIF2α and the potency of translational inhibition by this mechanism.

As an alternative model, PP5 may act directly upon Hsp90-chaperone machinery to regulate its function(s). While Hsp90 is often described as the "signal-transduction chaperone", due to its apparent specificity for signal transduction proteins, and the Hsp90 chaperone machinery is often described as "regulating" the function of its clients, few characterizations have attempted to discriminate between housekeeping roles for Hsp90 versus regulated roles for Hsp90 in signal transduction. Regarding this last possibility, our data could result from the direct action of PP5 on Hsp90 and/or its partner cochaperones. Consistent with this model, Hsp90 (65, 109, 132, 133, 252, 255), p50^{cdc37}

(21), p60/Hop (131, 135), and FKBP52 (157) are phosphoproteins, and recent studies suggest that the phosphorylation status of Hsp90 machinery may be linked to its chaperoning function (20, 106, 131, 135, 154, 157, 239, 268). Thus, PP5 might regulate Hsp90 function by modulating the phosphorylation status of one or more components of the Hsp90 machine. Models postulating regulated Hsp90 function are further supported by the apparent specificity of cohorts for individual Hsp90 clients (56, 199). This evidence for modulation of Hsp90 function is consistent with the finding that PP5 overexpression negatively regulates glucocorticoid-mediated growth arrest *in vivo* (272) and our observation that PP5 plays a negative role in HRI's Hsp90-dependent maturation/activation.

This negative role for PP5 in HRI's maturation/activation contrasts sharply with the previously described positive role that another Hsp90 partner protein $p50^{cdc37}$ plays during this process (215). Thus, PP5 and $p50^{cdc37}$ have opposing influences upon the Hsp90-dependent process of HRI maturation and activation, yet both can coexist in Hsp90-client kinase complexes. Within the context of regulated Hsp90 function, it is reasonable to speculate that these opposing effects must somehow be coordinated during proper execution of Hsp90 function *in vivo*. Furthermore, it is likely that coordination of the opposing effects of these two proteins plays a role in the regulation of the activity of other Hsp90-dependent signal transduction proteins in addition to HRI.

Irrespective of the finer details by which PP5 may act, our data indicate that this Hsp90 partner protein plays a negative role in regulating the activity of an Hsp90 client during its Hsp90-dependent maturational process. The finding that PP5 down-regulates

an Hsp90-dependent process supports models for regulated Hsp90 function and describes a novel potential substrate for PP5 function *in vivo*.

CHAPTER IV

Domain mapping and functional dissection of $p50^{cdc37}$

Introduction:

Originally identified in budding yeast as one of the START mutants arrested at the G1 phase (74, 197), the protein product of CDC37 gene in different species has been under extensive genetic and biochemical investigations over the past two decades. Its ability to control the cell cycle in yeast lies, at least partially on the fact that it functionally regulates both the stability and cyclin-binding affinity of cdc28, one of the key cyclin-dependent protein kinases (CDK) involved in cell cycle progression in eukaryotic cells through some unknown mechanism (71, 86). Along the same line of being important in cell cycle regulation in yeast, the CDC37 gene product has also been found to genetically interact with several other kinases including Mps1, a kinase required for spindle pole body duplication (214), Kin28, a putative CDK member of the $p34^{cdc2}$ family (251) and casein kinase II, an ubiquitous kinase also required for cell cycle progression in yeast (87) which were compromised in either their levels or activities or both in yeast strains with *cdc37* mutations. In *Drosophila*, genetic studies put a functional link between CDC37 and the sevenless receptor tyrosine kinase, suggesting that it is involved in mitogen-activated protein kinase (MAPK) pathway as well (48).

Unlike yeast and *Drosophila*, the vertebrate homolog of Cdc37 has long been known as the 50-kDa phospho-protein associated with the viral oncogenic protein kinase $pp60^{v\text{-}src}$ in the same complex with the 90-kDa heat shock protein Hsp90 (20, 22, 169, 256) before its identity was revealed in recent years (51, 175, 235). Subsequent studies have functionally linked it to a wide range of proteins most of which belong to the

eukaryotic protein kinase family. Examples include cyclin-dependent protein kinases, such as: CDK4 (51, 129, 235), CDK6 (129, 139) and CDK9 (69, 166); members of Src tyrosine kinase family such as $pp60^{v\text{-}src}$, Lck and Hck (59, 97, 175, 211); casein kinase II (87, 122); Raf-1 (89, 245); mitogen-activated protein kinase MOK (158); heme-regulated eIF2α kinase HRI (215); IκB kinase IKK (29); and most recently Akt (8). Significantly, all these kinases are known clients of Hsp90 which coexists in all the Cdc37/kinase heterocomplexes. As a result, it is dubbed the "kinase-specific cohort of Hsp90". However, with its new client proteins emerging rapidly, it appears that the substrate specificity of Cdc37 may be broader than was envisioned previously. Cdc37 has recently been found in association with the androgen receptor (77, 195) and reverse transcriptase (254) in mammalian systems both of which depend on the functional Cdc37 for their activities. Nonetheless, protein kinases still represent the vast majority of Cdc37 clients.

Working closely together, mammalian Cdc37 interacts directly with its partner Hsp90. This binding site has been assigned to the C-terminal half of the human Cdc37 (165-378) resulting from an arbitrary bisection (215). The same bisection also generated an N-terminal half of Cdc37 (1-164) which binds to several client proteins independently of Hsp90 (89, 215, 254). Therefore, mammalian Cdc37 seems to possess direct binding sites for the clients and partner Hsp90 at the N-terminal and C-terminal regions, respectively. Although it seems to agree with the model in which Cdc37 functions as the "kinase-targeting subunit of Hsp90" (89, 235), studies in our and other labs argue against such a simple role of Cdc37 as being the passive "tethering" adaptor between Hsp90 and the clients. First, under low ionic condition, geldanamycin (GA), an Hsp90-specific inhibitor, abolished the binding of Cdc37 to its client HRI completely while leaving that

of Hsp90 to HRI intact (97), indicating that 1) Hsp90 has the ability to bind client kinases independently of Cdc37 and 2) rather than rigidly bridging between Hsp90 and the clients, Cdc37 undergoes conformational change induced by nucleotide-modulated conformational switching of Hsp90 that affects its binding affinity for the clients. Second, overexpression of the N-terminal half of Cdc37, which is unable to bind Hsp90, similarly enhanced the binding of Hsp90 to Hck, although to a lesser extent than does the full length Cdc37, thus indicating that Cdc37, rather than simply recruiting Hsp90 to the clients, actually alters the clients allosterically in preparation for their high affinity binding to Hsp90 (211). Recently, a novel domain structure of mammalian Cdc37 has been proposed by Scholz *et al* based primarily on sequence alignment analyses. In contrast to the arbitrary bisection, they predicted a three-domain structure for the mammalian Cdc37 and showed that its middle domain (145-264 of human Cdc37) bears the Hsp90-binding site. However, no specific functions of the N-terminal and C-terminal domains of Cdc37 were suggested or identified (212).

Contrary to its mammalian homologues, yeast Cdc37 has proven contradictory regarding its ability to bind Hsp90 and the clients. Although Abbas-Terki *et al.* recently reported the detection of specific associations of yeast Cdc37 with Hsp90 and its putative client Ste11 (1), most attempts by other groups failed to observe such interactions (71, 86). It thus indicates a somewhat different mechanism by which the yeast Cdc37 functions *in vivo* relative to its mammalian homologues. In addition, the difference may also be expected based on the distant relationship of the yeast Cdc37 to its mammalian homologues at the amino acid sequence level. Yeast Cdc37 shares only 19% overall identity with its mammalian homologues, from which it differs considerably throughout

almost the entire sequence including the region that mediates Hsp90-binding by its corresponding mammalian homologues. Interestingly, the most conserved residues of Cdc37 are located at the N-terminal 30 or so residues, which are over 50% identical and 70% conserved among its homologues from yeast to human, suggesting that they are functionally important for some evolutionarily conserved activity of Cdc37 (51, 235). Consistent with such a hypothesis, previous studies in our lab have shown that the N-terminal eight amino acids of human Cdc37 are essential for its HRI-binding activity (215).

In order to better understand Cdc37 regarding its structure-function relationship, we attempted to unveil its true domain architecture, upon which further biochemical characterizations can be carried out. Utilizing the conventional limited protease-nicking technique in conjunction with the MALDI-TOF mass spectrometry analysis, we revealed a novel three-domain structure of Cdc37 that is slightly different from that proposed by Schulz *et al* (212). Biochemical characterizations assigned the kinase- and Hsp90-binding activities to its N-terminal and central domains, respectively. Additionally, we carried out alanine scanning site-directed mutagenesis at the N-terminus of human Cdc37, and identified four residues that are critical for its HRI-binding activity.

Materials and Methods:

Protein purification from E. coli-(His_6)-Cdc37 (in pQE32 expression vector) (215) was overexpressed in M15[pREP4] *E. coli* strain for 3 hr at 30 °C. Cells were harvested and lysed in 50 mM NaH_2PO_4 buffer (pH 8.0) containing 300 mM NaCl and 5 mM imidazole with sonication. Cell lysate was treated with DNase (5 μg/ml) and RNase A (10 μg/ml)

for 15 min on ice and centrifuged at 10,000×g for 30 min at 4 °C. Supernatant was mixed with 500 µl Ni^{2+}-NTA resin (Qiagen) for 2 hr at 4 °C, followed by washing with 50 mM NaH_2PO_4 buffer (pH 8.0) containing 300 mM NaCl and 20 mM imidazole. (His_6)-Cdc37 was eluted by 2 ml of 50 mM NaH_2PO_4 buffer (pH 8.0) containing 300 mM NaCl and 250 mM imidazole, and then dialyzed against 10 mM PIPES buffer (pH 7.2) containing 150 mM NaCl.

In-gel trypsin digestion-Gel pieces containing the major proteolytic fragments of (His_6)-Cdc37 were washed with water and 50% acetonitrile (ACN) sequentially for 15 min each. Gel pieces were subsequently dehydrated by a brief soaking in 100% ACN, which was then replaced by 50 mM NH_4HCO_3 to allow rehydration. Afterwards, the same volume of ACN was added and gel pieces were washed with 50% ACN/25mM NH_4HCO_3 for 15 min. Washes were repeated until little residual Coomassie blue is visible. Gel pieces were dried down completely in a speed vacuum centrifuge, rehydrated in 10 mM DTT/100 mM NH_4HCO_3 for 45 min at 56 °C (reduction), followed by 30 min incubation in 55 mM iodoacetamide/100 mM NH_4HCO_3 at room temperature (alkylation). They were then dried down again and rehydrated in 30 µl of 12.5 ng/µl trypsin (Promega, sequencing grade) prepared in 50 mM NH_4HCO_3 and 5 mM $CaCl_2$. After incubation at 37 °C for 12 hr or longer, the digestion fluid was removed and stored in separate tubes. Peptides trapped inside the gel pieces were further extracted with 50 µl of 50% acetonitrile/0.1% TFA twice, both of which was then combined with the digestion fluid removed earlier. Pooled peptide mixtures were subsequently concentrated in a speed vacuum centrifuge to a final volume of 10-20 µl.

MALDI-TOF mass spectrometry analysis-Saturated α-cyano-4-hydroxycinnamic acid (matrix) was prepared in 50% acetonitrile/0.1% TFA. 1.0 μl aliquot of the concentrated peptide mixtures was spotted onto the MALDI plate, which was immediately covered by the same volume of saturated matrix solution. After drying completely, peptide samples were analyzed using the Voyager "DE-PRO" matrix-assisted laser desorption-ionization time-of-flight mass spectrometer (MALDI-TOF) (Applied Biosystems). Mass spectra were acquired in both linear and reflector modes, and compared to the predicted peptide mass fingerprints of (His_6)-Cdc37 generated by trypsinolysis.

Immunoprecipitations from RRL-Various Cdc37 constructs were synthesized and radiolabeled with [^{35}S]Met in TnT RRL for 30 min at 30 °C, followed by 10 min chase with the addition of 60 μM protein synthesis initiation inhibitor aurintricarboxylic acid. To study their Hsp90-binding properties, they were either directly absorbed to the anti-(His_5) antibody-coupled agarose resin or coadsorbed to that bound with the monoclonal anti-Hsp90 antibody 8D3. Their interactions with Hsp90 were then assessed by Western blot or autoradiography, respectively. To examine their kinase-binding activities, non-His-tagged versions of the domains were mixed with the TnT RRL containing newly synthesized (His_7)-[^{35}S]HRI, coadsorbed by the anti-(His_5) antibody and then analyzed by autoradiography. Immunoresins were washed 4 times with 10 mM PIPES buffer (pH 7.2) containing 150 mM NaCl and 0.5% Tween-20.

Limited protease nicking in vitro-Purified recombinant (His_6)-Cdc37 was mixed with various concentrations of TPCK-treated trypsin (Sigma) in 10 mM Tris-HCl buffer (pH 7.4) containing 150 mM NaCl, 4 mM $CaCl_2$ and 0.1 mM EDTA. Digestion was carried out either on ice for 6 min or at 37 °C for 30 min, and immediately stopped by boiling in SDS sample buffer. Protein/enzyme ratio for trypsin digest (g/g) ranged from 2000:1 to 250:1 at 37 °C and from 200:1 to 10:1 on ice. Chymotrypsin digest was carried out at 37 °C for 20 min in the same buffer as described above and at similar protein/enzyme ratios to that for trypsin.

To affinity purify the N-terminal tryptic fragments of (His_6)-Cdc37, reactions were stopped by adding trypsin inhibitor (Sigma) at an inhibitor/trypsin ratio of 1:4 (g/g), 1% SDS and 100 mM β-mercaptoethanol (as the final concentrations). The reaction mixture was further diluted 5 times with NaH_2PO_4 buffer (50 mM final concentration, pH 8.0) to reduce the concentrations of SDS and β-mercaptoethanol, which would otherwise interfere with the binding of His-tagged fragments to Ni^{2+} resin. Diluted reactions were absorbed to Ni^{2+}-NTA resin (Qiagen) for 1 hr at room temperature, which were then washed 4 times with 50 mM NaH_2PO_4 buffer (pH 8.0) containing 1 M NaCl, 1% Triton X-100 and 8 M urea. Ni^{2+}-NTA resin was subsequently washed twice with TBS before boiling in SDS sample buffer.

Limited protease nicking in RRL-Wild-type and mutant Cdc37 were synthesized and radiolabeled with [^{35}S]-Met in TnT RRL at 30 °C for 30 min and matured for 1 hr in the presence of 60 μM aurintricarboxylic acid. RRL reactions were chilled on ice and the desired concentrations of TPCK-treated trypsin (Sigma) were applied in 10 mM Tris-HCl

buffer (pH 7.4) containing 150 mM NaCl, 4 mM $CaCl_2$ and 0.1 mM EDTA. Digestion was carried out on ice for 6 min and immediately terminated by boiling in SDS sample buffer. Samples were then separated on SDS-PAGE and analyzed by autoradiography.

Construction of plasmids for Cdc37 domains-PCR fragments were generated using oligonucleotide primers corresponding to the border regions of each different domain of human Cdc37 coding sequence. PCR products were digested with appropriate restriction enzymes whose consensus sites were built in the oligonucleotide primers (NcoI site in the 5' primers and SacI or BamHI in the 3' primers), and subsequently ligated into the corresponding sites of the expression vectors pSP64T and pSP64TL. This work was done by Wenjun Huang, who was a research technician in our lab during the course of this study.

Site-directed mutagenesis-Point mutations at the N-terminus of Cdc37 were introduced using standard PCR-based method. Seven sets of oligonucleotides (upper primers) corresponding to the N-terminus of human Cdc37 and containing the desired X-A mutations at the specific codons were synthesized to include a short 5' anchoring sequence with a BglII and NcoI sites immediately preceding the Cdc37 coding sequence. Another anti-sense oligonucleotide (lower primer) which corresponds to the region approximately 250 bp downstream of the unique DraIII site in the coding sequence of Cdc37 was used as the lower primer. PCR reactions were carried out using the wild-type pSP64T-Cdc37 (215) plasmid as the template. The PCR products (850 bp) were digested with BglII/DraIII and the resulting DNA fragments (550 bp) were used to replace the

corresponding region of the wild-type pSP64T-Cdc37 plasmid. Desired mutations were subsequently confirmed by sequencing. To introduce the N-terminal (His_6)-tag to Cdc37 mutants, their entire coding sequences were digested from the pSP64T vector as NcoI/EcoRI fragments and cloned into the corresponding sites of the pSP64TL vector (97).

Results:

1) Domain mapping of Cdc37:

Early studies in our and other laboratories have shown that the kinase-binding site of Cdc37 resides in its N-terminal half (Cdc37/ΔC) whereas the Hsp90-binding site is located in its C-terminal half (Cdc37/ΔN) (89, 215). However, this bisection of Cdc37 was rather arbitrary based on little knowledge of its true domain architecture. Here in this report, we attempted to determine the authentic domain structure of Cdc37 by limited protease nicking technique in conjunction with MALDI-TOF mass spectrometry analysis.

a) Generating the domain map: limited proteolytic fingerprint of purified recombinant Cdc37-Recombinant (His_6)-Cdc37 purified from *E. coli* was subjected to limited proteolysis *in vitro* with a wide range of concentrations of trypsin. The idea is to find the optimal condition under which only the most flexible and solvent accessible inter-domain regions of Cdc37 are cleaved, thus to generate a domain map of Cdc37. As shown in Fig. 23A, a nice proteolytic fingerprint of Cdc37 was generated at a protein/enzyme ratio (g/g) of 1: 200 on ice. It consisted of four major proteolytic fragments besides the full length

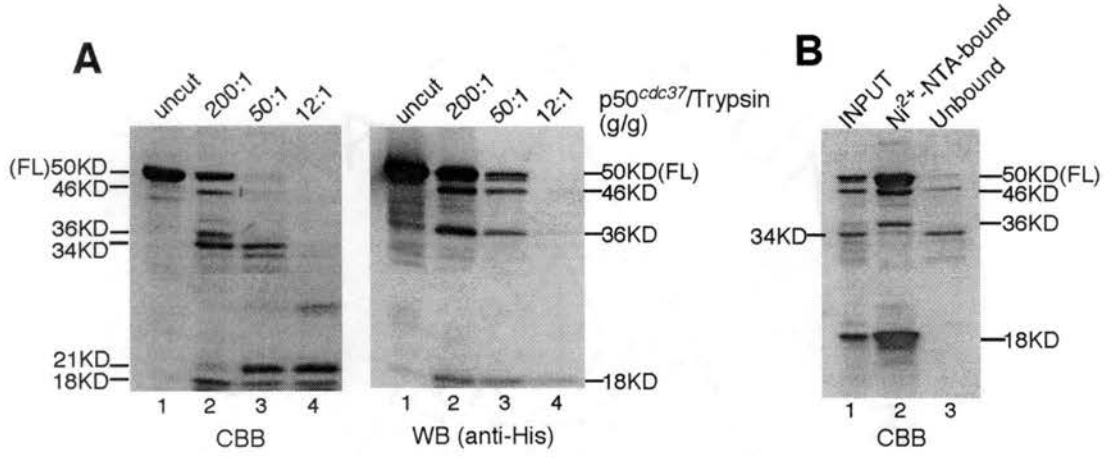

Figure 23. Limited trypsinolysis of purified recombinant (His_6)-Cdc37. **A)** 5 μg purified recombinant (His_6)-Cdc37 was digested with trypsin at substrate/enzyme ratios of 200:1 (*lane 2*), 50:1 (*lane 3*) and 12:1 (*lane 4*), respectively as described under "Materials and Methods". A mock digestion containing equal amount of trypsin-free buffer was set up in parallel as the uncut control (*lane 1*). Digestion was carried out for 6 min on ice and stopped immediately by mixing with boiling SDS sample buffer. Proteolytic fragments were subsequently separated on a 12% SDS-polyacrylamide gel, transferred to PVDF membrane and stained with Coomassie brilliant blue R250 (CBB, *left panel*). After imaging, the same membrane was bleached (with methanol to remove the dye) and immunoblotted with the anti-(His_5) antibody (WB, *right panel*). **B)** 10 μg purified recombinant (His_6)-Cdc37 was digested with trypsin at a substrate/enzyme ratio of 200:1 for 6 min on ice. Digestion was terminated by mixing with the trypsin inhibitor along with SDS and β-mercaptoethanol at concentrations as described under "Materials and Methods". Reaction was further diluted and absorbed to Ni^{2+}-NTA resin. After collecting the unbound material, resin was washed and the absorbed Cdc37 fragments were subsequently eluted by SDS sample buffer. Finally, both the bound and unbound Cdc37 fragments were analyzed side by side on a 12% SDS-polyacrylamide gel, transferred to PVDF membrane and detected by staining with Coomassie Brilliant Blue R250 (CBB). FL: full-length (His_6)-Cdc37.

protein, 46 kDa, 36 kDa, 34 kDa and 18 kDa. There were also some minor fragments which were likely to result from aggressive internal cleavage of Cdc37 domains. As the trypsin concentration increased, however, a novel 21 kDa fragment appeared and remained intact whereas most other fragments started to attenuate and disappear. The high protease-resistance of this particular fragment indicates that its tertiary structure is highly compact and solvent inaccessible, which are the main structural criteria for protein domains.

To assist interpreting the map, proteolytic fragments were transferred to PVDF membrane and immunoblotted with anti-His-tag antibody. In doing so, we determined that 46 kDa, 36 kDa and 18 kDa are N-terminal fragments, whereas 34 kDa and the most protease-resistant 21 kDa are either internal or C-terminal fragments (Fig. 23A). To further simplify the mapping process, we carried out the digestion at the optimal 1:200 ratio, and divided the entire mixture of tryptic fragments into two fractions by affinity purifying those N-terminal fragments with anti-His-tag antibody and leaving the internal and/or C-terminal fragments behind (Fig. 23B). For some reason, the 36 kDa fragment appeared to be a minor proteolytic product in this experiment (Fig. 23B: Lane 1). It could be due to slight inconsistency in experimental conditions such as substrate/enzyme ratio and/or the quality of purified Cdc37 between experiments. Despite the subtle variation, consistent with the Western blotting result, the 46 kDa, 36 kDa and 18 kDa fragments were specifically immunoadsorbed by anti-His-tag antibody whereas the 34 kDa fragment was not. These major proteolytic fragments were subsequently excised from the SDS-PAGE and subjected to further in-gel digest and MALDI-TOF mass spectrometry analysis.

b) Solving the domain map: in-gel trypsin digest and MALDI-TOF MS analysis of major proteolytic fragments of Cdc37-In-gel digestion by sequence-specific proteases coupled with matrix-assisted laser/desorption ionization-time of flight mass spectrometry (MALDI-TOF MS) analysis has emerged as a powerful and widely used tool for proteomic studies. It can be used for various purposes including protein identification which relies on the fact that each different protein gives its unique peptide mass fingerprint upon digestion with a sequence-specific protease. Here adopting the same principle, we used this integrated technique in an attempt to solve the domain structure of Cdc37. The idea is to digest each of the major Cdc37 fragments (resulting from trypsin nicking) representing its putative domains with trypsin, generate a unique peptide mass fingerprint for each of them using MALDI-TOF mass spectrometry, deduce their amino acid sequences and thus solve the domain structure of Cdc37.

As described above, the major proteolytic nicking fragments of Cdc37 were in-gel digested by trypsin and analyzed by MALDI-TOF MS. Their experimental peptide mass fingerprints were then compared to that predicted based on the amino acid sequence of full-length Cdc37 as a result of complete or partial trypsinolysis. Confident matches between the experimental and theoretical peptides are summarized in Table 3. Consistent with the Western blotting and immunoadsorption results, no N-terminal peptides of Cdc37 were identified for the 34 kDa and 21 kDa fragments. MS data indicated that they both start at Ser-127, which was later confirmed by Edman degradation sequencing. The 21 kDa fragment appears to end at Arg-283 as suggested by

Major Cdc37 fragments				Measured mass (Da)	Calculated mass (Da)	Covered sequences
46 kDa	36 kDa	18 kDa		810.28	810.38	$M^{40}EQFQK^{45}$
				1529.49[a]	1529.78[a]	$E^{70}LEVAEGGK\ AELER^{83}$
				1056.49	1056.58	$L^{84}QAEAQQLR^{92}$
				1335.43[a]	1335.64[a]	$S^{97}WEQK\ LEEMR^{106}$
				1811.71[a]	1811.86[a]	$S^{111}MPWNVDTLSK\ DGFSK^{126}$
		34 kDa	21 kDa	2493.69[a]	2493.18[a]	$S^{127}MVNTK\ PEK\ TEEDSEEVREQK^{147}$
				1043.60[a]	1043.54[a]	$T^{150}FVEK\ YEK^{157}$
				760.27	760.39	$H^{161}FGMLR^{166}$
				934.13[a]	934.44[a]	$R^{167}\ WDDSQK^{173}$
				1672.44[a]	1671.84[a]	$V^{228}DPR\ ACFR\ QFFTK^{240}$
				1721.45[a]	1720.75[a]	$Q^{247}YMEGFNDELEAFK\ ER^{262}$
				658.34[a]	658.43[a]	$L^{269}R\ IEK^{273}$
				1313.42[a]	1313.57[a]	$A^{274}MK\ EYEEEER^{283}$
				2269.62	2269.16	$L^{287}GPGGLDPVEVYESLPEELQK^{307}$
				2006.09[a]	2005.96[a]	$D^{313}VQMLQDAISK\ MDPTDAK^{330}$
				734.16	734.34	$Y^{331}HMQR^{335}$
				1707.65	1707.84	$E^{353}GEEAGPGDPLLEAVPK^{369}$

[a] peptides resulting from partial trypsin digestion

Table 3. Mass spectrometry analysis of major proteolytic fragments of Cdc37

the MS data. However, since Arg-283 is immediately followed by two Lys and one Arg residues, which would be cleaved off by trypsin upon complete digestion, the precise C-terminus of the 21 kDa fragment could not be determined. Nonetheless, it suggests that residues at or around $R^{283}KKR^{286}$ represent one of the major flexible and solvent accessible regions of Cdc37 which could be an inter-domain junction. Supporting this hypothesis, the 36 kDa fragment was mapped to a large N-terminal Cdc37 fragment which also ends around $R^{283}KKR^{286}$. As to the 34 kDa fragment, MS data suggested that it terminates at Lys-369. However, complete trypsinolysis of the last nine amino acids of Cdc37, $T^{370}GDEKDVSV^{378}$, should give rise to two rather short peptides, DVSV (418 Da) and TGDEK (549 Da), which are below the detection limit and buried under too many low mass noises of MALDI-TOF MS, respectively. Therefore, it remains unclear whether the 34 kDa fragment contains the last nine amino acids of Cdc37 or not.

Analysis of the 18 kDa fragment indicated that it contains amino acids 1-126 of Cdc37, which is consistent with the fact that it reacted with the anti-His-tag antibody. Most importantly, it suggested that the second inter-domain junction of Cdc37 resides between K^{126} and S^{127}, or at their proximity. Examination of the 46 kDa fragment assigned it to residues 1-347 or 1-352, indicating that another protease-sensitive region exists around K^{347} and/or K^{352}. However, since this region is very close to the C-terminus of Cdc37, it is probably not a true inter-domain junction. Instead, it may a flexible intra-domain region which structurally separates the last 25-30 amino acids of Cdc37 from the major part of its C-terminal domain. Take together, MS data successfully mapped all the major Cdc37 proteolytic nicking fragments to the full-length protein, and strongly suggested a three-domain structure of Cdc37 (Fig. 24).

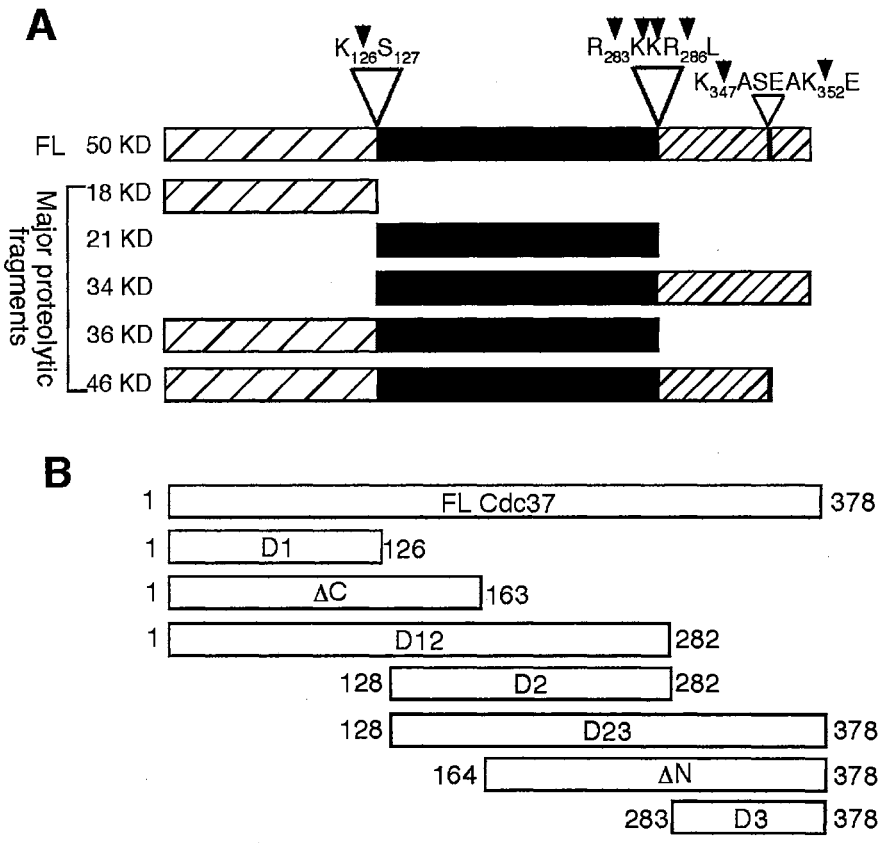

Figure 24. Domain structure of Cdc37. **A)** Mapping of the major proteolytic fragments of Cdc37 resulting from limited trypsinolysis by MALDI-TOF. Two major trypsin cutting sites representing putative inter-domain junctions are shown by large arrows pointing to the exact or approximate locations. One minor cutting site possibly representing an intra-domain junction is shown by a small arrow. Major proteolytic fragments of Cdc37 are also shown according to their individual locations. **B)** Dissection of Cdc37 based on its domain structure (shown in **A**). D1, D2 and D3 are the putative individual domains whereas D12 and D23 are fusions of adjacent domains. The arbitrary domains Cdc37/ΔC and Cdc37/ΔN which have been characterized previously are also shown here.

2) Characterizations of different Cdc37 domains regarding their abilities to bind HRI and Hsp90:

Early studies have assigned the kinase- and Hsp90-binding sites of Cdc37 to its arbitrary N-terminal (ΔC, 1-163) and C-terminal (ΔN, 164-378) regions, respectively (89, 215). Based on our novel domain structure of Cdc37, we predict that the authentic N-terminal domain (D1, 1-126) bears the kinase-binding site whereas the central domain (D2, 127-283) interacts with Hsp90. To characterize them in RRL, all three domains of Cdc37 were cloned into the pSP64T vector which drives efficient protein synthesis in RRL. Two additional constructs were also made to combine neighboring domains, named D12 and D23. This is to ensure that we do not miss any potential kinase and/or Hsp90 binding motifs of Cdc37 that are presented cooperatively by adjacent domains rather than solely by individual domains. Various Cdc37 constructs were synthesized in RRL, and their HRI- or Hsp90-binding abilities were subsequently assessed through immunoprecipitation coupled with Western blotting and autoradiography analyses.

a) Hsp90-binding site resides in the central domain (D2) of Cdc37-To examine the Hsp90-binding abilities of the individual Cdc37 domains, His-tagged versions of all five constructs were individually synthesized in RRL with concomitant radiolabeling with [^{35}S]Met and subsequently immunoadsorbed by anti-His-tag antibody. Full-length Cdc37 as well as the two arbitrary domains, ΔC and ΔN were also synthesized to serve as the controls. Coadsorption of endogenous Hsp90 with all these cdc37 constructs was then assessed through Western blot (Fig. 25). Consistent with the early data, full-length Cdc37 and ΔN specifically interacted with Hsp90. In agreement with our hypothesis the

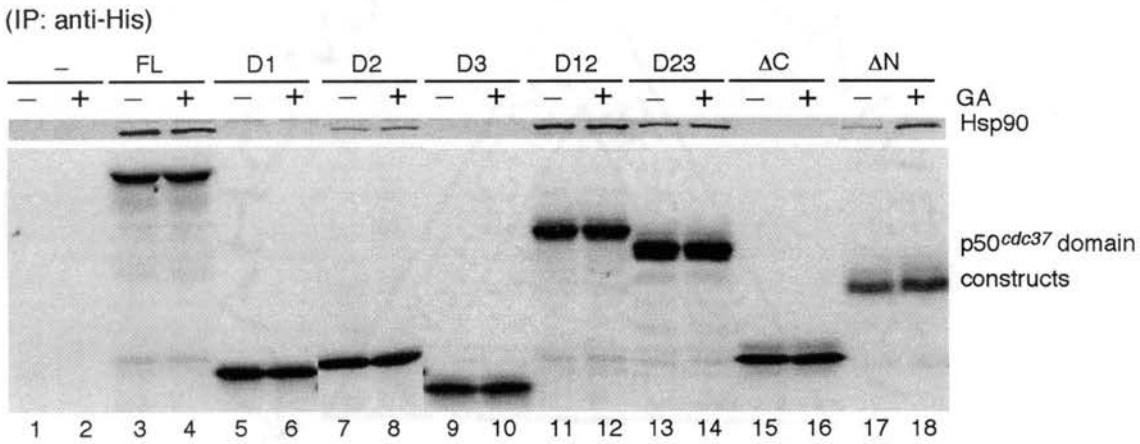

Figure 25. Hsp90-binding activities of Cdc37 dissection products. Eight different (His_6)-tagged Cdc37 constructs (full-length, D1, D2, D3, D12, D23, Cdc37/ΔC and Cdc37/ΔN) were synthesized with concomitant radiolabeling with [^{35}S]Met in TnT RRL containing (*even-number lanes*) or lacking (*odd-number lanes*) 10 μg/ml geldanamycin (GA) at 30 °C for 30 min followed by 10 min chase upon the addition of 60 μM aurintricarboxylic acid. Two mock RRL reactions lacking the exogenous DNA templates were assessed in parallel as the nonspecific controls (*lanes 1 and 2*). All the reactions were subsequently immunoprecipitated by the anti-(His_5) antibody and separated on a 10% SDS-polyacrylamide gel. Proteins were then transferred to PVDF membrane, and analyzed by autoradiography (*lower panel*, immunoadsorbed [^{35}S]-labeled Cdc37 domain constructs) or Western blotting (*upper panel*, coadsorbed endogenous Hsp90) analyses, respectively.

central domain D2 bound to Hsp90, whereas the other two domains D1 and D3 did not. As predicted, D12 and D23 both of which contain the central domain D2 also specifically pulled down endogenous Hsp90. Therefore, the Hsp90-binding site is located to the central domain D2 of Cdc37.

As a molecular chaperone, Hsp90 could interact with the Cdc37 domains simply because they are misfolded due to the lack of stabilizing interactions with other parts of the protein or because certain parts become exposed upon dissection which would be normally buried inside the full-length protein. To rule out such a possibility, GA was included in the same set of RRL reactions synthesizing different Cdc37 constructs as described above. If D2 is recognized by Hsp90 as an unfolded client, GA should disrupt such an interaction like it does to other clients of Hsp90 (29, 89, 97, 215). However, geldanamycin should not have any effect if D2 binds to Hsp90 as a cohort like full-length Cdc37. As expected, GA had no effect on the interaction between Hsp90 and D2, indicating that it is behaving as a cohort rather than a client of Hsp90. Consistently, GA also had no effect on the interactions of Hsp90 with full-length Cdc37, D12 and D23. However, quite surprisingly the interaction between Hsp90 and the arbitrary ΔN was actually enhanced several fold by GA treatment, a novel observation that we do not fully understand at this moment.

b) Kinase-binding site is located in the authentic N-terminal domain (D1) of Cdc37-To test the hypothesis that D1 possesses the kinase-binding site of Cdc37, it was synthesized and labeled with [^{35}S]Met in RRL, which was then mixed with RRL containing newly synthesized (His_7)-HRI. (His_7)-HRI was immunoadsorbed to anti-His-tag antibody and

the coadsorption of [^{35}S]D1 was assessed by autoradiography. D12 was also analyzed similarly regarding its HRI-binding activity (Fig. 26). Consistent with our hypothesis, both D1 and D12 were specifically coadsorbed by (His_7)-HRI, indicating that the authentic N-terminal domain of Cdc37 contains the kinase-binding site. To assess the possibility that Cdc37 possesses additional kinase-binding sites elsewhere in the protein, D2 and D23 were also examined for their abilities to bind HRI. However, neither of these constructs interacted with (His_7)-HRI specifically, further supporting the hypothesis that D1 is the only kinase-binding domain of Cdc37 (data not shown).

Early works have shown that Cdc37 binds to HRI in an Hsp90-dependent manner which can be fully disrupted by GA treatment. However, the interaction between the arbitrary ΔC and HRI was found to be GA-insensitive, which is presumably due to the fact that in the absence of the C-terminal Hsp90-binding domain, the kinase-binding site is no longer under control of the nucleotide-regulated conformational switching of Hsp90 (215). With no detectable ability to bind Hsp90, we predicted that D1 would interact with HRI in the same GA-insensitive fashion as ΔC, whereas D12 would behave the same as the full-length Cdc37 because of its Hsp90 binding by D2. Surprisingly, however GA not only disrupted the interaction between D12 and HRI, but also disrupted the interaction between D1 and HRI. Therefore, it seems that unlike ΔC, the kinase-binding activity of D1 is somehow regulated by Hsp90 through an unknown mechanism.

3) N-terminal residues of Cdc37 are essential for its interaction with HRI:

Sequence alignment classified the first 30 or so amino acids as the most conserved region of Cdc37 homologues from different species, indicating that they are

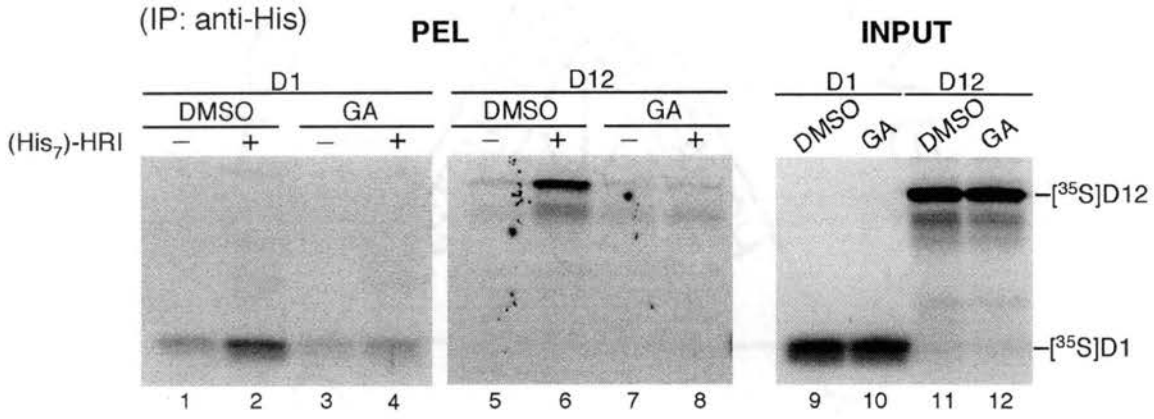

Figure 26. HRI-binding activities of D1 and D12 constructs of Cdc37. D1 and D12 were synthesized with concomitant radiolabeling with [^{35}S]Met in separate TnT RRL containing (*lanes 3, 4, 7 and 8*) or lacking (*lanes 1, 2, 5 and 6*) 10 μg/ml geldanamycin (GA) at 30 °C for 30 min. After 10 min chase with 60 μM aurintricarboxylic acid, they were mixed with either mock (*lanes 1, 3, 5 and 7*) or newly synthesized (His_7)-HRI-containing (*lanes 2, 4, 6 and 8*) TnT RRL and further incubated at 30 °C for 25 min. Resulting RRL mixtures were then subjected to immunoadsorption using the anti-(His_5) antibody and analyzed on a 10% SDS-polyacrylamide gel. Proteins were subsequently transferred to PVDF membrane, and the coasorbed [^{35}S]-labeled D1 (PEL, *left panel*) and D12 (PEL, *right panel*) were visualized by autoradiography analysis. Aliquots of RRL mixtures were taken prior to immunoadsorption and analyzed to show that geldanamycin had no effect on the synthesis level of D1 and D12 (INPUT).

functionally essential (51, 235). Our early studies on the Cdc37 mutant, N8aa whose first eight amino acids were replaced by a short irrelevant sequence, have indicated that these eight amino acids are critical for the kinase-binding, but not the Hsp90-binding activity of Cdc37 (215). This finding is also consistent with the fact that the N-terminal domain of Cdc37 (D1) interacts with the kinase. Here we sought to examine the first eight amino acids of Cdc37 individually by site-directed mutagenesis, attempting to pinpoint the ones that are directly involved in kinase-binding. Amino acids 2 through 8 of Cdc37 were mutated to alanine individually, and the resulting mutants were cloned into the pSP64T or pSP64TL vector for *in vitro* translation in RRL.

a) Val-2, Asp-3, Tyr-4 and Trp-7 are important for the HRI-binding activity of Cdc37-To examine the kinase-binding properties of the seven different mutants of Cdc37, their non-His-tagged versions were synthesized and labeled with [^{35}S]Met in TnT RRL reactions, which were then mixed with RRL containing newly synthesized (His_7)-HRI. Reaction mixtures were subjected to immunoadsorption by anti-His-tag antibody, and the coadsorption of [^{35}S]-labeled Cdc37 mutants with HRI were subsequently analyzed by autoradiography (Fig. 27). In doing so, we identified Tyr-4 and Trp-7 as two essential residues for the kinase-binding activity of Cdc37 as demonstrated by the observation that Y4A and W7A mutants completely failed to be coadsorbed with (His_7)-HRI. Asp-3 also seemed to be important for the kinase-binding of Cdc37 as well since its mutation to alanine reduced the interaction of Cdc37 with HRI by approximately 10 fold. Additionally, the binding affinity of V2A mutant for HRI was also decreased about 3 fold, indicating that Val-2 is also involved in the interaction of Cdc37 with the kinase.

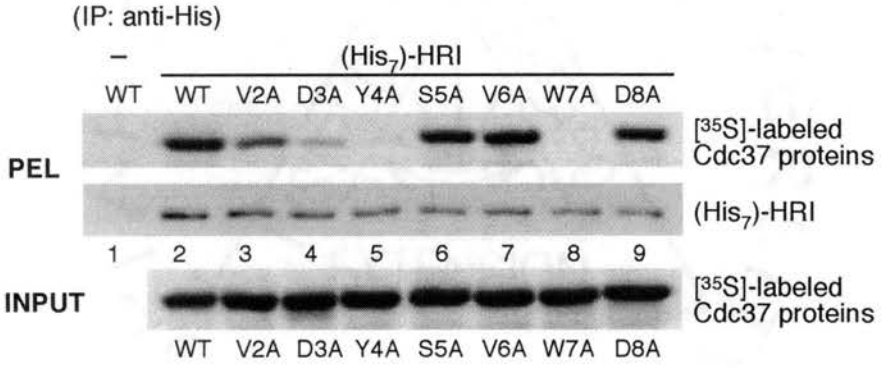

Figure 27. HRI-binding activities of the N-terminal point mutants of Cdc37. Wild type and the N-terminal point mutants of Cdc37 were synthesized and labeled with [^{35}S]Met in separate TnT RRL reactions at 30 °C for 30 min. Following a 10-min chase with 60 μM aurintricarboxylic acid, each RRL reaction was mixed with an equal volume of TnT RRL containing newly synthesized (His_7)-HRI and further incubated for 25 min (PEL, *lanes 2 to 9*). A duplicate TnT RRL reaction synthesizing the wild type Cdc37 was mixed with a mock TnT RRL mixture lacking (His_7)-HRI to serve as the nonspecific binding control (*lane 1*). Resulting mixtures were subjected to immunoadsorption with the anti-(His_5) antibody, separated on an 8% SDS-polyacrylamide gel and transferred to PVDF membrane. Immunoadsorbed (His_7)-HRI was detected by Western blot (PEL, *lower panel*), whereas the coadsorbed [^{35}S]-labeled Cdc37 mutants were analyzed by autoradiography (PEL, *upper panel*). Equivalent aliquots were taken from each different Cdc37 reaction prior to immunoadsorption to ensure the constructs were generated at comparable levels (INPUT).

Conversely, mutation of Ser-5, Val-6 and Asp-8 had no effect on the ability of Cdc37 to bind HRI, which thus ruled out their involvement in the kinase-binding by Cdc37. Thus, these mutagenesis studies identified four important residues out of the first eight amino acids of Cdc37 that are important for its interaction with HRI. These findings not only agree with the fact that D1 domain contains the kinase-binding site, but also suggests that such a function is mediated primarily by the highly conserved 30 or so N-terminal residues of Cdc37.

Working with mutants, there is always a chance for the altered function of the proteins to be caused by unwanted global conformational changes rather than by the expected change of properties of specific residues. To test whether the inability of the Cdc37 mutants to bind HRI was due to any mutation-induced global conformational changes, we carried out mild trypsin nicking experiments on all of the mutant constructs. Different fragmentation patterns and/or sensitivities to proteases are expected for mutants with compromised structures in comparison to the wild-type protein. As shown in Fig. 28, wild type and mutant Cdc37 proteins were synthesized and radiolabeled with [^{35}S]Met in separate TnT RRL reactions to which increasing amounts of trypsin were added subsequently. The resulting nicking reactions were then analyzed by SDS-PAGE and autoradiography. In doing so, we detected little differences in both the fragmentation patterns and sensitivities to trypsinolysis between the wild type Cdc37 and its mutants, indicating that no global conformational changes have been induced by the mutations. These findings further underscore the importance of these N-terminal amino acids in mediating the interaction of Cdc37 with its client proteins.

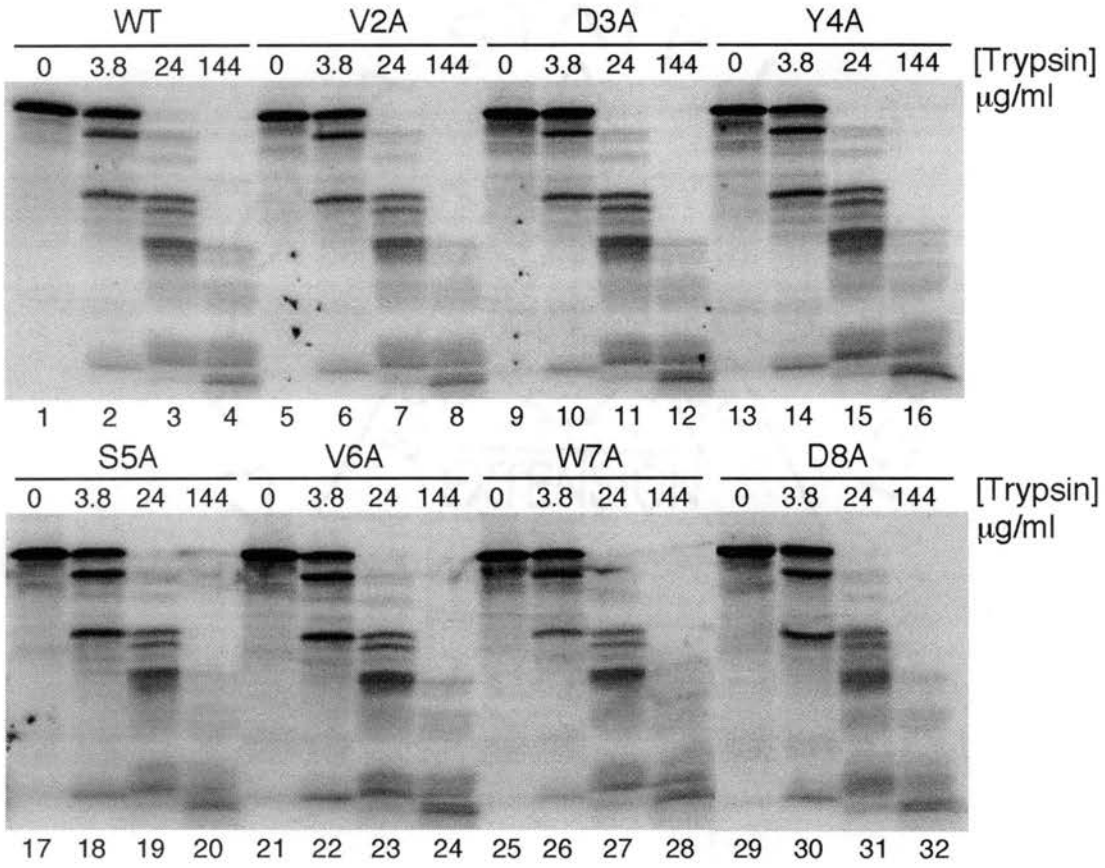

Figure 28. Comparison of proteolytic peptide mapping between wild type Cdc37 and its N-terminal mutants. Wild type (WT) and mutant forms of Cdc37 were synthesized with concomitant radiolabeling with [^{35}S]Met in separate TnT RRL reactions at 30 °C for 30 min, followed by a 1 hr maturation in the presence of 60 μM aurintricarboxylic acid. Reactions were chilled briefly on ice and diluted into 3 volumes of proteolysis buffer (as described under "Materials and Methods") containing four different concentrations of trypsin as specified in the figure. Digestion was carried out for 6 min on ice and terminated immediately by mixing the samples with boiling SDS sample buffer. Proteolytic peptide fragments were separated by 12% SDS-polyacrylamide gel, followed by autoradiography analysis. *FL* denotes full-length Cdc37.

b) The interaction of Cdc37 with Hsp90 is not affected by the N-terminal mutations-Early works done in our lab have indicated that the full-length Cdc37 requires functional Hsp90 to acquire its kinase-binding ability as the Hsp90-specific inhibitor, GA, completely abolishes its interaction with HRI (215). Therefore, another possible cause for the diminished or lost kinase-binding by the Cdc37 mutants is that, unlike the wild type Cdc37, they are unable to form complexes with Hsp90. To examine such a possibility, two reciprocal approaches were taken in which the interactions of different Cdc37 mutants with Hsp90 were compared to the wild type Cdc37. In the first approach, different Cdc37 mutants were synthesized and radiolabeled with [^{35}S]Met in RRL, followed by immunoprecipitation of the endogenous Hsp90 and coadsorption of [^{35}S]-labeled Cdc37 mutants (Fig. 29A). Autoradiogram showed that except for W7A, all of the other mutants bound Hsp90 at a similar level to the wild type Cdc37, indicating that their binding affinities for Hsp90 were not affected by the mutations. As to W7A, there was roughly 50% decrease in its binding to Hsp90 compared to the wild type Cdc37. Similar results were obtained in the reciprocal experiment in which the His-tagged Cdc37 mutants were synthesized in TnT RRL and immunoadsorbed by the anti-His-tag antibody. Coadsorption of the endogenous Hsp90 was subsequently detected by Western blotting (Fig. 29B). Again, W7A showed a loss of Hsp90-binding, whereas the other mutants interacted with Hsp90 at essentially the same level compared to the wild type Cdc37. Therefore, the data presented here further strengthen the hypothesis that the N-terminal amino acids including Val-2, Asp-3 and Tyr-4 are directly involved in the interaction of Cdc37 and its client kinase.

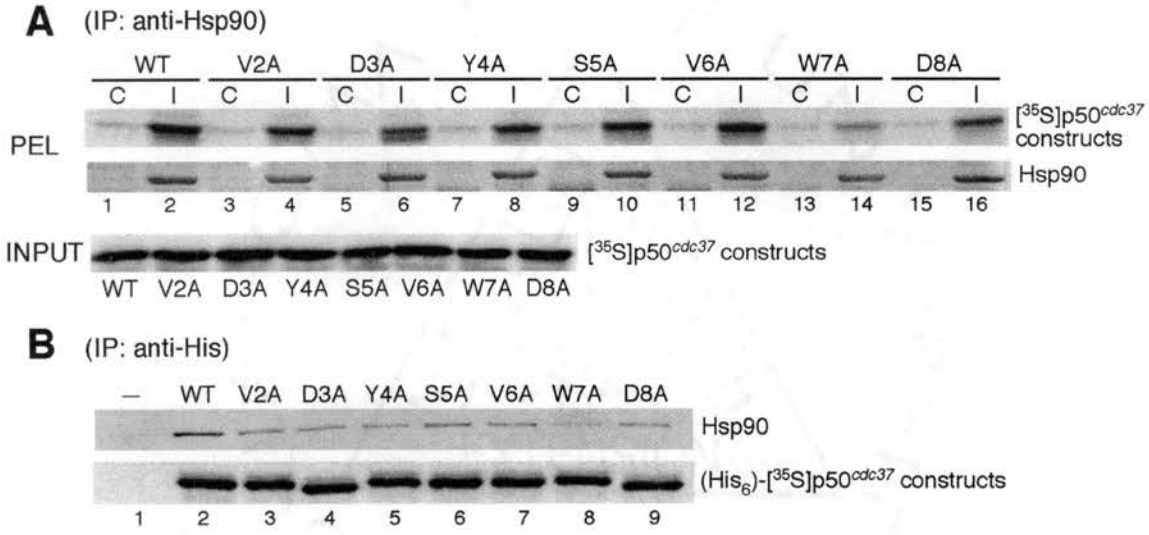

Figure 29. Hsp90-binding activities of the N-terminal point mutants of Cdc37. **A**) Wild type and mutant forms of Cdc37 were synthesized with concomitant radiolabeling with [^{35}S]Met in separate TnT RRL reactions at 30 °C for 30 min, followed by a 10 min chase with 60 μM aurintricarboxylic acid. They were then immunoadsorbed with the monoclonal anti-Hsp90 antibody 8D3 (*even-number lanes*) or nonimmune control IgM antibody (*odd-number lanes*) and separated on an 8% SDS-polyacrylamide gel. Proteins were transferred to PVDF membrane, and the immunoadsorbed endogenous Hsp90 and coadsorbed [^{35}S]-labeled Cdc37 proteins were subsequently detected by Western blotting and autoradiography analyses, respectively (PEL). Equivalent aliquots were taken from the Cdc37 translation mixtures prior to immunoadsorption to show that the constructs were synthesized at comparable levels (INPUT). **B)** (His_6)-tagged wild type and mutant forms of Cdc37 were synthesized and radiolabeled with [^{35}S]Met in separate TnT RRL reactions at 30 °C for 30 min. After a 10 min chase with 60 μM aurintricarboxylic acid, they were immunoadsorbed by the anti-(His_5) antibody and separated on an 8% SDS-polyacrylamide gel. Proteins were transferred to PVDF membrane, and analyzed by Western blotting (coadsorbed endogenous Hsp90) or autoradiography (different [^{35}S]-labeled Cdc37 proteins).

Discussion:

Data presented in this report indicate a three-domain structure of human Cdc37, which has also been suggested by Scholz *et al* recently (212). In their report, based on the amino acid sequence alignment of Cdc37 and Harc, an Hsp90-associating relative of Cdc37 from multiple species, they predict a three-domain structure of Cdc37 that is strikingly similar to ours. However, their middle domain D2 (120 amino acids ranging from 145-264) is 18 and 19 amino acids shorter than ours (157 amino acids ranging from 127-283) from the N- and C-terminal ends, respectively. Despite these minor differences, both D2 constructs are able to bind Hsp90, indicating that all or most of the Hsp90-interacting motifs occur within the central 120 amino acids of Cdc37. Indeed, the region of Cdc37 involved in the direct interaction with Hsp90 could even be minimized by 19 more residues based on the fact that the arbitrary C-terminal domain ΔN (starting at Met164) is also sufficient to bind Hsp90 (215). Therefore, it is quite likely that the extra 37 amino acids that lie outside of the central 120 residues, are either part of the middle domain of Cdc37 to which they may be structurally or functionally important, or representing an interdomain region that functionally couples the adjacent N-terminal domain (D1) and the middle domain (D2) of Cdc37. The hypothesis that these 37 amino acids are part of the middle domain of Cdc37 is strongly supported by the observation that our D2 fragment is highly resistant to proteolysis, a property usually possessed by intact domains with compact three-dimensional structures. Our confidence is further strengthened by the finding that limited proteolysis of Cdc37 by chymotrypsin generates a strikingly similar pattern of fragments to that by trypsin (data not shown).

Data presented here also allow us to identify a novel kinase-binding domain of Cdc37 (D1) which has not been reported previously. It contains the first 126 amino acids of Cdc37, 37 resides shorter than the previously characterized arbitrary N-terminal Cdc37/ΔC domain. D1 binds to HRI specifically, however unlike Cdc37/ΔC the interaction can be disrupted by the Hsp90-specific inhibitor geldanamycin. This result is rather puzzling considering the fact that D1 lacks any Hsp90-binding activity, which predicts that it is not controlled by the nucleotide-regulated conformational switching of Hsp90. Despite the lack of a convincing explanation, it seems reasonable to speculate that it is the 37 amino acids present in Cdc37/ΔC but missing from D1 that makes the difference in the geldanamycin-responsiveness of their HRI-binding activities. Interestingly, sequence alignment of the D1 domain of human Cdc37 with the Hsc70-interacting Bag domain suggests that they share a significant number of conserved residues that are critical for the direct binding of the Bag domain to the ATPase domain of Hsc70 (229). In one alignment, the conserved residues of Cdc37 (within amino acids 41-67) and the Bag domain correspond precisely with regards to their positions, suggesting that a similar binding surface for Hsc70 can be formed if this region of Cdc37 adopts a similar helical bundle structure with the identical length to that in the Bag domain (Fig. 30A). Alternatively, residues in the third helix of the Bag domain that are involved in its direct interaction with Hsc70 can also be aligned to a further downstream region of Cdc37 (within amino acids 92-100) with equal confidence (Fig. 30B). This implies that two or more potential helices, with different lengths relative to the two helices of the Bag domain, can be formed within the D1 domain of Cdc37 and arranged topologically to create a similar Hsc70 binding surface. Indeed, secondary structure

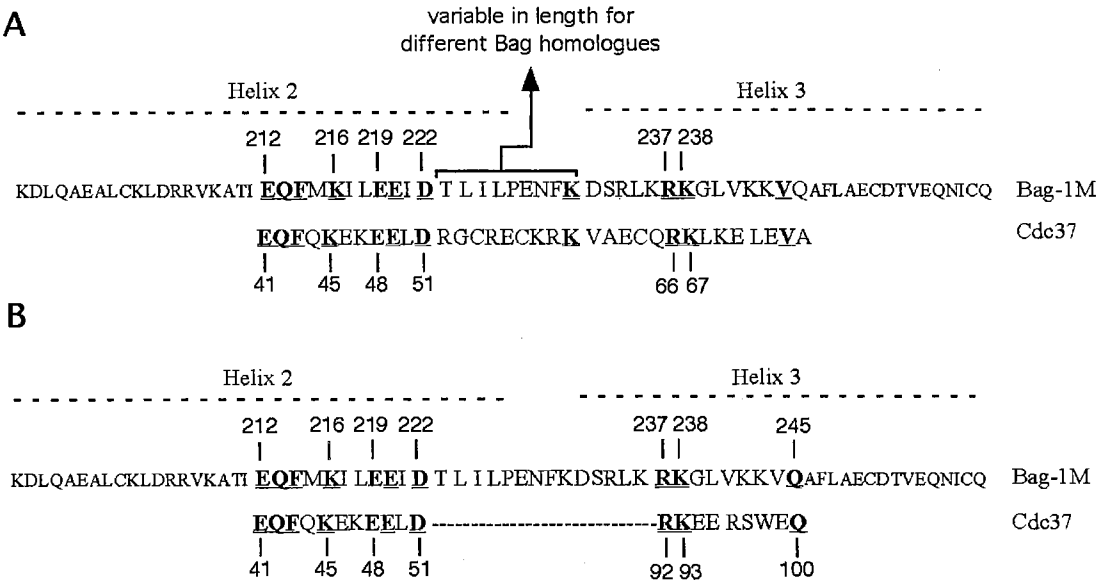

Figure 30. Sequence alignment of the D1 domain of Cdc37 (human) with the minimal Bag domain of Bag-1M (human, Genbank accession number Q99933). Only the region of D1 (41-73) that shares conserved residues with the Bag domain is shown here. The minimal Bag domain (151-264 for human Bag-1M) contains three α-helices in which the helix 2 and 3 interact directly with the ATPase domain of Hsc70 (Helix 1 is not shown) (229). Residues of the Bag domain that are both critical for the interaction with the ATPase domain of Hsc70 and absolutely conserved across species ranging from yeast to human are indicated by numbers. **A**) and **B**) represent two alternative alignments between the D1 domain of Cdc37 and the Bag domain of Bag-1M. Residues of Cdc37 located between the two conserved regions (to the Bag domain) are not shown in the second alignment (**B**).

prediction indicates that α-helices are highly possible for this region of mammalian Cdc37 (data not shown). Supporting such a hypothesis, we are able to observe specific interactions of full-length Cdc37, and to a lesser extent Cdc37/ΔC, with Hsc70 in RRL (data not shown). However, such an interaction can not be detected for D1, indicating that the extra 37 amino acids present in Cdc37/ΔC are required for the stable interaction between Cdc37 and Hsc70. Based on the fact that Hsc70 possesses its own Hsp90-independent kinase-binding activity (243, 248), it is tempting to speculate that in the presence of geldanamycin, Cdc37/ΔC interacts with HRI in an Hsc70-dependent, but Hsp90-independent fashion. However, in the context of the full-length Cdc37, geldanamycin can still exert its inhibitory effect on the HRI-binding of Cdc37 through its association with mediated by the central domain. As to D1, without the stable interaction with Hsc70, it relies solely on the geldanamycin-inhibitable Hsp90 function for its HRI-binding activity. Nonetheless, in this model another assumption needs to be made: that is the geldanamycin-inhibitable function of Hsp90 is required for HRI to achieve its Cdc37-binding competent conformation. This hypothesis then helps to explain the puzzle that even being physically free from Hsp90, the HRI-binding activity of D1 is still controlled by the nucleotide-regulated conformational switching of Hsp90.

The functional importance of these 37 amino acids for Cdc37 is also implicated by another interesting, yet puzzling finding. It appears that the presence or absence of these 37 amino acids from the middle domain of Cdc37 somehow determines whether its association with Hsp90 is sensitive to geldanamycin. Full-length Cdc37, D2 and D23 containing these residues interact with Hsp90 in a geldanamycin-insensitive fashion. However, the arbitrary Cdc37/ΔN construct which lacks these amino acids exhibits an

enhanced affinity for Hsp90 in the presence of geldanamycin (Fig. 25). Additionally, novobiocin, another Hsp90 inhibitor that targets the putative C-terminal nucleotide-binding pocket of Hsp90 (140, 141, 232), also seems to have a strange effect on the conformation of the Cdc37/ΔN construct. It surprisingly leads to a physical masking of the N-terminal His-tag of Cdc37/ΔN, which causes its inaccessibility to the anti-His antibody in the immunoprecipitation experiment (data not shown). Therefore, besides their potential roles in mediating the interaction of Cdc37 with Hsc70, these 37 amino acids may also be directly involved in modulating the interaction between Cdc37 and Hsp90 in response to the nucleotide-regulated conformational switching of Hsp90.

Site-directed mutagenesis of the N-terminal eight amino acids of Cdc37 (except the starting methionine) allowed us to pinpoint four residues that are critical for its interaction with HRI: V2; D3; Y4; and W7. It substantiates our early finding that replacing the first eight amino acids of Cdc37 with an unrelated sequence completely abolishes its ability to bind HRI, and also indicates that the actual kinase-recognition site(s) of Cdc37 may be located at the N-terminal region of the D1 domain. Sequence alignment of Cdc37 homologues from different species ranging from yeast to human reveals that the first 30 or so amino acids are the most conserved region of the whole protein, and three out of the four residues, D3, Y4 and W7, that we have identified to be critical for the HRI-binding of Cdc37 are absolutely invariant. Therefore, it implies that large aromatic amino acids at positions 4 and 7 (Y4 and W7) are required for the kinase-binding activity of Cdc37. Whereas alanine mutations at Y4 and W7 may have caused subtle conformational change at the N-terminal region of Cdc37 that contributes to its loss of kinase-binding (which was likely undetectable by protease nicking due to the

close proximity of Y4 and W7 to the N-terminus of Cdc37), future studies by mutating them to phenylalanine or aliphatic hydrophobic residues such as leucine should provide better evidence for whether large aromatic amino acids are absolutely required at these two positions for Cdc37 to bind kinases. As to V2, although it is replaced by an isoleucine residue in yeast Cdc37, the conserved hydrophobicity predicts a similar function for it in mediating protein-protein interactions. In contrast, V6 and D8, which do not seem to be important for the interaction of Cdc37 with HRI, are poorly conserved in lower species such as yeast and drosophila. It is noteworthy that the additional downstream residues within the first 30 or so amino acids of Cdc37 are also well conserved, suggesting that they are functionally or structurally important as well (51, 235). Considering that even the distantly related yeast Cdc37 has been reported to bind the protein kinase Ste11 (1), our data presented here strongly suggest an evolutionarily conserved function of these N-terminal amino acids in recognizing and binding the client proteins of Cdc37. Nonetheless, more mutagenesis studies of the additional conserved Cdc37 residues need to be carried out in order to fully understand their importance.

Despite their abolished or compromised abilities to bind HRI, these N-terminal Cdc37 mutants seem to be normal in their abilities to bind Hsp90 except for the W7A mutant whose interaction with Hsp90 is reduced by approximately 50% compared to that of the wild type Cdc37. Several significant implications can be derived from these observations. 1) It substantiates the notion that Cdc37 binds to the client proteins through direct interactions rather than the passive bridging by Hsp90. Such a notion has been well supported by several lines of evidence including the ability of the purified Cdc37 to interact with the purified CDK4 (235) and Raf-1 (223) *in vitro* and the ability of the

Hsp90-binding deficient Cdc37/ΔC mutant to interact with a number of kinases both *in vivo* and *in vitro* (89, 215). Here it is confirmed again by our data, since in a passive bridging model these defective N-terminal Cdc37 mutants should be present in the same heterocomplex with Hsp90 and HRI simply because they are able to bind Hsp90. 2) Hsp90 depends upon functional Cdc37 to bind its client kinases. This notion derives from the finding that the subpopulation of Hsp90 that is associated with the Cdc37 mutants becomes incapable of binding HRI as well. Although it may seem to agree with the prevalent model in which Cdc37 is the kinase-targeting subunit of Hsp90 (89, 235), several lines of evidence suggest that it is not simply acting as an adaptor between Hsp90 and the client kinases. First, as previously demonstrated, Cdc37 quantitatively dissociates from HRI upon GA treatment, whereas Hsp90 is still bound to HRI albeit the interaction becomes salt-labile (97). This observation thus argues against the passive tethering model in which Hsp90 is predicted to be incapable of binding HRI in the absence of the adaptor Cdc37. Although passively targeting of client kinases to Hsp90 may represent one possible aspect of its function, it appears that Cdc37 also actively facilitates the acquisition of the Hsp90-binding conformations of client kinases. This hypothesis has already been suggested by the limited ability of the Cdc37/ΔC mutant to promote the association between the temperature-sensitive mutant of Hck and Hsp90 despite its inability to bind Hsp90 (211). However, such a potential function of Cdc37 may be client-specific because Cdc37/ΔC actually decreases the interaction of Hsp90 with another kinase, Raf-1 (89). 3) Alternatively, the above mentioned data can also be interpreted by the possibility that these Cdc37 mutants abolish the kinase-binding ability of Hsp90. Since the kinase-binding activity of Cdc37 is controlled by Hsp90 through its

nucleotide-regulated conformational switching (29, 89, 97, 215), it is equally likely that the kinase-binding activity of Hsp90 is regulated by Cdc37 as well. However, in such a scenario the N-terminal residues of Cdc37 are expected to make contacts, which are possibly transient and labile, with Hsp90 that is bound to its central domain, or instead they may interact with residues from the middle domain of Cdc37 to affect the associated Hsp90 indirectly. 4) Indeed, such inter-domain communications of Cdc37 are also implied by other lines of evidence. For instance, we notice that compared to the full-length Cdc37 and D12, D2 and Cdc37/ΔN exhibit weaker binding affinity for Hsp90, suggesting that the N-terminal kinase-binding domain of Cdc37 may somehow facilitate the Hsp90-binding by the middle domain. Similarly, D1 seems to bind HRI weaker than the full length Cdc37 and D12, indicating that similar cooperation occurs between these two domains of Cdc37 with regards to its kinase-binding. 5) An additional line of evidence which supports a direct communication between the N-terminal kinase-binding domain and the central Hsp90-binding domain of Cdc37, is our observation that the W7A mutant of Cdc37 is not only compromised in its ability to bind HRI, but also its ability to interact with Hsp90.

Taken together, data presented in this report unveil to us a novel domain structure of Cdc37 that has not been reported previously. Biochemical characterizations allow us to assign the HRI- and Hsp90-binding activities of Cdc37 to its N-terminal and central domains, respectively. A 37-amino acid stretch immediately following the N-terminal domain of Cdc37 seems to be important in determining the geldanamycin-responsiveness of Cdc37's interaction with both HRI and Hsp90. In addition, site-directed mutagenesis studies pinpointed four amino acids at the N-terminus of Cdc37 that are critical for its

HRI-binding activity. Unfortunately, we failed to identify any biological functions for the C-terminal domain of Cdc37. It remains to be seen whether it is important for some yet unknown aspects of Cdc37 function.

CHAPTER V

Identification of post-translational phosphorylation sites on Met3 mutant of HRI and the TPR domain of PP5

Introduction:

The reversible phosphorylation of proteins is one of the most important post-translational modifications that regulate virtually all aspects of eukaryotic cell life. Since its discovery in mid-1950s, reversible phosphorylation has been found to alter protein functions in almost every conceivable way, such as changing their biological activities, stabilizing or signaling for degradation, facilitating or inhibiting subcellular translocation, and promoting or disrupting protein-protein interactions. It is now believed that 30% of cellular proteins encoded by the human genome contain covalently bound phosphate, and abnormal level of protein phosphorylation gives rise to various human diseases including cancer, diabetes, arthritis and neurodegenerative disease (43, 44).

Counteracting each other at the opposite sides of reversible phosphorylation, protein kinases and phosphatases are under tight functional controls *in vivo*. In fact, some of them proved to be modified and regulated by reversible phosphorylation events themselves. For protein kinases, with the knowledge on their structures and functions growing rapidly in recent years, a good number of them have been found to undergo reversible phosphorylation that plays important roles in regulating their biological activities. Phosphorylation of specific serine, threonine, or tyrosine residues may occur at various sites catalyzed either by the kinases themselves (autophosphorylation) or other kinases, and the impacts on their kinase activities may either be positive or negative (118). As described in the early chapters, the heme-regulated inhibitor of protein

synthesis (HRI) belongs to the small family of eukaryotic eIF2α kinases which also includes the double-stranded RNA-activated protein kinase (PKR), yeast GCN2 (general control non-derepressible-2) and the recently identified endoplasmic reticulum (ER)-localized PEK (pancreatic eIF2α kinase) or PERK (PKR-like ER kinase) (94, 217). These kinases share extensive homology within their catalytic domains (34), but differ substantially within their regulatory domains (32, 207). One common feature shared by these eIF2α kinases is that their activation is accompanied by autophosphorylation, which is believed to play an essential role in regulating their activities (32, 186, 207, 266). Recent studies on PKR have identified several autophosphorylation sites in both its regulatory and catalytic domains and their significance with regards to PKR kinase activity has also been characterized. Localized within the central region between the RNA-binding and catalytic domains, three adjacent residues, Ser-242, Thr-255 and Thr-258 all appear to undergo autophosphorylation upon PKR activation *in vitro*. Interestingly, mutation of Thr-258 to alanine reduces PKR function both *in vitro* and *in vivo*, whereas mutation of Ser-242 or Thr-255 to alanine exhibits no effect. And yet simultaneous mutations of all three sites to alanine further exacerbate the inhibitory effect caused by Thr-258 mutation (241). An additional autophosphorylation site has also been identified at Thr-446, which is located in the conserved activation loop of PKR catalytic domain. An adjacent residue, Thr-451 which is also located in the activation loop of PKR, was suggested to be a potential autophosphorylation site of PKR. Importantly, site-directed mutagenesis experiments demonstrated their importance in maintaining high-level kinase activity of PKR both *in vitro* and *in vivo*. Interestingly, Thr-882 and Thr-887 located in the activation loop of yeast GCN2 corresponding exactly to Thr-446 and Thr-

451 in PKR, were found to be important for GCN2 kinase activity and likely to undergo autophosphorylation upon GCN2 activation (201). Thus, it seems that phosphorylation at both conserved and unique sites of the eIF2α kinases plays important yet distinct roles in regulating their activities. Although it is known as a fact that both HRI and PERK/PEK undergo multiple phosphorylations which are essential for their kinase functions (9, 217, 246), no specific phosphorylation sites have been identified for either of these kinases so far.

As with protein kinases, there has been emerging evidence supporting the notion that protein phosphatases are under similar functional controls by reversible phosphorylation. Protein phosphatase 1 (PP1) and 2A (PP2A), two major serine/threonine-specific members of the eukaryotic PPP family (45), have been reported to become phosphorylated at the C-terminus of their catalytic subunits, which inhibits the activities of both phosphatases concomitantly. PP1c (PP1 catalytic subunit) is phosphorylated at Thr-320 by CDK2 and its phosphatase activity is inhibited in a cell-cycle-dependent manner (64, 260). As to PP2Ac, two neighboring residues, Thr-304 and Tyr-307 are the targets for the "autophosphorylation-activated protein kinase" and tyrosine kinases such as $p60^{v\text{-}src}$, $p56^{lck}$, and epidermal growth factor and insulin receptors. Like PP1c, phosphorylation of Thr-304 and Tyr-307 of PP2A correlates with its loss of activity as well (18, 30, 93). In addition, regulatory subunits of both PP1 and PP2A have been reported to harbor phosphorylation sites, whose modification functionally regulates the corresponding catalytic subunits in different ways. For instance, phosphorylation of the targeting GM subunit of PP1 at Ser-67 by cAMP-dependent protein kinase (PKA) disrupts its interaction with PP1c and hence releases

PP1c from glycogen and selectively inhibits its regulation of glycogen metabolism (57, 58). Interestingly, PKA has also been reported to phosphorylate the 74-kDa B'' subunit of PP2A at three serine residues without dissociating it from PP2Ac, and it stimulates the phosphatase activity of PP2A towards a certain subset of its substrates (249).

Identified by three different groups in 1994, protein phosphatase 5 (PP5) is a unique member of the PPP family in that its conserved catalytic domain is fused to an N-terminal tetratricopeptide repeat domain (TPR) (10, 37, 42). The basal activity of PP5 appears to be maintained at an extraordinarily low level *in vivo* due, at least in part, to the autoinhibition from its TPR domain. Polyunsaturated fatty acids stimulate PP5's activity *in vitro* presumably by relieving such autoinhibition through binding to the TPR domain (36, 224, 225). Although much effort has been made on elucidating the mechanisms by which PP5 is regulated by its TPR domain and potential physiological activators, little is known about whether reversible phosphorylation occurs on PP5 and plays any roles in modulating its function.

In this report, we attempted to identify the phosphorylation sites on HRI that become modified upon its activation induced by heme-deficiency utilizing MALDI-TOF mass spectrometry in conjunction with biochemical and molecular biological techniques. As a result, we found that heme-deficiency induces phosphorylation of HRI within its unique regulatory kinase insertion domain and it occurs at either Ser-255 or Ser-260. As to PP5, we found that its isolated TPR domain also undergoes phosphorylation upon incubation in okadaic acid (OA)-treated RRL, and phosphorylation is accompanied by a characteristic electrophoretic mobility shift on SDS-PAGE. Using MALDI-TOF mass spectrometry and site-directed mutagenesis analyses such a phosphorylation site was

located to Ser-160 which resides near the end of the extended α7 helix of the TPR domain (53). Mutating it to alanine completely abolished the OA-induced electrophoretic mobility shift of the TPR domain. Additionally, such a site seems to be phosphorylated by protein kinase A (PKA) *in vivo* as suggested by the finding that both cyclic AMP and purified PKA were able to quantitatively shift the TPR domain molecules to the slower migrating form as induced by OA *in vitro*. The potential significances of these phosphorylation sites on both proteins were further discussed.

Materials and Methods:

Construction of the plasmids-pET30a-PP5 (216) was digested with HindIII (One site exists in PP5 coding sequence between its TPR and phosphatase domains, and the other is in pET30a vector downstream of PP5 coding sequence) to cleave off the coding sequence for the C-terminal phosphatase domain, and the remaining large HindIII fragment with the TPR domain alone in the pET30a vector was self-annealed. The resulting construct gave rise to a His-tagged recombinant TPR domain with a relatively large leader sequence (around 50 aa) encoded by the pET30a vector followed by a FLAG-tag (originated from the parent plasmid pCMV6-FLAG-PP5) and the PP5 coding sequence. Due to the fact that the original stop codon in the PP5 coding sequence was cleaved off along with the phosphatase domain, the new TPR construct used the one present in pET30a (3' to the multiple cloning region), and subsequently added a short tail sequence (AAALEHHHHHH) along with another His-tag (engineered in pET30a as an alternative to the N-terminal tag) C-terminal to the TPR coding sequence. Therefore, the

resulting recombinant TPR domain contains two (His_6)-tags at both ends and a FLAG-tag proceeding the coding sequence.

Preparation of protein samples for MALDI-TOF mass spectrometry analysis-(His_6)-Met3 (192) was synthesized in TnT RRL at 30 °C for 40 min prior to chasing and maturing in 7 volumes of heme-supplemented or heme-deficient RRL mixtures containing or lacking 10 μg/ml geldanamycin for 3 hr. The maturation mixtures were subjected to immunoprecipitation using anti-(His_5) antibody, followed by washing with 20 mM PIPES buffer (pH 7.4) containing 500 mM NaCl and 0.5% Tween-20. Protein samples were separated on 7.5% SDS-PAGE, visualized subsequently via staining in 0.1% Coomassie brilliant blue R250 (dissolved in 50% methanol and 10% acetic acid) for 30 min and destaining in 50% methanol and 10% acetic acid for 3 hr. Gels were soaked in distilled water for 30 min, from which the pieces containing (His_6)-Met3 were subsequently excised.

The recombinant TPR domain of PP5 (pET30a-TPR) was overexpressed in *E. coli* BL21(DE3) strain and purified under non-denaturing condition as described previously (215). To cleave off the His-tag along with the large leader sequence (encoded by the pET30a vector), the purified recombinant TPR was treated with enterokinase (Novagen) at a protein/enzyme ratio of 50:1 μg/unit for 8 hr at 22 °C, followed by removal of the enterokinase using the Ekapture agarose (Novagen). Following reconstitution into heme-supplemented RRL containing or lacking 500 nM okadaic acid (Calbiochem) for 40 min, TPR was immunoprecipitated by M2 anti-FLAG antibody (Sigma), washed four times with 10 mM PIPES buffer (pH 7.2) containing 150

mM NaCl and 0.5% Tween-20, and analyzed on a 10% SDS-PAGE. After staining and destaining, gel pieces containing the TPR domain were excised.

In-gel protease digest-Gel pieces containing the proteins of interest were washed with water and 50% acetonitrile (ACN) sequentially for 15 min each. Gel slices were subsequently dehydrated by briefly soaking in 100% ACN, which was then replaced by 50 mM NH_4HCO_3 to allow rehydration. Afterwards, the same volume of ACN was added and gel pieces were washed with 50% ACN/25mM NH_4HCO_3 for 15 min. Washes were repeated until no residual Coomassie blue was visible. Gel pieces were dried down completely in a speed vacuum centrifuge, rehydrated in 10 mM DTT/100 mM NH_4HCO_3 for 45 min at 56 °C (reduction), followed by 30 min incubation in 55 mM iodoacetamide/100 mM NH_4HCO_3 at room temperature (alkylation). Gel slices were then dried down and rehydrated in 30 µl of 12.5 ng/µl trypsin (Promega, sequencing grade) prepared in 50 mM NH_4HCO_3 and 5 mM $CaCl_2$ or V8 Glu-C (Calbiochem, sequencing grade) in 50 mM NH_4HCO_3. After incubation at 37 °C for 12 hr or longer, the digestion fluid was removed and stored in separate tubes. Peptides trapped inside the gel pieces were further extracted with 50 µl of 50% acetonitrile/0.1% TFA twice, both of which was then combined with the digestion fluid removed earlier. Pooled peptide mixtures were subsequently concentrated in a speed vacuum centrifuge to a final volume of 10-20 µl.

MALDI-TOF mass spectrometry analysis-Saturated α-cyano-4-hydroxycinnamic acid (matrix) (Sigma) was prepared in 50% acetonitrile/0.1% TFA. 1.0 µl aliquot of the

concentrated peptide mixtures was spotted onto the MALDI plate, which was immediately covered by the same volume of saturated matrix solution. After drying completely, peptide samples were analyzed using the Voyager DE-PRO matrix-assisted laser desorption-ionization time-of-flight mass spectrometer (MALDI-TOF) (Applied Biosystems). Mass spectra were acquired in both linear and reflector modes, and compared to the predicted peptide mass fingerprints of HRI-Met3 or PP5-TPR generated by trypsin or V8 Glu-C. Additionally, peptide samples of Met3 were also analyzed by the Bruker Reflex III MALDI-TOF mass spectrometer. To gain sequence information on the 2757.26-Da peptide of Met3 which seemed to correspond to residues 249-272 (of wild-type HRI), it was selected by the ion gate and subjected to the post-source decay (PSD) analysis in the reflector mode using the Bruker Reflex III MALDI-TOF mass spectrometer. Amino acid sequence was deduced based on the fragmentation pattern of the peptide, and it was matched to residues 249-272 of HRI as expected.

In vitro phosphorylation assay-PKA-catalyzed phosphorylation reaction was carried out following the procedures as described elsewhere (249). Enterokinase-cleaved purified recombinant TPR domain (5 μg) was incubated with the catalytic subunit of PKA (15 units) (Sigma) in a 70 μl reaction for 1 hr at 30 °C in 20 mM HEPES-NaOH buffer (pH 7.4) containing 5 mM $Mg(CH_3COO)_2$, 0.5 mM dithiothreitol and 50 μM ATP. A control reaction including everything but PKA was carried out in parallel. Reactions were terminated by mixing with boiling SDS sample buffer, and subsequently analyzed on SDS-PAGE.

As to [^{32}P]-labeling in RRL, enterokinase-cleaved purified recombinant TPR domain (2 μg) was reconstituted into 40 μl RRL mixture containing 500 nM okadaic acid or its inactive analog okadaic acid-7,10,24,28-tetraacetate (Calbiochem) and incubated at 30 °C for 5 min. 15 μCi of [γ-^{32}P]ATP was then added to the RRL mixtures followed by 15 min incubation. Reactions were subsequently immunoadsorbed to the M2 anti-FLAG-tag antibody (Sigma), followed by washing four times with 10 mM PIPES buffer (pH 7.2) containing 150 mM NaCl and 0.5% Tween-20. Samples were separated on SDS-PAGE and analyzed by autoradiography.

Treatment of TPR domain with okadaic acid and cyclic AMP in RRL-Enterokinase-cleaved purified recombinant TPR domain of PP5 (1 μg) (wild type, S160A or S164A mutant) was reconstituted into the heme-supplemented normal RRL (30 μl) containing okadaic acid (Calbiochem) (concentrations specified in figure legends) and/or cyclic AMP (Sigma) (concentrations specified in figure legends). After incubation at 30 °C for 30-40 min (as specified in figure legends), RRL reactions were subjected to immunoadsorption with the M2 anti-FLAG-tag antibody (Sigma) followed by washing four times with 10 mM PIPES (pH 7.2) buffer containing 150 mM NaCl and 0.5% Tween-20. Samples were subsequently separated on SDS-PAGE, transferred to PVDF membrane and analyzed by staining with Coomassie brilliant blue R250 or Western blot using the anti-FLAG-tag antibody.

Alkaline phosphatase (AP) treatment of the TPR domain-Enterokinase-cleaved purified recombinant TPR domain (1 μg) was reconstituted into RRL mixtures (40 μl) containing

500 nM okadaic acid or its inactive analog okadaic acid-7,10,24,28-tetraacetate (Calbiochem) and incubated at 30 °C for 40 min. Reactions were then subjected to immunoadsorption using the anti-FLAG-tag antibody (Sigma) and washed four times with 10 mM PIPES buffer (pH 7.2) containing 150 mM NaCl and 0.5% Tween-20. Resin-bound TPR proteins were subsequently treated with alkaline phosphatase (5 units, Promega) in the 50 mM Tris-HCl (pH 9.3) buffer containing 1 mM $MgCl_2$, 0.1 mM $ZnCl_2$ and 1 mM spermidine (Promega) at 37 °C for 1 hr. Reaction was terminated by mixing with the boiling SDS sample buffer and analyzed on SDS-PAGE. Proteins were transferred to PVDF membrane and immunoblotted using the anti-FLAG-tag antibody.

Site-directed mutagenesis-Point mutations of Ser-255 and Ser-260 of HRI were carried out using a PCR-based method. We took advantage of two unique internal restriction sites within the cDNA sequence of HRI, DraIII and AflII that are about 400 bps apart. DraIII is located approximately 70 and 80 bps upstream of the Ser-255 and Ser-260 codons, respectively. To introduce the S-A mutations at Ser-255 and Ser-260, two oligonucleotides (5' primers for PCR) corresponding to the region of HRI spanning from the DraIII site to the downstream codons encoding either Ser-255 or Ser-260 were synthesized, and the desired mutations were engineered at either Ser codon. For the 3' primer, another oligonucleotide was synthesized which corresponds to the region of HRI that harbors the unique AflII site. PCR reactions were carried out using the pSP64T-HRI plasmid (246) as the template and the resulting DNA fragments were digested with DraIII and AflII and used to replace the corresponding region in the wild-type pSP64T-HRI plasmid. The desired mutations were subsequently confirmed by sequencing. To make

the double mutations at both Ser-255 and Ser-260, the PCR reaction was carried out using the 5' primer containing the S260A mutation and the pSP64T-HRI-S255A plasmid as the template. Additionally, to add the (His_6)-tag to the N-terminus of the HRI mutants, they were cleaved from the pSP64T vector as a NcoI/MluI fragment and cloned into the corresponding sites of pSP64TL which is a modified version of pSP64T that encodes an (His_6)-tag preceding the NcoI site (97).

Similar strategy was used to introduce the S-A mutations to Ser-160 and Ser-164 of the TPR domain of PP5. A unique HindIII site that sits between the N-terminal TPR and C-terminal phosphatase domains of PP5 was used to clone the TPR domain out of the full-length PP5 by PCR. Two oligonucleotides (3' primers) encoding the inter-domain region of PP5 were synthesized to include the S-A mutations at either Ser-160 or Ser-164 along with the HindIII site that is approximately 50 and 60 bps downstream of the two Ser codons, respectively. Another oligonucleotide (5' primer) encoding the N-terminus of PP5 was also engineered to include an EcoRI and a BamHI site preceding the start codon. They were coupled in PCR reactions using the wild type pSP64T-PP5 plasmid (216) as the template. The 600-bp PCR product was digested with BamHI/HindIII and cloned into the corresponding sites of pET30a vector, and the desired mutations were confirmed by sequencing. To introduce these mutations into the full-length PP5, the phosphatase domain of PP5 was excised from the pCMV6 vector (35) as a HindIII fragment and inserted into the same site of the pET30a-TPR mutants (S160A or S164A). To transfer the full-length PP5 mutants into the RRL-specialized pSP64T and pSP64TL (encoding an (His_6)-tag) vectors, they were excised from pET30a as an EcoRI fragment and subcloned into the same site of pSP64T and pSP64TL vectors.

Results:

1) TPR domain of PP5:

a) Okadaic acid induces phosphorylation of the TPR domain of PP5-To investigate whether post-translational phosphorylation occurs on PP5, we first examined whether it is able to undergo any electrophoretic mobility shift on SDS-PAGE which often serves as an indicator of protein phosphorylation events. Rabbit reticulocyte lysate (RRL) was used as a quasi-physiological system in which purified recombinant PP5 was reconstituted and analyzed. Okadaic acid (OA), a serine-threonine phosphatase inhibitor, was included in the reaction mix to prevent any possible dephosphorylation of PP5 from occurring either catalyzed by itself or by other endogenous protein phosphatase(s) in RRL. In addition to the full-length protein, we also analyzed the isolated recombinant TPR domain of PP5 in the same experiment based on a potential protein kinase A (PKA) phosphorylation site near its C-terminus (DEHRRS160VVDS for rat and DEHKRS160VVDS for human PP5). As shown in Fig. 31, there was no detectable level of electrophoretic mobility shift for the full-length PP5 in response to OA treatment. This was confirmed in a separate experiment in which the *de novo* synthesized PP5 was analyzed in RRL (data not shown). Interestingly, an electrophoretic mobility shift was observed for a portion of the TPR molecules (less than 50%) in OA-treated RRL (Fig. 31), indicating that phosphorylation occurs on the TPR domain of PP5 when it is separated from the phosphatase domain.

To confirm that it is phosphorylation that correlates with the electrophoretic mobility shift of the TPR domain, we took on two different approaches. In the first

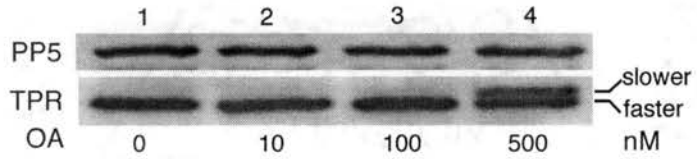

Figure 31. Okadaic acid (OA) induces electrophoretic mobility shift of the TPR domain of PP5. Purified recombinant full-length PP5 or its isolated TPR domain was reconstituted into RRL mixtures lacking (*lane 1*) or containing 10 nM (*lane 2*), 100 nM (*lane 3*) or 500 nM (*lane 4*) okadaic acid. Following incubation at 30 °C for 40 min, they were immunoprecipitated by the anti-FLAG-tag antibody and analyzed on a 10% SDS-polyacrylamide gel. Proteins were transferred to PVDF membrane and subsequently stained with Coomassie brilliant blue R250. Slower: slower migrating form of the TPR domain; Faster: faster migrating form of the TPR domain.

approach, we treated the recombinant TPR domain with OA in RRL, immunoprecipitated it using anti-FLAG-tag antibody and treated it with alkaline phosphatase (AP) *in vitro*. Consistent with being caused by phosphorylation, the electrophoretic mobility shift of TPR induced by OA was abolished by AP treatment (Fig. 32A). In the second and more straightforward approach, we radiolabeled the recombinant TPR domain with [γ-^{32}P]ATP in RRL in the presence or absence of OA. Whereas trace level of [^{32}P]-labeling of TPR was observed in the absence of OA, the labeling intensity was enhanced substantially in its presence. More importantly, after superimposing the [^{32}P]-autoradiogram with the immunoblotted membrane, we found that the [^{32}P]-labeled protein band corresponded precisely to the slower migrating form of TPR, further supporting our hypothesis that phosphorylation occurs on the TPR domain of PP5 and correlates directly with its electrophoretic mobility shift on SDS-PAGE (Fig. 32B). The fact that only in the presence of OA did we observe the significant level of phosphorylation on TPR also suggests that it is a reversible process controlled by specific protein kinase(s) and phosphatase(s).

b) Protein kinase A phosphorylates the TPR domain of PP5-To investigate whether the OA-induced phosphorylation of the TPR domain occurs on the potential PKA site mentioned above, we examined the effect of cyclic AMP (cAMP), the physiological activator of PKA, on the electrophoretic mobility of the recombinant TPR in RRL. As shown in Fig. 33A, cAMP caused a small fraction of the TPR molecules to undergo the same electrophoretic mobility shift as that caused by OA. More significantly, simultaneous treatment of cAMP and OA quantitatively shifted all TPR molecules to

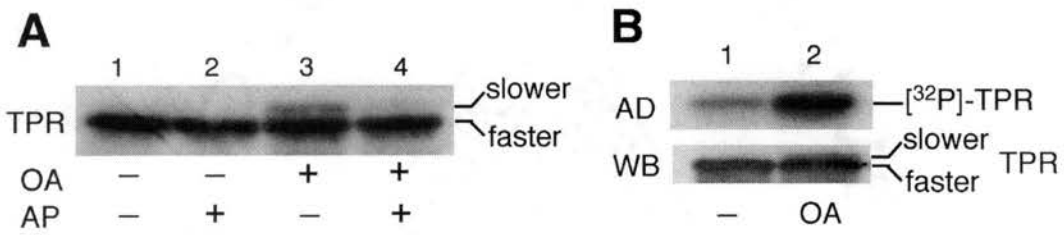

Figure 32. The okadaic acid (OA)-induced electrophoretic mobility shift of TPR results from phosphorylation. **A)** Alkaline phosphatase (AP) treatment of the TPR domain. Purified recombinant TPR domain was reconstituted into RRL mixtures containing 500 nM okadaic acid (*lanes 3 and 4*) or its inactive analog okadaic acid-7,10,24,28-tetraacetate (*lanes 1 and 2*) and incubated at 30 °C for 40 min. Reactions were then subjected to immunoadsorption using the anti-FLAG-tag antibody, and the resin-bound TPR domain was treated with alkaline phosphatase (AP) (*lanes 2 and 4*) or equal volumes of enzyme-free buffer (*lanes 1 and 3*) at 37 °C for 1 hr as described under "Materials and Methods". Reactions were terminated by boiling SDS sample buffer and samples were subsequently analyzed on a 10% SDS-polyacrylamide gel. Proteins were transferred to PVDF membrane and immunoblotted with the anti-FLAG-tag antibody. **B)** [^{32}P]-labeling of the reconstituted TPR domain in RRL. Purified recombinant TPR domain was reconstituted into RRL containing 500 nM okadaic acid (*lane 2*) or okadaic acid-7,10,24,28-tetraacetate (*lane 1*), incubated at 30 °C for 5 min followed by addition of [γ-^{32}P]ATP and another 15 min incubation. RRL mixtures were subsequently immunoadsorbed by the anti-FLAG-tag antibody, separated on a 10% SDS-polyacrylamide gel, transferred to PVDF membrane and analyzed by autoradiography (AD). The same membrane was also Western blotted with the anti-FLAG-tag antibody and used to superimpose against the [^{32}P]-autoradiogram (WB). Slower: slower migrating form of the TPR domain; Faster: faster migrating form of the TPR domain.

their slower migrating form. These findings strongly suggest that PKA phosphorylates the TPR domain of PP5 at the above mentioned consensus site (Ser-160), and that such a site is readily dephosphorylated in RRL, and possibly *in vivo*, by certain protein phosphatase(s).

To confirm these observations, we carried out an *in vitro* PKA kinase assay using the recombinant TPR domain as the substrate (Fig. 33B). The constitutively active catalytic subunit of PKA was used and cAMP (which activates PKA through binding to the regulatory subunit) was omitted from the reaction. As we expected, incubation with the PKA catalytic subunit shifted almost the entire population of the TPR molecules to the slower migrating form, showing that the TPR domain was nearly quantitatively phosphorylated by PKA *in vitro*. Taken together, our data strongly suggested that PKA phosphorylates PP5 in its TPR domain, which may represent an important mechanism by which PP5 function is regulated *in vivo*.

c) MALDI-TOF mass spectrometry analysis of phosphorylation site(s) in PP5 TPR-To gain more direct evidence for the PKA-catalyzed phosphorylation at Ser-160 of the TPR domain of PP5, we analyzed its two distinct migrating forms using MALDI-TOF mass spectrometry. Purified recombinant TPR was treated with OA in RRL, immunoprecipitated and separated on SDS-PAGE. Gel pieces containing faster or slower migrating forms of TPR were excised and subjected to in-gel digestion with trypsin or V8 Glu-C. Resulting peptide mixtures were subsequently analyzed by MALDI-TOF MS. Useful information was obtained by comparing the experimental peptide mass fingerprint with that predicted based on the amino acid sequence of the recombinant TPR

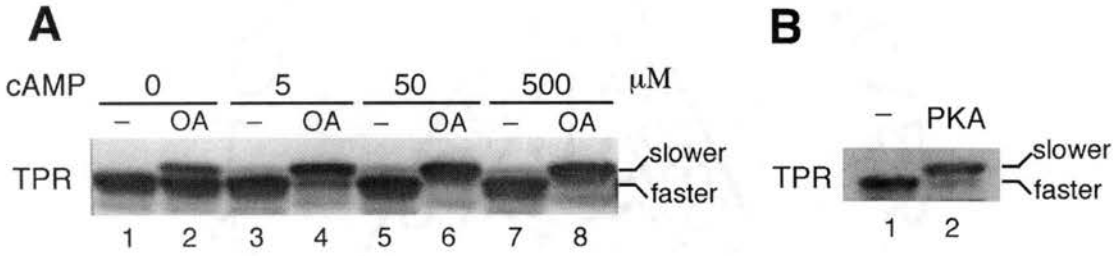

Figure 33. Protein kinase A (PKA) phosphorylates the TPR domain of PP5 *in vitro*. **A)** Purified recombinant TPR domain of PP5 was reconstituted into RRL containing 500 nM okadaic acid (OA, *even-number lanes*) or its inactive analog okadaic acid-7,10,24,28-tetraacetate (-, *odd-number lanes*) in the absence (*lanes 1 and 2*) or presence of 5 μM (*lanes 3 and 4*), 50 μM (*lanes 5 and 6*) and 500 μM (*lanes 7 and 8*) cyclic AMP (cAMP). Reactions were incubated at 30 °C for 40 min and immunoabsorbed by the anti-FLAG-tag antibody. Proteins were analyzed on a 10 % SDS-polyacrylamide gel, transferred to PVDF membrane, and immunoblotted with the anti-FLAG-tag antibody. **B)** Purified recombinant TPR domain was treated with the catalytic subunit of PKA at 30 °C for 1 hr (*lane 2*) as described under "Materials and Methods". A control reaction containing the same amount of TPR but lacking PKA was carried out in parallel (*lane 1*). Reactions were terminated by mixing with the SDS sample buffer, separated on a 10% SDS-polyacrylamide gel, transferred to PVDF membrane and analyzed by staining with Coomassie brilliant blue R250. Slower: slower migrating form of the TPR domain; Faster: faster migrating form of the TPR domain.

domain as a result of partial or complete digestion by trypsin or V8 Glu-C. In doing so with the trypsin digestion of the faster TPR migrating form, we identified a peptide with a measured mass of 2313.67 Da which corresponds to the calculated mass (2314.06 Da) of a predicted TPR fragment spanning residues 160-180 and containing the consensus PKA site Ser-160 along with three other serines and one threonine (Ser-164, Ser-169, Ser-177 and Thr-171). Interestingly, this peptide was not found in the spectrum of the slower migrating form of TPR. Instead, we detected a 2394.46 Da peptide, which is approximately 80 Da higher than that found for the faster migrating form of TPR. Similarly, a predicted TPR peptide resulting from partial trysinolysis that spans residues 159-180 (2470.17 Da) and contains all five above mentioned serine/threonine residues was identified for the faster, but not the slower migrating form of TPR, whereas a peptide of 80 Da higher (2549.16 Da) was found for the slower migrating form of TPR only (Table 4). These findings suggest that one of the five serine/threonine residues within the TPR peptide containing residues 160-180 is phosphorylated in response to OA and cAMP treatment, which correlates with the electrophoretic mobility shift. It is also important to note that the consensus phosphorylation site for PKA, Ser-160, resides in this peptide.

To more closely define the phosphorylation site, in-gel digest of the TPR domain was carried out using a different protease, V8 Glu-C which is capable of generating an entirely different peptide mass fingerprint of a protein from that generated by trypsin. In doing so, we detected a peptide of 1425.99 Da that corresponds to the calculated mass (1425.74 Da) of a predicted TPR fragment spanning residues 157-168 and containing Ser-160 and Ser-164 for the faster but not the slower migrating form of TPR, whereas a peptide with a molecular mass roughly 80 Da higher (1505.57 Da) was

Recombinant TPR		Measured mass (Da)	Calculated mass (Da)	Covered sequence
Slower form	Faster form			
	√	2313.67	2314.06	S^{160}VVDSLDIESMTIEDEYSGPK^{180}
√		2394.46	2314.06+80(PO_3)	**S**^{160}VVD**S**LDIE**S**M**T**IEDEY**S**GPK^{180}
	√	2470.23[a]	2470.17[a]	R^{159}SVVDSLDIESMTIEDEYSGPK^{180}
√		2549.16[a]	2470.17+80(PO_3)[a]	R^{159}**S**VVD**S**LDIE**S**M**T**IEDEY**S**GPK^{180}

[a] peptides resulting from partial trypsin digest

Bold and underlined serine residues represent the potential phosphorylation sites

Table 4. MALDI-TOF MS analysis of tryptic peptides of recombinant TPR domain

only observed for the slower migrating form. Additionally, a peptide (2138.09 Da) spanning residues 150-168 which resulted from partial V8 Glu-C digestion was identified for the faster migrating form of TPR, whereas a peptide with a molecular mass approximately 80 Da higher (2218.09 Da) was found for its slower migrating form instead (Table 5). Therefore, the putative phosphorylation site of TPR was successfully narrowed down to two candidates, Ser-160 and Ser-164 one of which is the consensus phosphorylation site for PKA.

d) Site-directed mutagenesis studies of Ser-160 and Ser-164 in PP5 TPR--To verify the MALDI-TOF MS data and identify the exact phosphorylation site in the TPR domain of PP5, we mutated the two candidate residues, Ser-160 and Ser-164 to alanines individually and examined their electrophoretic behaviors in response to OA and cAMP treatments. Significantly, the recombinant S160A mutant of TPR lost its ability to undergo the electrophoretic mobility shift in response to OA and cAMP treatments, whereas the S164A mutant behaved the same as the wild type TPR (Fig 34A & B). Therefore, our data clearly demonstrated that Ser-160 is the phosphorylation site in the TPR domain of PP5 whose modification by PKA is stimulated by OA and cAMP treatments.

2) Met-3 mutant of HRI:

a) Quantitative transformation of Met-3 mutant of HRI in response to heme-deficiency in RRL-Transformation and activation of HRI is accompanied by autophosphorylation as well as its characteristic electrophoretic mobility shift on SDS-PAGE. To identify the phosphorylation sites on HRI which become modified upon activation, we faced the

Recombinant TPR		Measured mass (Da)	Calculated mass (Da)	Covered sequence
Slower form	Faster form			
	√	1425.99	1425.74	H^{157}RRSVVDSLDIE^{168}
√		1505.57	1425.74+80(PO_3)	H^{157}RR<u>S</u>VVD<u>S</u>LDIE^{168}
	√	2138.64 [a]	2138.09 [a]	R^{150}AIAGDEHRRSVVDSLDIE^{168}
√		2219.05 [a]	2138.09+80(PO_3) [a]	R^{150}AIAGDEHRR<u>S</u>VVD<u>S</u>LDIE^{168}

[a] peptides resulting from partial V8 Glu-C digest

Table 5. MALDI-TOF MS analysis of V8 Glu-C-generated peptides of recombinant TPR domain

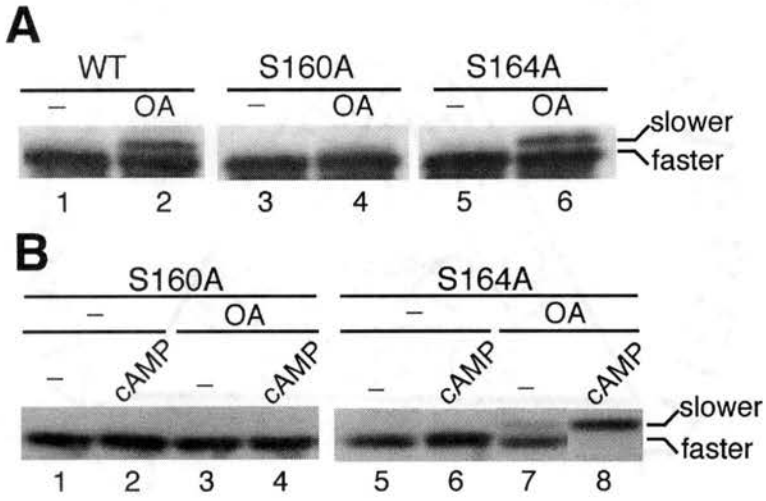

Figure 34. S160A mutant of the TPR domain is unable to undergo the electrophoretic mobility shift induced by okadaic acid (OA) and cyclic AMP (cAMP). **A)** Purified recombinant wild type (*lanes 1 and 2*), S160A (*lanes 3 and 4*) and S164A (*lanes 5 and 6*) mutants of the TPR domain were reconstituted into separate RRL reactions containing 500 nM okadaic acid (OA, *lanes 2, 4 and 6*) or its inactive analog okadaic acid-7,10,24,28-tetraacetate (-, *lanes 1, 3 and 5*) and incubated at 30 °C for 40 min. Proteins were separated on a 10% SDS-polyacrylamide gel, transferred to PVDF membrane and immunoblotted with the anti-FLAG-tag antibody. **B)** Purified recombinant S160A (*lanes 1-4*) and S164A (*lanes 5-8*) mutants of the TPR domain were reconstituted into RRL reactions lacking (*lanes 1 and 5*) or containing 500 nM okadaic acid (OA, *lanes 3 and 7*), 50 μM cAMP (*lanes 2 and 6*) or a combination of both (*lanes 4 and 8*), and incubated at 30 °C for 40 min. Proteins were separated on a 10% SDS-polyacrylamide gel, transferred to PVDF membrane and immunoblotted with the anti-FLAG-tag antibody. Slower: slower migrating form of the TPR domain; Faster: faster migrating form of the TPR domain.

challenge of obtaining a homogenous population of transformed/activated HRI molecules. Unfortunately in RRL, for some unknown reasons only half of the *de novo* synthesized HRI molecules are able to transform into the slower migrating form in response to heme-deficiency. Due to the difficulty in separating the two closely-migrating forms of wild-type HRI on SDS-PAGE, we turned to the Met-3 mutant of HRI which lacks the majority of the N-terminal heme-binding domain. Previous studies have indicated that it is much less heme-responsive than the wild-type HRI, therefore it may be regulated differently in terms of the ability to autophosphorylate and activate in response to heme-deficiency (192). Surprisingly, upon incubation in heme-deficient RRL for 3 hours, newly synthesized Met-3 almost quantitatively transformed into the slower migrating form, an observation that has never been made for the wild-type HRI under the same condition (Fig. 35). Based on the assumption that the electrophoretic mobility is caused, at least partially, by phosphorylation events, Met-3 mutant appeared to be a better choice for identifying phosphorylation sites of HRI than the wild-type protein because of the ease of obtaining its transformed and phosphorylated form in homogeneity.

b) MALDI-TOF mass spectrometry analysis of phosphorylation sites in Met-3 mutant of HRI--Following quantitative transformation in heme-deficient RRL, (His_7)-Met-3 was immunoprecipitated and applied on SDS-PAGE from which gel pieces containing the transformed (His_7)-Met-3 were excised and subjected to in-gel trypsin digestion. As the presumed hypophosphorylated control, (His_7)-Met-3 was also synthesized and matured in heme-supplemented RRL containing GA (a specific inhibitor of Hsp90 which is essential for HRI maturation) to prevent any transformation and activation from occurring, and

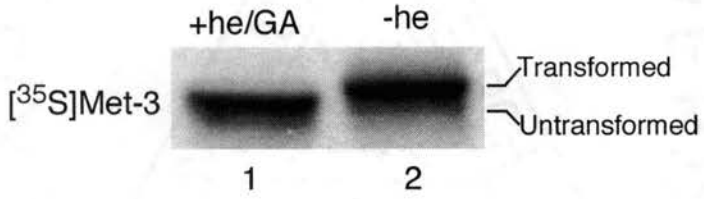

Figure 35. Met-3 mutant of HRI undergoes quantitative transformation into the slower migrating form on SDS-PAGE upon 3 hr incubation in heme-deficient RRL. Met-3 mutant of HRI was synthesized in TnT RRL at 30 °C for 15 min, followed by a 4-min pulse-label with [^{35}S]Met. [^{35}S]-Met3-containing TnT RRL was subsequently transferred into 7 volumes of heme-supplemented RRL containing geldanamycin (*lane 1*) or normal heme-deficient RRL mix (*lane 2*) and incubated at 30 °C for 1 hr. Aliquots of both reactions were analyzed on an 8% SDS-polyacrylamide gel and visualized by autoradiography. Transformed: transformed HRI with slower electrophoretic mobility; Untransformed: untransformed HRI with faster electrophoretic mobility.

subjected to the same in-gel digest procedures. The resulting peptide mixtures of both forms of (His_7)-Met-3 were then analyzed by MALDI-TOF mass spectrometry. After comparing the experimental spectra with the calculated peptide mass fingerprint produced by partial or complete trypsin digestion of (His_7)-Met-3, we identified a peptide with a measured mass of 2067.01 Da which corresponds to the calculated mass (2067.06 Da) of a predicted (His_7)-Met-3 peptide spanning residues 249-266 (numbering based on the wild-type rabbit HRI) and containing two serines, Ser-255 and Ser-260. However, this peptide was only observed for the untransformed (His_7)-Met-3. As to the transformed (His_7)-Met-3, a different peptide with a molecular mass roughly 80 Da higher (2147.04 Da) was detected in the spectrum, indicating that the peptide spanning residues 249-266 was phosphorylated either on Ser-255 or 260. Supporting this hypothesis, partial trypsin digestion of the untransformed (His_7)-Met-3 generated a peptide (2757.34 Da) that corresponds to a predicted fragment (2757.39 Da) spanning residues 249-272 and harboring the same two serines. However, in the spectrum of the transformed (His_7)-Met-3, a peptide with a measured mass approximately 80 Da higher (2837.25 Da) was found instead (Table 6). Further evidence for the single-site phosphorylation between residues 249 and 272 included the finding that following post-source decay (PSD) of the 2837.25 Da peptide, a novel fragment (2739.25 Da) of 98 Da smaller was detected, characteristic of the metastable decomposition of the phosphate group (H_3PO_4) from the parent peptide. Furthermore, PSD-assisted amino acid sequencing of the 2757.34 Da peptide confirmed its identity as the region spanning residues 249-272 of HRI. Therefore, our data suggested that either Ser-255 or Ser-260

(His_7)-Met-3		Measured mass (Da)	Calculated mass (Da)	Covered sequence
transformed	untranformed			
	√	2067.01	2067.06	V^{249}PIQLPSLEVLSDQEEDR^{266}
√		2147.04	2067.06+80(PO_3)	V^{249}PIQLP**S**^{255}LEVL**S**^{260}DQEEDR^{266}
	√	2757.34[a,b]	2757.39[b]	V^{249}PIQLPSLEVLSDQEEDR DQYGVK^{272}
√		2837.25[b]	2757.39+80(PO_3)[b]	V^{249}PIQLP**S**^{255}LEVL**S**^{260}DQEEDR DQYGVK^{272}

[a] peptide sequenced by post-source decay (PSD)
[b] peptides resulting from partial trypsin digest
Bold and underlined serine residues represent the candidate phosphorylation sites.

Table 6. MALDI-TOF MS analysis of tryptic peptides of (His_7)-Met-3

becomes phosphorylated upon HRI transformation and activation in response to heme-deficiency.

Discussion:

Driven by the hypothesis that reversible phosphorylation occurs on and functionally regulates both HRI and PP5, we have searched and found strong evidence for specific phosphorylation sites on both proteins using a combination of biochemical, molecular biological and MALDI-TOF mass spectrometry analyses. Out of multiple elusive phosphorylation sites on HRI (9), we have successfully detected one in its unique kinase insertion sequence (between the two conserved kinase subdomains) and narrowed the possibility down to two candidates, Ser-255 or Ser-260. As to PP5, a novel phosphorylation site was identified at Ser-160, which is located near the end of the extended seventh helix of its N-terminal TPR domain (53). The possible significances of these two sites are discussed below.

Early studies indicated that phosphorylation level of HRI correlate with its kinase activity (70). Recently, Bauer *et al* found that HRI is multiply phosphorylated at serine, thereonine and to a lesser extent, tyrosine residues upon activation, which is essential for HRI to adopt the stable and active conformation as a homodimer (9). However, their identities remain elusive. Based on the recent identification of two conserved phosphorylation sites in the activation loop of PKR (Thr-446, Thr-451) and GCN2 (Thr-882, Thr-887) (201) and the striking similarities within the kinase domains of eIF2α kinases (34), it is tempting to speculate that the corresponding sites (Thr-483, Thr-488) in the activation loop of HRI are also phosphorylated upon activation. As with most other kinases, possible phosphorylation of the activation loop of HRI is expected to activate it

by inducing local conformational changes within its active site and consequently altering its binding affinities for substrate (55, 265) or ATP, or changing the phosphoryl transfer reaction itself (2, 119).

One common feature shared by many protein kinases is the ability of phosphorylation within their regulatory domains/sequences to alter their functions in distinct ways. Besides the conserved kinase domain, HRI contains two additional regulatory domains: an N-terminal heme-binding domain (HBD) and an insertion sequence (KIS) located between its two kinase lobes (32). The HBD bears the major heme-binding site of HRI whose stable occupation by heme is thought to play a role in facilitating the proper folding and maintaining the stability of HRI in reticulocytes (247). Interestingly, KIS has recently been identified as the possible second heme-binding domain of HRI. In contrast to HBD, KIS binds heme rather weakly but reversibly, and is thought to be responsible for the rapid down-regulation of HRI activity by heme (192). In addition, KIS seems to undergo multiple phosphorylations as indicated by the reproducible laddering appearance of its different electrophoretic migrating forms on SDS-PAGE (data not shown). Significantly, such a hypothesis was strongly supported by our evidence here for specific phosphorylation of Ser-255 or Ser-260 within KIS upon activation of HRI by heme-deficiency. However, its functional importance remains unclear at this point. Our initial studies in which either Ser-255 or Ser-260 was mutated to alanine failed to result in any significant changes in the eIF2α kinase activity of HRI in response to heme-deficiency (data not shown). It then seems that this particular phosphorylation event in KIS is not essential for the activation of HRI by heme-deficiency. This is not totally unexpected given the huge number of potential

phosphorylation sites on HRI and the complexity and possible redundancy of their individual and/or coordinated effects on HRI function. Therefore, simply mutating one of its autophosphorylation sites may not be able to generate detectable, if any, phenotypic changes of the HRI protein.

Alternatively, phosphorylation of Ser-255 or Ser-260 may alter functional aspect(s) of HRI other than the activation process induced by heme-deficiency *per se*. One good candidate is the heme-binding ability of KIS. We speculate that phosphorylation within KIS inhibits its ability to bind heme and conversely heme-binding to KIS inhibits its multiple phosphorylation. This speculation is based on several lines of evidence. 1) Heme-binding and multiple phosphorylation have opposing effects on HRI function. While the former down regulates HRI kinase activity (70, 246), the latter is essential for its activation (9). 2) Heme-binding has been reported to inhibit ATP binding by HRI (33), which may potentially prevent HRI from autophosphorylating within and/or outside the KIS and transforming into the active state. 3) The phosphorylation level of HRI reciprocally correlates with its readiness of being repressed and bound by heme. While transformed HRI with moderate level of phosphorylation is readily repressed by heme, hyperactivated and hyperphosphorylated HRI becomes much less sensitive to inhibition by heme (32, 70). Considering the possible role of KIS in reversible heme-binding and rapid down-regulation of HRI activity, it is tempting to speculate that multiple phosphorylations within KIS primarily regulate the transition of HRI from the low-activity/heme-sensitive state to the high-activity/heme-resistant state. Future experiments designed to compare the heme-responsiveness of transformed wild type and S255A or S260A mutants of HRI at finer scales may shed light on such a

hypothesis. Nonetheless, the exact mechanism by which heme-binding and multiple phosphorylation of HRI counteract each other is probably very complicated and difficult to determine until more phosphorylation sites are identified in future studies.

Over the past few years, various studies on PP5 clearly demonstrated the importance of its TPR domain for its biological function. First, TPR domain targets the catalytic domain of PP5 to specific client and partner proteins. Second, TPR domain inhibits the phosphatase activity of PP5, presumably by binding directly to and interfering with the catalytic domain. Finally, TPR domain is believed to possess the binding site for the polyunsaturated fatty acid activators of PP5, such as arachidonic acid, which relieves the autoinhibition by freeing the catalytic domain from the physical masking by the TPR domain (41). Here in this report this domain becomes more interesting with our novel finding that it undergoes reversible phosphorylation. The phosphorylation site, Ser-160, is located near the end of the last α helix of the TPR domain, which is positioned at the junction between the TPR and phosphatase domains (Fig. 36) (53). One could easily imagine that introducing a phosphate group at an inter-domain junction would cause dramatic conformational changes of the protein as a result of tightening or loosening of the domain-domain interactions. Such examples have been well established in many protein kinases where single-site phosphorylation of the activation loop, sandwiched by two kinase lobes, triggers conformational changes far beyond the phosphorylation site, and ultimately leads to kinase activation (119). As for PP5, such a global conformational change induced by single-site phosphorylation at Ser-160 is also possible, and the controlled opening and closing of the two-domain structure

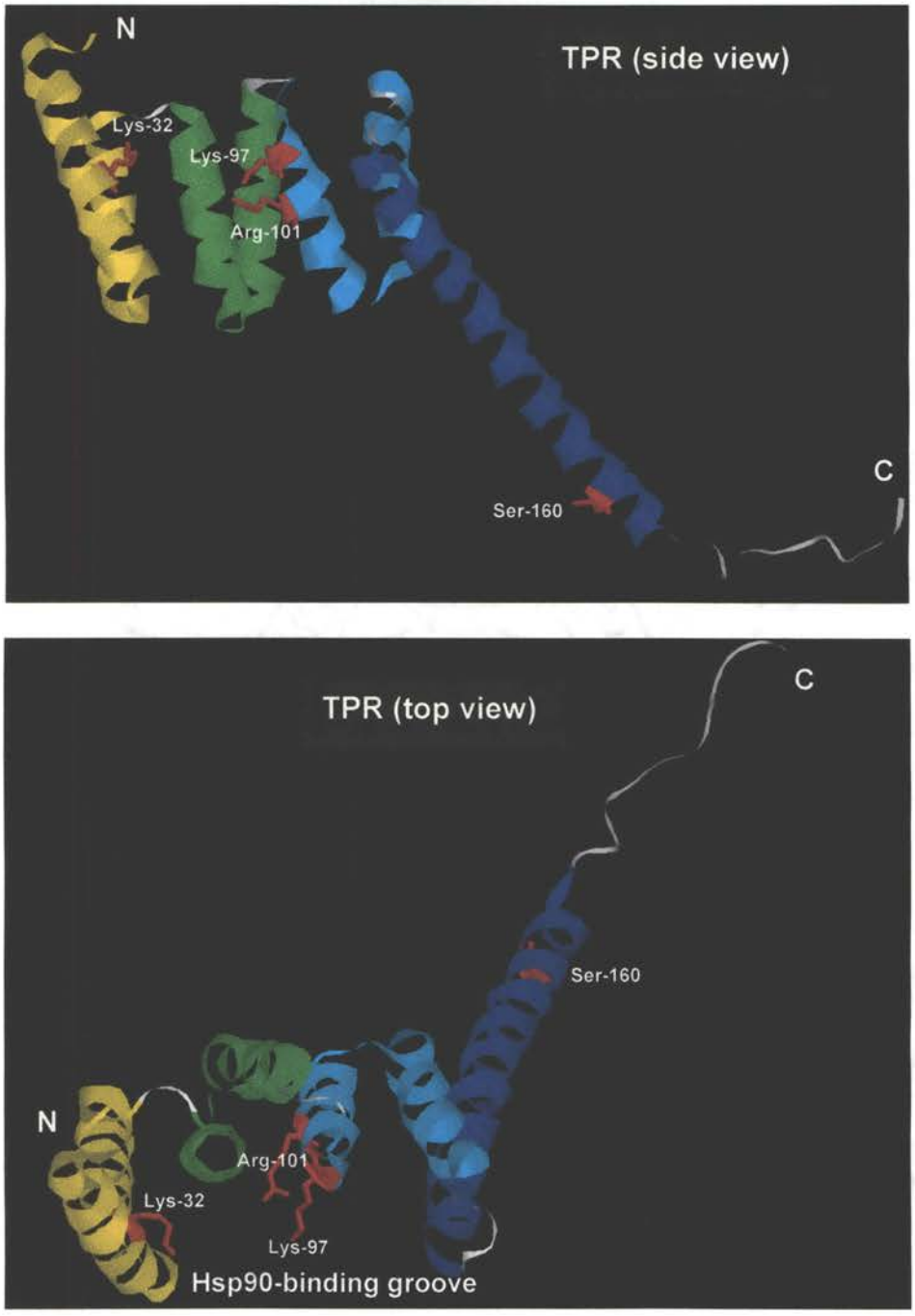

Figure 36. Crystal structure of the isolated TPR domain of PP5 (PDB code, 1A17) shown in ribbons. Ser-160 which was identified as the *in vitro* phosphorylation site is labeled and shown in sticks. It is located towards the end of the extended seventh α-helix of the TPR domain. Lys-32, Lys-97 and Arg-101 which are involved in interacting with the C-terminus of Hsp90 are also labeled and shown in sticks. They are located in the first and fifth α-helices but all within and pointing to the center of the Hsp90-binding groove of the TPR domain (*top view*).

of PP5 may consequently relieve or maintain the autoinhibition of its phosphatase activity by the TPR domain.

Unfortunately, our preliminary data do not seem to support such a hypothesis. Mutagenesis studies in which Ser-160 is mutated to either alanine or glutamate showed little impact on the phosphatase activity of PP5 when assayed *in vitro* using p-nitrophenyl phosphate (pNPP) as the substrate. Although we can not rule out the possibility that phosphorylation of Ser-160 is functionally unimportant to PP5, the failure of the mutations to alter the phosphatase activity of PP5 could be due to other reasons. 1) PP5 purified from *E. coli* is likely to be quantitatively unphosphorylated due to its efficient auto-dephosphorylation and the lack of appropriate protein kinases. This hypothesis is supported by the finding that even in the eukaryotic RRL system which contains its putative kinase PKA, little phosphorylation of TPR could be detected without addition of the phosphatase inhibitor (Fig. 31), suggesting that the equilibrium of the reversible phosphorylation on Ser-160 is normally in favor of the dephosphorylation reaction. Therefore, it is highly possible that both the wild type PP5 and the S160A mutant that we tested were equally unphosphorylated, which then explains their same levels of phosphatase activities. As to the S160E mutant, although in many cases the monoanionic glutamate closely mimics the dianionic phospho-serine, subtle differences still exist in their three-dimensional structures, hydrogen bonding properties and charges, which are the key determinants of specific phosphorylation-induced structural and functional changes of proteins. Therefore it is possible that the S160E mutant can not imitate the phosphorylated state of PP5 well enough, which then explains their similar levels of phosphatase activity. 2) Although pNPP is routinely used as the *in vitro* substrate for

most protein phosphatases, its simple structure must be very different from those of the true physiological substrates of the phosphatases. Therefore, subtle conformational changes of PP5 caused by phosphorylation (or the phosphorylation-mimicking S/E mutation) that are sufficient to alter its activity towards the true clients might be blind to the small pNPP molecule. It thus seems difficult to address the true functional significance of this phosphorylation event for PP5 until its physiological substrates are identified.

Alternatively, instead of affecting the catalytic activity of PP5, phosphorylation of Ser-160 may be regulating other aspects of PP5 function. One possible mechanism is that it alters the binding affinity of the TPR domain for specific set(s) of PP5 substrates and/or partners. TPR domains consisting of multiple TPR motifs have the potential to possess distinct binding sites for different proteins (128, 244). Containing three TPR motifs, the single TPR domain of PP5 may be able to interact with different proteins via different binding sites. In fact, such a possibility has already been suggested by the recent finding that an edge of the TPR domain of PP5 that is outside the main Hsp90-binding groove may be interacting with its phosphatase domain and responsible for autoinhibition (121). It is also similarly implicated by our observation that the TPR domain of PP5 interacts with Hsp90 and HRI simultaneously and its interaction with HRI is not entirely mediated by Hsp90, which indicates a separate binding site of the TPR domain for HRI that is different from that for Hsp90 (Chapter III, Figure 16). Reversible phosphorylation of Ser-160 may serve as a conformational switch for the TPR domain of PP5 which shifts its binding affinity in favor or disfavor of specific client or partner proteins in response to different cellular conditions. Indeed, mounting evidence suggests

a general role of reversible phosphorylation in regulating protein-protein association/dissociation (118). Such examples include phosphorylation-induced association between the CREB (cyclic AMP response element binding protein) and CBP (CREB binding protein) (190, 191), phosphorylation-promoted dimerization of STAT (signal transducers and activators of transcription) (40), and phosphorylation-induced dissociation of the inactivation domain from the K^+ channel (4) and that of Rb (Retinoblastoma tumor suppressor protein) from its various targets (123). Three-dimensional structures of these protein revealed that in some cases phosphorylation alters protein-protein interaction through electrostatic repulsion or attraction, which causes conformational changes near or distant from the phosphorylation sites. Nonetheless, novel physiological interacting proteins of PP5 need to be identified in order to examine such a hypothesis. Finally, phosphorylation of Ser-160 may be involved in some yet unknown aspects of PP5 function, or it may regulate PP5 in redundancy with other unidentified phosphorylation site(s), because of which mutating one can not generate phenotypic changes.

CHAPTER VI

Summary

The 90-kDa heat shock protein (Hsp90) is an abundant and essential molecular chaperone in eukaryotic cells. Contrary to other members of the chaperone family, only a small number of *in vivo* substrates have been identified for Hsp90 to date, and the most common feature shared by these known Hsp90 clients is that the majority of them play critical roles in cellular signal transduction. In all these cases, association of the client proteins with Hsp90 is essential for their stability and/or activity. While the underlying mechanism of Hsp90 function still remains largely unknown, studies over the past decade revealed that its *in vivo* chaperone activity is differentially, yet coordinately regulated by a highly conserved group of proteins, the so-called cohorts or co-chaperones. In this study, we focused on two of these co-chaperones, namely $p50^{cdc37}$ and protein phosphatase 5 (PP5) and examined their roles in the Hsp90-dependent biogenesis of the heme-regulated eIF2α kinase (HRI), which has been previously established to be an *in vivo* substrate of Hsp90. In addition, we also studied the structure-function relationship of $p50^{cdc37}$ and obtained an authentic domain structure in which its kinase- and Hsp90-binding activities are segregated into two different regions. Finally, since regulatory proteins are often subjected to functional controls themselves, we sought to examine the possibility that PP5 undergoes post-translational phosphorylation and if so, where the phosphorylation site(s) is (are). Summarized below are the key points of this study which shed new light on our current understanding of the Hsp90 chaperone system and require further investigations.

$p50^{cdc37}$ and PP5-"nonexclusive rivals on the same team": Functional analyses of the client protein HRI clearly demonstrated the difference between the two Hsp90 cohorts, $p50^{cdc37}$ and PP5, with regards to their regulatory effects on HRI and possibly other substrates. $p50^{cdc37}$, in concert with Hsp90, facilitates the maturation and activation of HRI in response to its natural stimulus, heme-deficiency. In contrast, pharmacological evidence suggests that PP5 inhibits such a process. While the actions of these two Hsp90 co-chaperones on HRI are poorly understood mechanistically at this moment, one surprising finding was that both $p50^{cdc37}$ and PP5 can be recovered in the same Hsp90 heterocomplex, and their coexistence can be further enhanced by the presence of the client protein HRI. Although this result is contradictory to the prevailing hypothesis that $p50^{cdc37}$ and the TPR-containing cohorts of Hsp90 are mutually exclusive with regards to their binding to Hsp90 (223), it strongly supports the authenticity of our earlier finding that $p50^{cdc37}$ and another TPR-containing cohort of Hsp90, FKBP52, coexist in both the basal and client-bound Hsp90 heterocomplexes (97). As discussed in the early sections, the apparent discrepancy between our finding and others is likely related to the fact that Hsp90 exists and functions as a dimer in which each monomer binds a different cohort (Fig. 37). It is possible that within the simple reductionist system of an *in vitro* competition assay, which has been primarily used to build the "mutually exclusive" model (as opposed to the quasi-physiological RRL system that we used here), certain elements could be missing that are critical for the formation of a "proper" Hsp90 dimer, which has the ability to accommodate both $p50^{cdc37}$ and a TPR-containing cohort. Considering the dynamic and complex nature of Hsp90 structure and function, which are controlled by both nucleotides and various binding partners, a better and more complete

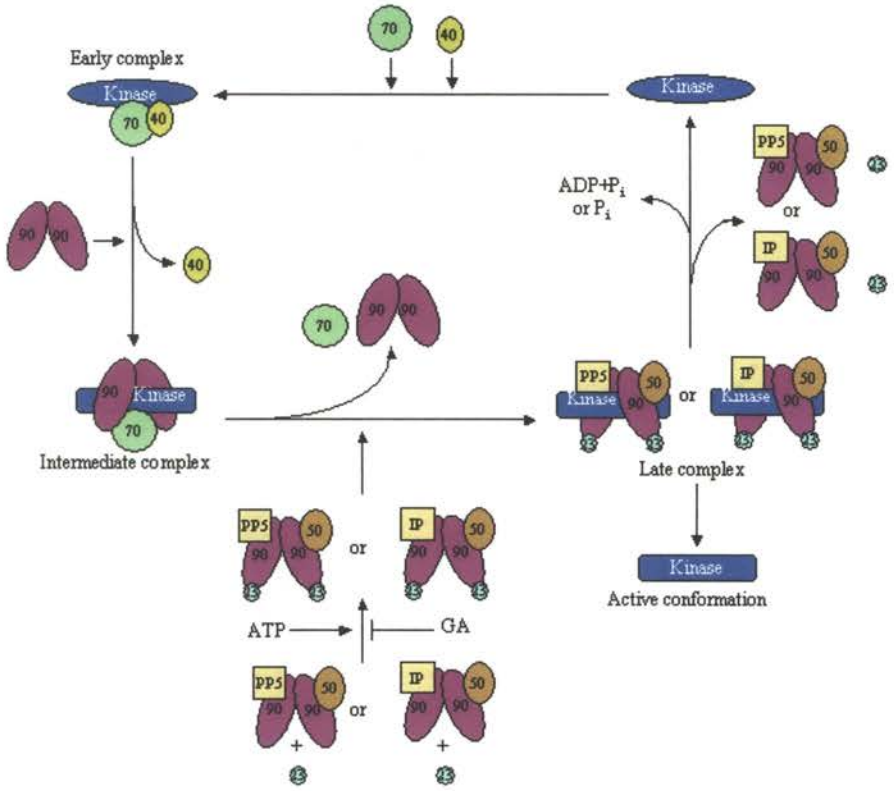

Figure 37. Proposed chaperone pathway for the maturation/activation of protein kinases by Hsp90 machinery. This model was built upon our current knowledge of the maturation and activation of some of the Hsp90-dependent protein kinases as well as the postulation that protein kinases share a similar Hsp90-mediated folding pathway as the steroid hormone receptors (SHRs) (Fig. 1). However, this is very likely to be a simplified model, and inaccuracy may exsit due to our incomplete understanding of this pathway. Hsp90-dependent protein kinases enter the cyclic pathway by binding to the Hsp70 system containing its co-chaperone Hsp40/DnaJ. Currently, it is not known whether p48/Hip and p60/Hop (see Chapter 1) are involved in the folding pathway of protein kinases, thus they are not included here. We call this kinase/Hsp70/Hsp40 heterocomplex "the early complex" based on the presumed similarity between the folding pathways of Hsp90-dependent protein kinases and SHRs. The early complex proceeds to the "intermediate complex" as a result of dissociation of Hsp40/DnaJ (which is proposed on the basis of the SHR folding pathway) and association of an Hsp90 dimer. Hsp90 and Hsp70 in the intermediate complex are subsequently replaced by an Hsp90 dimer, which is bound by p50^{cdc37} at one monomer and an immunophilin or protein phosphatase 5 (PP5) at the other. The coexistence of p50^{cdc37} and a TPR-containing cohort on an Hsp90 dimer is suggested by our recent finding that p50^{cdc37} can be co-adsorbed from the rabbit reticulocyte lysate in anti-FKBP52 and anti-PP5 immunoprecipitations (97, 215). The same Hsp90 dimer also contains p23, whose binding requires the ATP-bound conformation of Hsp90 and is inhibited by geldanamycin. The resulting "late complex" subsequently dissociates, which is supposedly promoted by ATP hydrolysis of Hsp90. The protein kinases either become folded, active and Hsp90-independent, or reenter the pathway for further rounds of folding until they reach their folded and active states.

understanding of its *in vivo* function seems to require experimental approaches of more than one type.

The above mentioned data also suggested a model in which the chaperone activity of Hsp90 complexes towards HRI and possibly other client proteins, are functionally coordinated by opposing actions of the two coexisting cohorts, $p50^{cdc37}$ and PP5. This model is consistent with the arising notion that multiprotein complexes or so-called regulatory modules exist *in vivo*, which harbor enzymes or proteins with opposing regulatory activities towards their common targets, thereby enhancing their regulatory efficiency and/or specificity. Within the Hsp90 heterocomplex, although $p50^{cdc37}$ is likely to exert its positive effect on HRI directly (as a chaperone), it is not clear what the true target(s) of PP5 is (are) at this moment. Assuming it is the serine-threonine phosphatase activity of PP5 that is responsible for down-regulating HRI activity, PP5 could dephosphorylate the client protein HRI directly, or alternatively dephosphorylate Hsp90 and/or its other cohorts and alter their chaperone activities. Future studies should be directed towards identifying the true target(s) of PP5 in the Hsp90/client heterocomplexes.

Potential functional regulation of PP5 by post-translational phosphorylation: Studies here successfully identified a post-translational phosphorylation site at Ser-160 in the TPR domain of PP5. Ser-160 is within a consensus phosphorylation site for protein kinase A (PKA) which is able to phosphorylate this site *in vitro*. The phosphorylation site Ser-160 is located at the inter-domain region between the TPR and phosphatase domains of PP5. Despite of the obvious potential of Ser-160 as a phosphorylation-

controlled conformational switch of PP5, mutating it to either alanine or glutamate failed to cause any significant changes in the phosphatase activity of PP5 towards the artificial substrate p-nitrophenyl phosphate. Nonetheless, phosphorylation at Ser-160 could still be important to PP5, with regards to either its phosphatase activity or other functional aspects such as TPR-domain mediated protein-protein interactions with potential substrates and/or partners. To unveil the significance of this phosphorylation site of PP5, future studies should be directed towards identifying more *in vivo* clients or partner proteins of PP5, towards whom its phosphatase activity or binding affinity may be altered by the reversible phosphorylation at Ser-160. Despite of this uncertainty, our result raises the possibility that *in vivo* PP5 function is controlled by post-translational phosphorylation, and tentatively adds it to the growing list of phosphorylation-regulated cohorts of Hsp90, substantiating the notion that regulatory proteins such as molecular chaperones are subjected to functional regulations *in vivo* as well.

Hsc70-a possible binding partner of p50^{cdc37}: Data presented here indicate for the first time, that an interaction between p50^{cdc37} and Hsc70 exists. Supporting this observation is our finding that p50^{cdc37}, within its N-terminal kinase-binding domain (D1), shares a number of conserved residues with the Bag domain, that are directly involved in the binding of Bag-1 to the ATPase domain of Hsc70. The possibility of a direct interaction between p50^{cdc37} and Hsc70, however, does not agree with the current belief that p50^{cdc37} is a component of the late Hsp90/kinase heterocomplex, because Hsp70 is thought to enter the Hsp90 chaperone cycle at the early stages. Nonetheless, given the fact that the current Hsp90 chaperone cycle is built primarily on studies of the steroid hormone

receptors, the chaperone cycle of Hsp90 with the kinase and/or other Hsp90 clients could be quite different. Alternatively, $p50^{cdc37}$ may not be a true Hsp90-specific cohort. Instead, it may cooperate with other chaperones, such as Hsp70 as well, given the complexity and sometimes overlapping pathways of the different molecular chaperone machines *in vivo*. Moreover, considering the existence of a possible Bag domain-like binding surface for Hsp70 in $p50^{cdc37}$, $p50^{cdc37}$ may potentially regulate Hsp70 with regards to its ATP cycle upon binding to its ATPase domain. Thus, $p50^{cdc37}$ may coordinate Hsp70 and Hsp90 functions in a manner that is similar to the proposed function of p60/Hop. Nonetheless, future studies need to be carried out in order to test these speculations.

BIBLIOGRAPHY:

1. **Abbas-Terki, T., O. Donze, and D. Picard.** 2000. The molecular chaperone Cdc37 is required for Ste11 function and pheromone-induced cell cycle arrest. FEBS Lett **467:**111-6.
2. **Adams, J. A., M. L. McGlone, R. Gibson, and S. S. Taylor.** 1995. Phosphorylation modulates catalytic function and regulation in the cAMP-dependent protein kinase. Biochemistry **34:**2447-54.
3. **Anfinsen, C. B.** 1973. Principles that govern the folding of protein chains. Science **181:**223-30.
4. **Antz, C., T. Bauer, H. Kalbacher, R. Frank, M. Covarrubias, H. R. Kalbitzer, J. P. Ruppersberg, T. Baukrowitz, and B. Fakler.** 1999. Control of K+ channel gating by protein phosphorylation: structural switches of the inactivation gate. Nat Struct Biol **6:**146-50.
5. **Bahl, R., K. C. Bradley, K. J. Thompson, R. A. Swain, S. Rossie, and R. L. Meisel.** 2001. Localization of protein Ser/Thr phosphatase 5 in rat brain. Brain Res Mol Brain Res **90:**101-9.
6. **Ban, C., M. Junop, and W. Yang.** 1999. Transformation of MutL by ATP binding and hydrolysis: a switch in DNA mismatch repair. Cell **97:**85-97.
7. **Bardwell, J. C., and E. A. Craig.** 1987. Eukaryotic Mr 83,000 heat shock protein has a homologue in Escherichia coli. Proc Natl Acad Sci U S A **84:**5177-81.
8. **Basso, A. D., D. B. Solit, G. Chiosis, B. Giri, P. Tsichlis, and N. Rosen.** 2002. Akt forms an intracellular complex with Hsp90 and Cdc37 and is destabilized by inhibitors of Hsp90 function. J Biol Chem **9:**9.
9. **Bauer, B. N., M. Rafie-Kolpin, L. Lu, A. Han, and J. J. Chen.** 2001. Multiple autophosphorylation is essential for the formation of the active and stable homodimer of heme-regulated eIF2alpha kinase. Biochemistry **40:**11543-51.
10. **Becker, W., H. Kentrup, S. Klumpp, J. E. Schultz, and H. G. Joost.** 1994. Molecular cloning of a protein serine/threonine phosphatase containing a putative regulatory tetratricopeptide repeat domain. J Biol Chem **269:**22586-92.
11. **Bergerat, A., B. de Massy, D. Gadelle, P. C. Varoutas, A. Nicolas, and P. Forterre.** 1997. An atypical topoisomerase II from Archaea with implications for meiotic recombination. Nature **386:**414-7.
12. **Bijlmakers, M. J., and M. Marsh.** 2000. Hsp90 is essential for the synthesis and subsequent membrane association, but not the maintenance, of the Src-kinase p56(lck). Mol Biol Cell **11:**1585-95.
13. **Blatch, G. L., and M. Lassle.** 1999. The tetratricopeptide repeat: a structural motif mediating protein-protein interactions. Bioessays **21:**932-9.
14. **Blond-Elguindi, S., S. E. Cwirla, W. J. Dower, R. J. Lipshutz, S. R. Sprang, J. F. Sambrook, and M. J. Gething.** 1993. Affinity panning of a library of peptides displayed on bacteriophages reveals the binding specificity of BiP. Cell **75:**717-28.
15. **Bohen, S. P., A. Kralli, and K. R. Yamamoto.** 1995. Hold 'em and fold 'em: chaperones and signal transduction. Science **268:**1303-4.

16. **Borthwick, E. B., T. Zeke, A. R. Prescott, and P. T. Cohen.** 2001. Nuclear localization of protein phosphatase 5 is dependent on the carboxy-terminal region. FEBS Lett **491:**279-84.
17. **Bose, S., T. Weikl, H. Bugl, and J. Buchner.** 1996. Chaperone function of Hsp90-associated proteins. Science **274:**1715-7.
18. **Brautigan, D. L.** 1995. Flicking the switches: phosphorylation of serine/threonine protein phosphatases. Semin Cancer Biol **6:**211-7.
19. **Brown, L., E. B. Borthwick, and P. T. Cohen.** 2000. Drosophila protein phosphatase 5 is encoded by a single gene that is most highly expressed during embryonic development. Biochim Biophys Acta **1492:**470-6.
20. **Brugge, J. S.** 1986. Interaction of the Rous sarcoma virus protein pp60src with the cellular proteins pp50 and pp90. Curr Top Microbiol Immunol **123:**1-22.
21. **Brugge, J. S., and D. Darrow.** 1982. Rous sarcoma virus-induced phosphorylation of a 50,000-molecular weight cellular protein. Nature **295:**250-3.
22. **Brugge, J. S., E. Erikson, and R. L. Erikson.** 1981. The specific interaction of the Rous sarcoma virus transforming protein, pp60src, with two cellular proteins. Cell **25:**363-72.
23. **Buchner, J.** 1999. Hsp90 & Co. - a holding for folding. Trends Biochem Sci **24:**136-41.
24. **Buchner, J.** 1996. Supervising the fold: functional principles of molecular chaperones. Faseb J **10:**10-9.
25. **Bukau, B., and A. L. Horwich.** 1998. The Hsp70 and Hsp60 chaperone machines. Cell **92:**351-66.
26. **Caplan, A. J.** 1999. Hsp90's secrets unfold: new insights from structural and functional studies. Trends Cell Biol **9:**262-8.
27. **Carver, L. A., J. J. LaPres, S. Jain, E. E. Dunham, and C. A. Bradfield.** 1998. Characterization of the Ah receptor-associated protein, ARA9. J Biol Chem **273:**33580-7.
28. **Chadli, A., I. Bouhouche, W. Sullivan, B. Stensgard, N. McMahon, M. G. Catelli, and D. O. Toft.** 2000. Dimerization and N-terminal domain proximity underlie the function of the molecular chaperone heat shock protein 90. Proc Natl Acad Sci U S A **97:**12524-9.
29. **Chen, G., P. Cao, and D. V. Goeddel.** 2002. TNF-induced recruitment and activation of the IKK complex require Cdc37 and Hsp90. Mol Cell **9:**401-10.
30. **Chen, J., B. L. Martin, and D. L. Brautigan.** 1992. Regulation of protein serine-threonine phosphatase type-2A by tyrosine phosphorylation. Science **257:**1261-4.
31. **Chen, J.-J.** 1993. p. 349-372. *In* J. Ilan (ed.), Translational Regulation of Gene Expression 2. Plenum Press, New York.
32. **Chen, J. J., and I. M. London.** 1995. Regulation of protein synthesis by heme-regulated eIF-2 alpha kinase. Trends Biochem Sci **20:**105-8.
33. **Chen, J. J., J. K. Pal, R. Petryshyn, I. Kuo, J. M. Yang, M. S. Throop, L. Gehrke, and I. M. London.** 1991. Amino acid microsequencing of internal tryptic peptides of heme-regulated eukaryotic initiation factor 2 alpha subunit kinase: homology to protein kinases. Proc Natl Acad Sci U S A **88:**315-9.

34. **Chen, J. J., M. S. Throop, L. Gehrke, I. Kuo, J. K. Pal, M. Brodsky, and I. M. London.** 1991. Cloning of the cDNA of the heme-regulated eukaryotic initiation factor 2 alpha (eIF-2 alpha) kinase of rabbit reticulocytes: homology to yeast GCN2 protein kinase and human double-stranded-RNA-dependent eIF-2 alpha kinase. Proc Natl Acad Sci U S A **88:**7729-33.
35. **Chen, M. S., A. M. Silverstein, W. B. Pratt, and M. Chinkers.** 1996. The tetratricopeptide repeat domain of protein phosphatase 5 mediates binding to glucocorticoid receptor heterocomplexes and acts as a dominant negative mutant. J Biol Chem **271:**32315-20.
36. **Chen, M. X., and P. T. Cohen.** 1997. Activation of protein phosphatase 5 by limited proteolysis or the binding of polyunsaturated fatty acids to the TPR domain. FEBS Lett **400:**136-40.
37. **Chen, M. X., A. E. McPartlin, L. Brown, Y. H. Chen, H. M. Barker, and P. T. Cohen.** 1994. A novel human protein serine/threonine phosphatase, which possesses four tetratricopeptide repeat motifs and localizes to the nucleus. Embo J **13:**4278-90.
38. **Chen, S., V. Prapapanich, R. A. Rimerman, B. Honore, and D. F. Smith.** 1996. Interactions of p60, a mediator of progesterone receptor assembly, with heat shock proteins hsp90 and hsp70. Mol Endocrinol **10:**682-93.
39. **Chen, S., W. P. Sullivan, D. O. Toft, and D. F. Smith.** 1998. Differential interactions of p23 and the TPR-containing proteins Hop, Cyp40, FKBP52 and FKBP51 with Hsp90 mutants. Cell Stress Chaperones **3:**118-29.
40. **Chen, X., U. Vinkemeier, Y. Zhao, D. Jeruzalmi, J. E. Darnell, Jr., and J. Kuriyan.** 1998. Crystal structure of a tyrosine phosphorylated STAT-1 dimer bound to DNA. Cell **93:**827-39.
41. **Chinkers, M.** 2001. Protein phosphatase 5 in signal transduction. Trends Endocrinol Metab **12:**28-32.
42. **Chinkers, M.** 1994. Targeting of a distinctive protein-serine phosphatase to the protein kinase-like domain of the atrial natriuretic peptide receptor. Proc Natl Acad Sci U S A **91:**11075-9.
43. **Cohen, P.** 2002. The origins of protein phosphorylation. Nat Cell Biol **4:**E127-30.
44. **Cohen, P.** 2000. The regulation of protein function by multisite phosphorylation--a 25 year update. Trends Biochem Sci **25:**596-601.
45. **Cohen, P. T.** 1997. Novel protein serine/threonine phosphatases: variety is the spice of life. Trends Biochem Sci **22:**245-51.
46. **Csermely, P., J. Kajtar, M. Hollosi, G. Jalsovszky, S. Holly, C. R. Kahn, P. Gergely, Jr., C. Soti, K. Mihaly, and J. Somogyi.** 1993. ATP induces a conformational change of the 90-kDa heat shock protein (hsp90). J Biol Chem **268:**1901-7.
47. **Csermely, P., T. Schnaider, C. Soti, Z. Prohaszka, and G. Nardai.** 1998. The 90-kDa molecular chaperone family: structure, function, and clinical applications. A comprehensive review. Pharmacol Ther **79:**129-68.
48. **Cutforth, T., and G. M. Rubin.** 1994. Mutations in Hsp83 and cdc37 impair signaling by the sevenless receptor tyrosine kinase in Drosophila. Cell **77:**1027-36.

49. **Czar, M. J., J. K. Owens-Grillo, K. D. Dittmar, K. A. Hutchison, A. M. Zacharek, K. L. Leach, M. R. Deibel, Jr., and W. B. Pratt.** 1994. Characterization of the protein-protein interactions determining the heat shock protein (hsp90.hsp70.hsp56) heterocomplex. J Biol Chem **269:**11155-61.
50. **Czar, M. J., J. K. Owens-Grillo, A. W. Yem, K. L. Leach, M. R. Deibel, Jr., M. J. Welsh, and W. B. Pratt.** 1994. The hsp56 immunophilin component of untransformed steroid receptor complexes is localized both to microtubules in the cytoplasm and to the same nonrandom regions within the nucleus as the steroid receptor. Mol Endocrinol **8:**1731-41.
51. **Dai, K., R. Kobayashi, and D. Beach.** 1996. Physical interaction of mammalian CDC37 with CDK4. J Biol Chem **271:**22030-4.
52. **Dalman, F. C., L. C. Scherrer, L. P. Taylor, H. Akil, and W. B. Pratt.** 1991. Localization of the 90-kDa heat shock protein-binding site within the hormone-binding domain of the glucocorticoid receptor by peptide competition. J Biol Chem **266:**3482-90.
53. **Das, A. K., P. W. Cohen, and D. Barford.** 1998. The structure of the tetratricopeptide repeats of protein phosphatase 5: implications for TPR-mediated protein-protein interactions. Embo J **17:**1192-9.
54. **Davies, T. H., Y. M. Ning, and E. R. Sanchez.** 2002. A new first step in activation of steroid receptors: hormone-induced switching of FKBP51 and FKBP52 immunophilins. J Biol Chem **277:**4597-600.
55. **De Bondt, H. L., J. Rosenblatt, J. Jancarik, H. D. Jones, D. O. Morgan, and S. H. Kim.** 1993. Crystal structure of cyclin-dependent kinase 2. Nature **363:**595-602.
56. **Denny, W. B., D. L. Valentine, P. D. Reynolds, D. F. Smith, and J. G. Scammell.** 2000. Squirrel monkey immunophilin FKBP51 is a potent inhibitor of glucocorticoid receptor binding. Endocrinology **141:**4107-13.
57. **Dent, P., D. G. Campbell, M. J. Hubbard, and P. Cohen.** 1989. Multisite phosphorylation of the glycogen-binding subunit of protein phosphatase-1G by cyclic AMP-dependent protein kinase and glycogen synthase kinase-3. FEBS Lett **248:**67-72.
58. **Dent, P., A. Lavoinne, S. Nakielny, F. B. Caudwell, P. Watt, and P. Cohen.** 1990. The molecular mechanism by which insulin stimulates glycogen synthesis in mammalian skeletal muscle. Nature **348:**302-8.
59. **Dey, B., J. J. Lightbody, and F. Boschelli.** 1996. CDC37 is required for p60v-src activity in yeast. Mol Biol Cell **7:**1405-17.
60. **Dill, K. A., S. Bromberg, K. Yue, K. M. Fiebig, D. P. Yee, P. D. Thomas, and H. S. Chan.** 1995. Principles of protein folding--a perspective from simple exact models. Protein Sci **4:**561-602.
61. **Dinner, A. R., A. Sali, L. J. Smith, C. M. Dobson, and M. Karplus.** 2000. Understanding protein folding via free-energy surfaces from theory and experiment. Trends Biochem Sci **25:**331-9.
62. **Dittmar, K. D., D. R. Demady, L. F. Stancato, P. Krishna, and W. B. Pratt.** 1997. Folding of the glucocorticoid receptor by the heat shock protein (hsp) 90-based chaperone machinery. The role of p23 is to stabilize receptor.hsp90 heterocomplexes formed by hsp90.p60.hsp70. J Biol Chem **272:**21213-20.

63. **Dittmar, K. D., K. A. Hutchison, J. K. Owens-Grillo, and W. B. Pratt.** 1996. Reconstitution of the steroid receptor.hsp90 heterocomplex assembly system of rabbit reticulocyte lysate. J Biol Chem **271:**12833-9.
64. **Dohadwala, M., E. F. da Cruz e Silva, F. L. Hall, R. T. Williams, D. A. Carbonaro-Hall, A. C. Nairn, P. Greengard, and N. Berndt.** 1994. Phosphorylation and inactivation of protein phosphatase 1 by cyclin-dependent kinases. Proc Natl Acad Sci U S A **91:**6408-12.
65. **Dougherty, J. J., D. A. Rabideau, A. M. Iannotti, W. P. Sullivan, and D. O. Toft.** 1987. Identification of the 90 kDa substrate of rat liver type II casein kinase with the heat shock protein which binds steroid receptors. Biochim Biophys Acta **927:**74-80.
66. **Duina, A. A., J. A. Marsh, R. B. Kurtz, H. C. Chang, S. Lindquist, and R. F. Gaber.** 1998. The peptidyl-prolyl isomerase domain of the CyP-40 cyclophilin homolog Cpr7 is not required to support growth or glucocorticoid receptor activity in Saccharomyces cerevisiae. J Biol Chem **273:**10819-22.
67. **Dutta, R., and M. Inouye.** 2000. GHKL, an emergent ATPase/kinase superfamily. Trends Biochem Sci **25:**24-8.
68. **Ellis, R. J.** 1994. Molecular chaperones. Opening and closing the Anfinsen cage. Curr Biol **4:**633-5.
69. **Estable, M. C., M. H. Naghavi, H. Kato, H. Xiao, J. Qin, A. Vahlne, and R. G. Roeder.** 2002. MCEF, the Newest Member of the AF4 Family of Transcription Factors Involved in Leukemia, Is a Positive Transcription Elongation Factor-b-Associated Protein. J Biomed Sci **9:**234-45.
70. **Fagard, R., and I. M. London.** 1981. Relationship between phosphorylation and activity of heme-regulated eukaryotic initiation factor 2 alpha kinase. Proc Natl Acad Sci U S A **78:**866-70.
71. **Farrell, A., and D. O. Morgan.** 2000. Cdc37 promotes the stability of protein kinases Cdc28 and Cak1. Mol Cell Biol **20:**749-54.
72. **Felts, S. J., B. A. Owen, P. Nguyen, J. Trepel, D. B. Donner, and D. O. Toft.** 2000. The hsp90-related protein TRAP1 is a mitochondrial protein with distinct functional properties. J Biol Chem **275:**3305-12.
73. **Fenton, W. A., J. S. Weissman, and A. L. Horwich.** 1996. Putting a lid on protein folding: structure and function of the co-chaperonin, GroES. Chem Biol **3:**157-61.
74. **Ferguson, J., J. Y. Ho, T. A. Peterson, and S. I. Reed.** 1986. Nucleotide sequence of the yeast cell division cycle start genes CDC28, CDC36, CDC37, and CDC39, and a structural analysis of the predicted products. Nucleic Acids Res **14:**6681-97.
75. **Fisher, D. L., E. Mandart, and M. Doree.** 2000. Hsp90 is required for c-Mos activation and biphasic MAP kinase activation in Xenopus oocytes. Embo J **19:**1516-24.
76. **Flaherty, K. M., C. DeLuca-Flaherty, and D. B. McKay.** 1990. Three-dimensional structure of the ATPase fragment of a 70K heat-shock cognate protein. Nature **346:**623-8.

77. **Fliss, A. E., Y. Fang, F. Boschelli, and A. J. Caplan.** 1997. Differential in vivo regulation of steroid hormone receptor activation by Cdc37p. Mol Biol Cell **8:**2501-9.
78. **Flynn, G. C., J. Pohl, M. T. Flocco, and J. E. Rothman.** 1991. Peptide-binding specificity of the molecular chaperone BiP. Nature **353:**726-30.
79. **Freeman, B. C., S. J. Felts, D. O. Toft, and K. R. Yamamoto.** 2000. The p23 molecular chaperones act at a late step in intracellular receptor action to differentially affect ligand efficacies. Genes Dev **14:**422-34.
80. **Freeman, B. C., D. O. Toft, and R. I. Morimoto.** 1996. Molecular chaperone machines: chaperone activities of the cyclophilin Cyp-40 and the steroid aporeceptor-associated protein p23. Science **274:**1718-20.
81. **Freeman, B. C., and K. R. Yamamoto.** 2002. Disassembly of transcriptional regulatory complexes by molecular chaperones. Science **296:**2232-5.
82. **Frydman, J.** 2001. Folding of newly translated proteins in vivo: the role of molecular chaperones. Annu Rev Biochem **70:**603-47.
83. **Frydman, J., and J. Hohfeld.** 1997. Chaperones get in touch: the Hip-Hop connection. Trends Biochem Sci **22:**87-92.
84. **Galigniana, M. D., C. Radanyi, J. M. Renoir, P. R. Housley, and W. B. Pratt.** 2001. Evidence that the peptidylprolyl isomerase domain of the hsp90-binding immunophilin FKBP52 is involved in both dynein interaction and glucocorticoid receptor movement to the nucleus. J Biol Chem **276:**14884-9.
85. **Geissler, S., K. Siegers, and E. Schiebel.** 1998. A novel protein complex promoting formation of functional alpha- and gamma-tubulin. Embo J **17:**952-66.
86. **Gerber, M. R., A. Farrell, R. J. Deshaies, I. Herskowitz, and D. O. Morgan.** 1995. Cdc37 is required for association of the protein kinase Cdc28 with G1 and mitotic cyclins. Proc Natl Acad Sci U S A **92:**4651-5.
87. **Glover, C. V., 3rd.** 1998. On the physiological role of casein kinase II in Saccharomyces cerevisiae. Prog Nucleic Acid Res Mol Biol **59:**95-133.
88. **Grammatikakis, N., A. Grammatikakis, M. Yoneda, Q. Yu, S. D. Banerjee, and B. P. Toole.** 1995. A novel glycosaminoglycan-binding protein is the vertebrate homologue of the cell cycle control protein, Cdc37. J Biol Chem **270:**16198-205.
89. **Grammatikakis, N., J. H. Lin, A. Grammatikakis, P. N. Tsichlis, and B. H. Cochran.** 1999. p50(cdc37) acting in concert with Hsp90 is required for Raf-1 function. Mol Cell Biol **19:**1661-72.
90. **Grenert, J. P., B. D. Johnson, and D. O. Toft.** 1999. The importance of ATP binding and hydrolysis by hsp90 in formation and function of protein heterocomplexes. J Biol Chem **274:**17525-33.
91. **Grenert, J. P., W. P. Sullivan, P. Fadden, T. A. Haystead, J. Clark, E. Mimnaugh, H. Krutzsch, H. J. Ochel, T. W. Schulte, E. Sausville, L. M. Neckers, and D. O. Toft.** 1997. The amino-terminal domain of heat shock protein 90 (hsp90) that binds geldanamycin is an ATP/ADP switch domain that regulates hsp90 conformation. J Biol Chem **272:**23843-50.
92. **Gross, M., and S. Hessefort.** 1996. Purification and characterization of a 66-kDa protein from rabbit reticulocyte lysate which promotes the recycling of hsp 70. J Biol Chem **271:**16833-41.

93. **Guo, H., and Z. Damuni.** 1993. Autophosphorylation-activated protein kinase phosphorylates and inactivates protein phosphatase 2A. Proc Natl Acad Sci U S A **90:**2500-4.
94. **Harding, H. P., Y. Zhang, and D. Ron.** 1999. Protein translation and folding are coupled by an endoplasmic-reticulum-resident kinase. Nature **397:**271-4.
95. **Harrison, C. J., M. Hayer-Hartl, M. Di Liberto, F. Hartl, and J. Kuriyan.** 1997. Crystal structure of the nucleotide exchange factor GrpE bound to the ATPase domain of the molecular chaperone DnaK. Science **276:**431-5.
96. **Hartl, F. U.** 1996. Molecular chaperones in cellular protein folding. Nature **381:**571-9.
97. **Hartson, S. D., A. D. Irwin, J. Shao, B. T. Scroggins, L. Volk, W. Huang, and R. L. Matts.** 2000. p50(cdc37) is a nonexclusive Hsp90 cohort which participates intimately in Hsp90-mediated folding of immature kinase molecules. Biochemistry **39:**7631-44.
98. **Hartson, S. D., E. A. Ottinger, W. Huang, G. Barany, P. Burn, and R. L. Matts.** 1998. Modular folding and evidence for phosphorylation-induced stabilization of an hsp90-dependent kinase. J Biol Chem **273:**8475-82.
99. **Hartson, S. D., V. Thulasiraman, W. Huang, L. Whitesell, and R. L. Matts.** 1999. Molybdate inhibits hsp90, induces structural changes in its C-terminal domain, and alters its interactions with substrates. Biochemistry **38:**3837-49.
100. **Hendrick, J. P., and F. U. Hartl.** 1995. The role of molecular chaperones in protein folding. Faseb J **9:**1559-69.
101. **Hoffmann, K., and R. E. Handschumacher.** 1995. Cyclophilin-40: evidence for a dimeric complex with hsp90. Biochem J **307:**5-8.
102. **Hohfeld, J., and S. Jentsch.** 1997. GrpE-like regulation of the hsc70 chaperone by the anti-apoptotic protein BAG-1. Embo J **16:**6209-16.
103. **Hohfeld, J., Y. Minami, and F. U. Hartl.** 1995. Hip, a novel cochaperone involved in the eukaryotic Hsc70/Hsp40 reaction cycle. Cell **83:**589-98.
104. **Honkanen, R. E., B. A. Codispoti, K. Tse, A. L. Boynton, and R. E. Honkanan.** 1994. Characterization of natural toxins with inhibitory activity against serine/threonine protein phosphatases. Toxicon **32:**339-50.
105. **Honkanen, R. E., M. Dukelow, J. Zwiller, R. E. Moore, B. S. Khatra, and A. L. Boynton.** 1991. Cyanobacterial nodularin is a potent inhibitor of type 1 and type 2A protein phosphatases. Mol Pharmacol **40:**577-83.
106. **Honore, B., H. Leffers, P. Madsen, H. H. Rasmussen, J. Vandekerckhove, and J. E. Celis.** 1992. Molecular cloning and expression of a transformation-sensitive human protein containing the TPR motif and sharing identity to the stress-inducible yeast protein STI1. J Biol Chem **267:**8485-91.
107. **Hutchison, K. A., L. C. Scherrer, M. J. Czar, Y. Ning, E. R. Sanchez, K. L. Leach, M. R. Deibel, Jr., and W. B. Pratt.** 1993. FK506 binding to the 56-kilodalton immunophilin (Hsp56) in the glucocorticoid receptor heterocomplex has no effect on receptor folding or function. Biochemistry **32:**3953-7.
108. **Hutchison, K. A., L. F. Stancato, J. K. Owens-Grillo, J. L. Johnson, P. Krishna, D. O. Toft, and W. B. Pratt.** 1995. The 23-kDa acidic protein in reticulocyte lysate is the weakly bound component of the hsp foldosome that is

required for assembly of the glucocorticoid receptor into a functional heterocomplex with hsp90. J Biol Chem **270:**18841-7.

109. **Iannotti, A. M., D. A. Rabideau, and J. J. Dougherty.** 1988. Characterization of purified avian 90,000-Da heat shock protein. Arch Biochem Biophys **264:**54-60.
110. **Itoh, H., and Y. Tashima.** 1993. Domain structure of the 90-kDa stress protein: heparin- and antibody-binding domain. Int J Biochem **25:**157-61.
111. **Jaenicke, R.** 1987. Folding and association of proteins. Prog Biophys Mol Biol **49:**117-237.
112. **Jakob, U., H. Lilie, I. Meyer, and J. Buchner.** 1995. Transient interaction of Hsp90 with early unfolding intermediates of citrate synthase. Implications for heat shock in vivo. J Biol Chem **270:**7288-94.
113. **Johnson, B. D., A. Chadli, S. J. Felts, I. Bouhouche, M. G. Catelli, and D. O. Toft.** 2000. Hsp90 chaperone activity requires the full-length protein and interaction among its multiple domains. J Biol Chem **275:**32499-507.
114. **Johnson, B. D., R. J. Schumacher, E. D. Ross, and D. O. Toft.** 1998. Hop modulates Hsp70/Hsp90 interactions in protein folding. J Biol Chem **273:**3679-86.
115. **Johnson, J. L., T. G. Beito, C. J. Krco, and D. O. Toft.** 1994. Characterization of a novel 23-kilodalton protein of unactive progesterone receptor complexes. Mol Cell Biol **14:**1956-63.
116. **Johnson, J. L., and D. O. Toft.** 1995. Binding of p23 and hsp90 during assembly with the progesterone receptor. Mol Endocrinol **9:**670-8.
117. **Johnson, J. L., and D. O. Toft.** 1994. A novel chaperone complex for steroid receptors involving heat shock proteins, immunophilins, and p23. J Biol Chem **269:**24989-93.
118. **Johnson, L. N., and R. J. Lewis.** 2001. Structural basis for control by phosphorylation. Chem Rev **101:**2209-42.
119. **Johnson, L. N., M. E. Noble, and D. J. Owen.** 1996. Active and inactive protein kinases: structural basis for regulation. Cell **85:**149-58.
120. **Kampranis, S. C., A. D. Bates, and A. Maxwell.** 1999. A model for the mechanism of strand passage by DNA gyrase. Proc Natl Acad Sci U S A **96:**8414-9.
121. **Kang, H., S. L. Sayner, K. L. Gross, L. C. Russell, and M. Chinkers.** 2001. Identification of amino acids in the tetratricopeptide repeat and C-terminal domains of protein phosphatase 5 involved in autoinhibition and lipid activation. Biochemistry **40:**10485-90.
122. **Kimura, Y., S. L. Rutherford, Y. Miyata, I. Yahara, B. C. Freeman, L. Yue, R. I. Morimoto, and S. Lindquist.** 1997. Cdc37 is a molecular chaperone with specific functions in signal transduction. Genes Dev **11:**1775-85.
123. **Knudsen, E. S., and J. Y. Wang.** 1996. Differential regulation of retinoblastoma protein function by specific Cdk phosphorylation sites. J Biol Chem **271:**8313-20.
124. **Kono, Y., K. Maeda, K. Kuwahara, H. Yamamoto, E. Miyamoto, K. Yonezawa, K. Takagi, and N. Sakaguchi.** 2002. MCM3-binding GANP DNA-primase is associated with a novel phosphatase component G5PR. Genes Cells **7:**821-34.

125. **Koyasu, S., E. Nishida, T. Kadowaki, F. Matsuzaki, K. Iida, F. Harada, M. Kasuga, H. Sakai, and I. Yahara.** 1986. Two mammalian heat shock proteins, HSP90 and HSP100, are actin-binding proteins. Proc Natl Acad Sci U S A **83:**8054-8.
126. **Krieg, P. A., and D. A. Melton.** 1984. Functional messenger RNAs are produced by SP6 in vitro transcription of cloned cDNAs. Nucleic Acids Res **12:**7057-70.
127. **Krone, P. H., and J. B. Sass.** 1994. HSP 90 alpha and HSP 90 beta genes are present in the zebrafish and are differentially regulated in developing embryos. Biochem Biophys Res Commun **204:**746-52.
128. **Lamb, J. R., S. Tugendreich, and P. Hieter.** 1995. Tetratrico peptide repeat interactions: to TPR or not to TPR? Trends Biochem Sci **20:**257-9.
129. **Lamphere, L., F. Fiore, X. Xu, L. Brizuela, S. Keezer, C. Sardet, G. F. Draetta, and J. Gyuris.** 1997. Interaction between Cdc37 and Cdk4 in human cells. Oncogene **14:**1999-2004.
130. **Langer, T., C. Lu, H. Echols, J. Flanagan, M. K. Hayer, and F. U. Hartl.** 1992. Successive action of DnaK, DnaJ and GroEL along the pathway of chaperone-mediated protein folding. Nature **356:**683-9.
131. **Lassle, M., G. L. Blatch, V. Kundra, T. Takatori, and B. R. Zetter.** 1997. Stress-inducible, murine protein mSTI1. Characterization of binding domains for heat shock proteins and in vitro phosphorylation by different kinases. J Biol Chem **272:**1876-84.
132. **Lees-Miller, S. P., and C. W. Anderson.** 1989. The human double-stranded DNA-activated protein kinase phosphorylates the 90-kDa heat-shock protein, hsp90 alpha at two NH2-terminal threonine residues. J Biol Chem **264:**17275-80.
133. **Lees-Miller, S. P., and C. W. Anderson.** 1989. Two human 90-kDa heat shock proteins are phosphorylated in vivo at conserved serines that are phosphorylated in vitro by casein kinase II. J Biol Chem **264:**2431-7.
134. **Leroux, M. R., and F. U. Hartl.** 2000. Protein folding: versatility of the cytosolic chaperonin TRiC/CCT. Curr Biol **10:**R260-4.
135. **Longshaw, V. M., H. W. Dirr, G. L. Blatch, and M. Lassle.** 2000. The in vitro phosphorylation of the co-chaperone mSTI1 by cell cycle kinases substantiates a predicted casein kinase II-p34cdc2-NLS (CcN) motif. Biol Chem **381:**1133-8.
136. **Louvion, J. F., R. Warth, and D. Picard.** 1996. Two eukaryote-specific regions of Hsp82 are dispensable for its viability and signal transduction functions in yeast. Proc Natl Acad Sci U S A **93:**13937-42.
137. **Lu, L., A. P. Han, and J. J. Chen.** 2001. Translation initiation control by heme-regulated eukaryotic initiation factor 2alpha kinase in erythroid cells under cytoplasmic stresses. Mol Cell Biol **21:**7971-80.
138. **Lubert, E. J., Y. Hong, and K. D. Sarge.** 2001. Interaction between protein phosphatase 5 and the A subunit of protein phosphatase 2A: evidence for a heterotrimeric form of protein phosphatase 5. J Biol Chem **276:**38582-7.
139. **Mahony, D., D. A. Parry, and E. Lees.** 1998. Active cdk6 complexes are predominantly nuclear and represent only a minority of the cdk6 in T cells. Oncogene **16:**603-11.
140. **Marcu, M. G., A. Chadli, I. Bouhouche, M. Catelli, and L. M. Neckers.** 2000. The heat shock protein 90 antagonist novobiocin interacts with a previously

unrecognized ATP-binding domain in the carboxyl terminus of the chaperone. J Biol Chem **275:**37181-6.

141. **Marcu, M. G., T. W. Schulte, and L. Neckers.** 2000. Novobiocin and related coumarins and depletion of heat shock protein 90-dependent signaling proteins. J Natl Cancer Inst **92:**242-8.
142. **Maruya, M., M. Sameshima, T. Nemoto, and I. Yahara.** 1999. Monomer arrangement in HSP90 dimer as determined by decoration with N and C-terminal region specific antibodies. J Mol Biol **285:**903-7.
143. **Matsuda, S., T. Suzuki-Fujimoto, A. Minowa, H. Ueno, K. Katamura, and S. Koyasu.** 1999. Temperature-sensitive ZAP70 mutants degrading through a proteasome-independent pathway. Restoration of a kinase domain mutant by Cdc37. J Biol Chem **274:**34515-8.
144. **Matts, R. L., and R. Hurst.** 1989. Evidence for the association of the heme-regulated eIF-2 alpha kinase with the 90-kDa heat shock protein in rabbit reticulocyte lysate in situ. J Biol Chem **264:**15542-7.
145. **Matts, R. L., R. Hurst, and Z. Xu.** 1993. Denatured proteins inhibit translation in hemin-supplemented rabbit reticulocyte lysate by inducing the activation of the heme-regulated eIF-2 alpha kinase. Biochemistry **32:**7323-8.
146. **Matts, R. L., Z. Xu, J. K. Pal, and J. J. Chen.** 1992. Interactions of the heme-regulated eIF-2 alpha kinase with heat shock proteins in rabbit reticulocyte lysates. J Biol Chem **267:**18160-7.
147. **Maxwell, A.** 1993. The interaction between coumarin drugs and DNA gyrase. Mol Microbiol **9:**681-6.
148. **Mayhew, M., A. C. da Silva, J. Martin, H. Erdjument-Bromage, P. Tempst, and F. U. Hartl.** 1996. Protein folding in the central cavity of the GroEL-GroES chaperonin complex. Nature **379:**420-6.
149. **McCarty, J. S., A. Buchberger, J. Reinstein, and B. Bukau.** 1995. The role of ATP in the functional cycle of the DnaK chaperone system. J Mol Biol **249:**126-37.
150. **McLaughlin, S. H., H. W. Smith, and S. E. Jackson.** 2002. Stimulation of the weak ATPase activity of human hsp90 by a client protein. J Mol Biol **315:**787-98.
151. **Mendez, R., and C. de Haro.** 1994. Casein kinase II is implicated in the regulation of heme-controlled translational inhibitor of reticulocyte lysates. J Biol Chem **269:**6170-6.
152. **Meng, X., J. Devin, W. P. Sullivan, D. Toft, E. E. Baulieu, and M. G. Catelli.** 1996. Mutational analysis of Hsp90 alpha dimerization and subcellular localization: dimer disruption does not impede "in vivo' interaction with estrogen receptor. J Cell Sci **109:**1677-87.
153. **Meyer, B. K., and G. H. Perdew.** 1999. Characterization of the AhR-hsp90-XAP2 core complex and the role of the immunophilin-related protein XAP2 in AhR stabilization. Biochemistry **38:**8907-17.
154. **Mimnaugh, E. G., P. J. Worland, L. Whitesell, and L. M. Neckers.** 1995. Possible role for serine/threonine phosphorylation in the regulation of the heteroprotein complex between the hsp90 stress protein and the pp60v-src tyrosine kinase. J Biol Chem **270:**28654-9.

155. **Minami, Y., J. Hohfeld, K. Ohtsuka, and F. U. Hartl.** 1996. Regulation of the heat-shock protein 70 reaction cycle by the mammalian DnaJ homolog, Hsp40. J Biol Chem **271:**19617-24.
156. **Minami, Y., Y. Kimura, H. Kawasaki, K. Suzuki, and I. Yahara.** 1994. The carboxy-terminal region of mammalian HSP90 is required for its dimerization and function in vivo. Mol Cell Biol **14:**1459-64.
157. **Miyata, Y., B. Chambraud, C. Radanyi, J. Leclerc, M. C. Lebeau, J. M. Renoir, R. Shirai, M. G. Catelli, I. Yahara, and E. E. Baulieu.** 1997. Phosphorylation of the immunosuppressant FK506-binding protein FKBP52 by casein kinase II: regulation of HSP90-binding activity of FKBP52. Proc Natl Acad Sci U S A **94:**14500-5.
158. **Miyata, Y., Y. Ikawa, M. Shibuya, and E. Nishida.** 2001. Specific association of a set of molecular chaperones including HSP90 and Cdc37 with MOK, a member of the mitogen-activated protein kinase superfamily. J Biol Chem **276:**21841-8.
159. **Moore, S. K., C. Kozak, E. A. Robinson, S. J. Ullrich, and E. Appella.** 1989. Murine 86- and 84-kDa heat shock proteins, cDNA sequences, chromosome assignments, and evolutionary origins. J Biol Chem **264:**5343-51.
160. **Morita, K., M. Saitoh, K. Tobiume, H. Matsuura, S. Enomoto, H. Nishitoh, and H. Ichijo.** 2001. Negative feedback regulation of ASK1 by protein phosphatase 5 (PP5) in response to oxidative stress. Embo J **20:**6028-36.
161. **Nathan, D. F., M. H. Vos, and S. Lindquist.** 1997. In vivo functions of the Saccharomyces cerevisiae Hsp90 chaperone. Proc Natl Acad Sci U S A **94:**12949-56.
162. **Nemoto, T., Y. Ohara-Nemoto, M. Ota, T. Takagi, and K. Yokoyama.** 1995. Mechanism of dimer formation of the 90-kDa heat-shock protein. Eur J Biochem **233:**1-8.
163. **Nemoto, T., N. Sato, H. Iwanari, H. Yamashita, and T. Takagi.** 1997. Domain structures and immunogenic regions of the 90-kDa heat-shock protein (HSP90). Probing with a library of anti-HSP90 monoclonal antibodies and limited proteolysis. J Biol Chem **272:**26179-87.
164. **Nicolet, C. M., and E. A. Craig.** 1989. Isolation and characterization of STI1, a stress-inducible gene from Saccharomyces cerevisiae. Mol Cell Biol **9:**3638-46.
165. **Obermann, W. M., H. Sondermann, A. A. Russo, N. P. Pavletich, and F. U. Hartl.** 1998. In vivo function of Hsp90 is dependent on ATP binding and ATP hydrolysis. J Cell Biol **143:**901-10.
166. **O'Keeffe, B., Y. Fong, D. Chen, S. Zhou, and Q. Zhou.** 2000. Requirement for a kinase-specific chaperone pathway in the production of a Cdk9/cyclin T1 heterodimer responsible for P-TEFb-mediated tat stimulation of HIV-1 transcription. J Biol Chem **275:**279-87.
167. **Ollendorff, V., and D. J. Donoghue.** 1997. The serine/threonine phosphatase PP5 interacts with CDC16 and CDC27, two tetratricopeptide repeat-containing subunits of the anaphase-promoting complex. J Biol Chem **272:**32011-8.
168. **O'Neil, B. J., T. R. McKeown, D. J. DeGracia, S. S. Alousi, J. A. Rafols, and B. C. White.** 1999. Cell death, calcium mobilization, and immunostaining for phosphorylated eukaryotic initiation factor 2-alpha (eIF2alpha) in neuronally

differentiated NB-104 cells: arachidonate and radical-mediated injury mechanisms. Resuscitation **41:**71-83.

169. **Oppermann, H., W. Levinson, and J. M. Bishop.** 1981. A cellular protein that associates with the transforming protein of Rous sarcoma virus is also a heat-shock protein. Proc Natl Acad Sci U S A **78:**1067-71.
170. **Owens-Grillo, J. K., M. J. Czar, K. A. Hutchison, K. Hoffmann, G. H. Perdew, and W. B. Pratt.** 1996. A model of protein targeting mediated by immunophilins and other proteins that bind to hsp90 via tetratricopeptide repeat domains. J Biol Chem **271:**13468-75.
171. **Owens-Grillo, J. K., K. Hoffmann, K. A. Hutchison, A. W. Yem, M. R. Deibel, Jr., R. E. Handschumacher, and W. B. Pratt.** 1995. The cyclosporin A-binding immunophilin CyP-40 and the FK506-binding immunophilin hsp56 bind to a common site on hsp90 and exist in independent cytosolic heterocomplexes with the untransformed glucocorticoid receptor. J Biol Chem **270:**20479-84.
172. **Panaretou, B., C. Prodromou, S. M. Roe, R. O'Brien, J. E. Ladbury, P. W. Piper, and L. H. Pearl.** 1998. ATP binding and hydrolysis are essential to the function of the Hsp90 molecular chaperone in vivo. Embo J **17:**4829-36.
173. **Pearl, L. H., and C. Prodromou.** 2000. Structure and in vivo function of Hsp90. Curr Opin Struct Biol **10:**46-51.
174. **Pellecchia, M., T. Szyperski, D. Wall, C. Georgopoulos, and K. Wuthrich.** 1996. NMR structure of the J-domain and the Gly/Phe-rich region of the Escherichia coli DnaJ chaperone. J Mol Biol **260:**236-50.
175. **Perdew, G. H., H. Wiegand, J. P. Vanden Heuvel, C. Mitchell, and S. S. Singh.** 1997. A 50 kilodalton protein associated with raf and pp60(v-src) protein kinases is a mammalian homolog of the cell cycle control protein cdc37. Biochemistry **36:**3600-7.
176. **Pirkl, F., and J. Buchner.** 2001. Functional analysis of the Hsp90-associated human peptidyl prolyl cis/trans isomerases FKBP51, FKBP52 and Cyp40. J Mol Biol **308:**795-806.
177. **Pirkl, F., E. Fischer, S. Modrow, and J. Buchner.** 2001. Localization of the chaperone domain of FKBP52. J Biol Chem **276:**37034-41.
178. **Pratt, W. B.** 1998. The hsp90-based chaperone system: involvement in signal transduction from a variety of hormone and growth factor receptors. Proc Soc Exp Biol Med **217:**420-34.
179. **Pratt, W. B., A. M. Silverstein, and M. D. Galigniana.** 1999. A model for the cytoplasmic trafficking of signalling proteins involving the hsp90-binding immunophilins and p50cdc37. Cell Signal **11:**839-51.
180. **Pratt, W. B., and D. O. Toft.** 1997. Steroid receptor interactions with heat shock protein and immunophilin chaperones. Endocr Rev **18:**306-60.
181. **Pratt, W. B., and M. J. Welsh.** 1994. Chaperone functions of the heat shock proteins associated with steroid receptors. Semin Cell Biol **5:**83-93.
182. **Prodromou, C., B. Panaretou, S. Chohan, G. Siligardi, R. O'Brien, J. E. Ladbury, S. M. Roe, P. W. Piper, and L. H. Pearl.** 2000. The ATPase cycle of Hsp90 drives a molecular 'clamp' via transient dimerization of the N-terminal domains. Embo J **19:**4383-92.

183. **Prodromou, C., S. M. Roe, R. O'Brien, J. E. Ladbury, P. W. Piper, and L. H. Pearl.** 1997. Identification and structural characterization of the ATP/ADP-binding site in the Hsp90 molecular chaperone. Cell **90:**65-75.
184. **Prodromou, C., S. M. Roe, P. W. Piper, and L. H. Pearl.** 1997. A molecular clamp in the crystal structure of the N-terminal domain of the yeast Hsp90 chaperone. Nat Struct Biol **4:**477-82.
185. **Prodromou, C., G. Siligardi, R. O'Brien, D. N. Woolfson, L. Regan, B. Panaretou, J. E. Ladbury, P. W. Piper, and L. H. Pearl.** 1999. Regulation of Hsp90 ATPase activity by tetratricopeptide repeat (TPR)-domain co-chaperones. Embo J **18:**754-62.
186. **Proud, C. G.** 1995. PKR: a new name and new roles. Trends Biochem Sci **20:**241-6.
187. **Qian, Y. Q., D. Patel, F. U. Hartl, and D. J. McColl.** 1996. Nuclear magnetic resonance solution structure of the human Hsp40 (HDJ-1) J-domain. J Mol Biol **260:**224-35.
188. **Queitsch, C., T. A. Sangster, and S. Lindquist.** 2002. Hsp90 as a capacitor of phenotypic variation. Nature **417:**618-24.
189. **Radanyi, C., B. Chambraud, and E. E. Baulieu.** 1994. The ability of the immunophilin FKBP59-HBI to interact with the 90-kDa heat shock protein is encoded by its tetratricopeptide repeat domain. Proc Natl Acad Sci U S A **91:**11197-201.
190. **Radhakrishnan, I., G. C. Perez-Alvarado, H. J. Dyson, and P. E. Wright.** 1998. Conformational preferences in the Ser133-phosphorylated and non-phosphorylated forms of the kinase inducible transactivation domain of CREB. FEBS Lett **430:**317-22.
191. **Radhakrishnan, I., G. C. Perez-Alvarado, D. Parker, H. J. Dyson, M. R. Montminy, and P. E. Wright.** 1997. Solution structure of the KIX domain of CBP bound to the transactivation domain of CREB: a model for activator:coactivator interactions. Cell **91:**741-52.
192. **Rafie-Kolpin, M., P. J. Chefalo, Z. Hussain, J. Hahn, S. Uma, R. L. Matts, and J. J. Chen.** 2000. Two heme-binding domains of heme-regulated eukaryotic initiation factor-2alpha kinase. N terminus and kinase insertion. J Biol Chem **275:**5171-8.
193. **Ramsey, A. J., and M. Chinkers.** 2002. Identification of potential physiological activators of protein phosphatase 5. Biochemistry **41:**5625-32.
194. **Ramsey, A. J., L. C. Russell, S. R. Whitt, and M. Chinkers.** 2000. Overlapping sites of tetratricopeptide repeat protein binding and chaperone activity in heat shock protein 90. J Biol Chem **275:**17857-62.
195. **Rao, J., P. Lee, S. Benzeno, C. Cardozo, J. Albertus, D. M. Robins, and A. J. Caplan.** 2001. Functional interaction of human Cdc37 with the androgen receptor but not with the glucocorticoid receptor. J Biol Chem **276:**5814-20.
196. **Ratajczak, T., and A. Carrello.** 1996. Cyclophilin 40 (CyP-40), mapping of its hsp90 binding domain and evidence that FKBP52 competes with CyP-40 for hsp90 binding. J Biol Chem **271:**2961-5.
197. **Reed, S. I.** 1980. The selection of S. cerevisiae mutants defective in the start event of cell division. Genetics **95:**561-77.

198. **Renoir, J. M., S. Le Bihan, C. Mercier-Bodard, A. Gold, M. Arjomandi, C. Radanyi, and E. E. Baulieu.** 1994. Effects of immunosuppressants FK506 and rapamycin on the heterooligomeric form of the progesterone receptor. J Steroid Biochem Mol Biol **48:**101-10.
199. **Reynolds, P. D., Y. Ruan, D. F. Smith, and J. G. Scammell.** 1999. Glucocorticoid resistance in the squirrel monkey is associated with overexpression of the immunophilin FKBP51. J Clin Endocrinol Metab **84:**663-9.
200. **Richter, K., and J. Buchner.** 2001. Hsp90: chaperoning signal transduction. J Cell Physiol **188:**281-90.
201. **Romano, P. R., M. T. Garcia-Barrio, X. Zhang, Q. Wang, D. R. Taylor, F. Zhang, C. Herring, M. B. Mathews, J. Qin, and A. G. Hinnebusch.** 1998. Autophosphorylation in the activation loop is required for full kinase activity in vivo of human and yeast eukaryotic initiation factor 2alpha kinases PKR and GCN2. Mol Cell Biol **18:**2282-97.
202. **Ruddon, R. W., and E. Bedows.** 1997. Assisted protein folding. J Biol Chem **272:**3125-8.
203. **Rudiger, S., L. Germeroth, J. Schneider-Mergener, and B. Bukau.** 1997. Substrate specificity of the DnaK chaperone determined by screening cellulose-bound peptide libraries. Embo J **16:**1501-7.
204. **Russell, L. C., S. R. Whitt, M. S. Chen, and M. Chinkers.** 1999. Identification of conserved residues required for the binding of a tetratricopeptide repeat domain to heat shock protein 90. J Biol Chem **274:**20060-3.
205. **Rutherford, S. L., and S. Lindquist.** 1998. Hsp90 as a capacitor for morphological evolution. Nature **396:**336-42.
206. **Rutherford, S. L., and C. S. Zuker.** 1994. Protein folding and the regulation of signaling pathways. Cell **79:**1129-32.
207. **Samuel, C. E.** 1993. The eIF-2 alpha protein kinases, regulators of translation in eukaryotes from yeasts to humans. J Biol Chem **268:**7603-6.
208. **Scheibel, T., and J. Buchner.** 1998. The Hsp90 complex--a super-chaperone machine as a novel drug target. Biochem Pharmacol **56:**675-82.
209. **Scheibel, T., T. Weikl, and J. Buchner.** 1998. Two chaperone sites in Hsp90 differing in substrate specificity and ATP dependence. Proc Natl Acad Sci U S A **95:**1495-9.
210. **Scheufler, C., A. Brinker, G. Bourenkov, S. Pegoraro, L. Moroder, H. Bartunik, F. U. Hartl, and I. Moarefi.** 2000. Structure of TPR domain-peptide complexes: critical elements in the assembly of the Hsp70-Hsp90 multichaperone machine. Cell **101:**199-210.
211. **Scholz, G., S. D. Hartson, K. Cartledge, N. Hall, J. Shao, A. R. Dunn, and R. L. Matts.** 2000. p50(Cdc37) can buffer the temperature-sensitive properties of a mutant of Hck. Mol Cell Biol **20:**6984-95.
212. **Scholz, G. M., K. Cartledge, and N. E. Hall.** 2001. Identification and characterization of Harc, a novel Hsp90-associating relative of Cdc37. J Biol Chem **276:**30971-9.
213. **Scholz, G. M., S. D. Hartson, K. Cartledge, L. Volk, R. L. Matts, and A. R. Dunn.** 2001. The molecular chaperone Hsp90 is required for signal transduction

by wild-type Hck and maintenance of its constitutively active counterpart. Cell Growth Differ **12:**409-17.

214. **Schutz, A. R., T. H. Giddings, Jr., E. Steiner, and M. Winey.** 1997. The yeast CDC37 gene interacts with MPS1 and is required for proper execution of spindle pole body duplication. J Cell Biol **136:**969-82.
215. **Shao, J., N. Grammatikakis, B. T. Scroggins, S. Uma, W. Huang, J. J. Chen, S. D. Hartson, and R. L. Matts.** 2001. Hsp90 regulates p50(cdc37) function during the biogenesis of the activeconformation of the heme-regulated eIF2 alpha kinase. J Biol Chem **276:**206-14.
216. **Shao, J., S. D. Hartson, and R. L. Matts.** 2002. Evidence that protein phosphatase 5 functions to negatively modulate the maturation of the Hsp90-dependent heme-regulated eIF2alpha kinase. Biochemistry **41:**6770-9.
217. **Shi, Y., K. M. Vattem, R. Sood, J. An, J. Liang, L. Stramm, and R. C. Wek.** 1998. Identification and characterization of pancreatic eukaryotic initiation factor 2 alpha-subunit kinase, PEK, involved in translational control. Mol Cell Biol **18:**7499-509.
218. **Shtilerman, M., G. H. Lorimer, and S. W. Englander.** 1999. Chaperonin function: folding by forced unfolding. Science **284:**822-5.
219. **Siegers, K., T. Waldmann, M. R. Leroux, K. Grein, A. Shevchenko, E. Schiebel, and F. U. Hartl.** 1999. Compartmentation of protein folding in vivo: sequestration of non-native polypeptide by the chaperonin-GimC system. Embo J **18:**75-84.
220. **Siligardi, G., B. Panaretou, P. Meyer, S. Singh, D. N. Woolfson, P. W. Piper, L. H. Pearl, and C. Prodromou.** 2002. Regulation of Hsp90 ATPase activity by the co-chaperone Cdc37p/p50cdc37. J Biol Chem **277:**20151-9.
221. **Silverstein, A. M., M. D. Galigniana, M. S. Chen, J. K. Owens-Grillo, M. Chinkers, and W. B. Pratt.** 1997. Protein phosphatase 5 is a major component of glucocorticoid receptor.hsp90 complexes with properties of an FK506-binding immunophilin. J Biol Chem **272:**16224-30.
222. **Silverstein, A. M., M. D. Galigniana, K. C. Kanelakis, C. Radanyi, J. M. Renoir, and W. B. Pratt.** 1999. Different regions of the immunophilin FKBP52 determine its association with the glucocorticoid receptor, hsp90, and cytoplasmic dynein. J Biol Chem **274:**36980-6.
223. **Silverstein, A. M., N. Grammatikakis, B. H. Cochran, M. Chinkers, and W. B. Pratt.** 1998. p50(cdc37) binds directly to the catalytic domain of Raf as well as to a site on hsp90 that is topologically adjacent to the tetratricopeptide repeat binding site. J Biol Chem **273:**20090-5.
224. **Sinclair, C., C. Borchers, C. Parker, K. Tomer, H. Charbonneau, and S. Rossie.** 1999. The tetratricopeptide repeat domain and a C-terminal region control the activity of Ser/Thr protein phosphatase 5. J Biol Chem **274:**23666-72.
225. **Skinner, J., C. Sinclair, C. Romeo, D. Armstrong, H. Charbonneau, and S. Rossie.** 1997. Purification of a fatty acid-stimulated protein-serine/threonine phosphatase from bovine brain and its identification as a homolog of protein phosphatase 5. J Biol Chem **272:**22464-71.

226. **Smith, D. F.** 1993. Dynamics of heat shock protein 90-progesterone receptor binding and the disactivation loop model for steroid receptor complexes. Mol Endocrinol **7:**1418-29.
227. **Smith, D. F., B. A. Stensgard, W. J. Welch, and D. O. Toft.** 1992. Assembly of progesterone receptor with heat shock proteins and receptor activation are ATP mediated events. J Biol Chem **267:**1350-6.
228. **Smith, D. F., W. P. Sullivan, T. N. Marion, K. Zaitsu, B. Madden, D. J. McCormick, and D. O. Toft.** 1993. Identification of a 60-kilodalton stress-related protein, p60, which interacts with hsp90 and hsp70. Mol Cell Biol **13:**869-76.
229. **Sondermann, H., C. Scheufler, C. Schneider, J. Hohfeld, F. U. Hartl, and I. Moarefi.** 2001. Structure of a Bag/Hsc70 complex: convergent functional evolution of Hsp70 nucleotide exchange factors. Science **291:**1553-7.
230. **Song, H. Y., J. D. Dunbar, Y. X. Zhang, D. Guo, and D. B. Donner.** 1995. Identification of a protein with homology to hsp90 that binds the type 1 tumor necrosis factor receptor. J Biol Chem **270:**3574-81.
231. **Sorger, P. K., and H. R. Pelham.** 1987. The glucose-regulated protein grp94 is related to heat shock protein hsp90. J Mol Biol **194:**341-4.
232. **Soti, C., A. Racz, and P. Csermely.** 2002. A Nucleotide-dependent molecular switch controls ATP binding at the C-terminal domain of Hsp90. N-terminal nucleotide binding unmasks a C-terminal binding pocket. J Biol Chem **277:**7066-75.
233. **Stancato, L. F., Y. H. Chow, K. A. Hutchison, G. H. Perdew, R. Jove, and W. B. Pratt.** 1993. Raf exists in a native heterocomplex with hsp90 and p50 that can be reconstituted in a cell-free system. J Biol Chem **268:**21711-6.
234. **Stebbins, C. E., A. A. Russo, C. Schneider, N. Rosen, F. U. Hartl, and N. P. Pavletich.** 1997. Crystal structure of an Hsp90-geldanamycin complex: targeting of a protein chaperone by an antitumor agent. Cell **89:**239-50.
235. **Stepanova, L., X. Leng, S. B. Parker, and J. W. Harper.** 1996. Mammalian p50Cdc37 is a protein kinase-targeting subunit of Hsp90 that binds and stabilizes Cdk4. Genes Dev **10:**1491-502.
236. **Stewart, S., M. Sundaram, Y. Zhang, J. Lee, M. Han, and K. L. Guan.** 1999. Kinase suppressor of Ras forms a multiprotein signaling complex and modulates MEK localization. Mol Cell Biol **19:**5523-34.
237. **Sullivan, W., B. Stensgard, G. Caucutt, B. Bartha, N. McMahon, E. S. Alnemri, G. Litwack, and D. Toft.** 1997. Nucleotides and two functional states of hsp90. J Biol Chem **272:**8007-12.
238. **Szabo, A., R. Korszun, F. U. Hartl, and J. Flanagan.** 1996. A zinc finger-like domain of the molecular chaperone DnaJ is involved in binding to denatured protein substrates. Embo J **15:**408-17.
239. **Szyszka, R., G. Kramer, and B. Hardesty.** 1989. The phosphorylation state of the reticulocyte 90-kDa heat shock protein affects its ability to increase phosphorylation of peptide initiation factor 2 alpha subunit by the heme-sensitive kinase. Biochemistry **28:**1435-8.

240. **Takayama, S., D. N. Bimston, S. Matsuzawa, B. C. Freeman, C. Aime-Sempe, Z. Xie, R. I. Morimoto, and J. C. Reed.** 1997. BAG-1 modulates the chaperone activity of Hsp70/Hsc70. Embo J **16:**4887-96.
241. **Taylor, D. R., S. B. Lee, P. R. Romano, D. R. Marshak, A. G. Hinnebusch, M. Esteban, and M. B. Mathews.** 1996. Autophosphorylation sites participate in the activation of the double-stranded-RNA-activated protein kinase PKR. Mol Cell Biol **16:**6295-302.
242. **Thulasiraman, V., and R. L. Matts.** 1996. Effect of geldanamycin on the kinetics of chaperone-mediated renaturation of firefly luciferase in rabbit reticulocyte lysate. Biochemistry **35:**13443-50.
243. **Thulasiraman, V., Z. Xu, S. Uma, Y. Gu, J. J. Chen, and R. L. Matts.** 1998. Evidence that Hsc70 negatively modulates the activation of the heme-regulated eIF-2alpha kinase in rabbit reticulocyte lysate. Eur J Biochem **255:**552-62.
244. **Tzamarias, D., and K. Struhl.** 1995. Distinct TPR motifs of Cyc8 are involved in recruiting the Cyc8-Tup1 corepressor complex to differentially regulated promoters. Genes Dev **9:**821-31.
245. **Tzivion, G., Z. Luo, and J. Avruch.** 1998. A dimeric 14-3-3 protein is an essential cofactor for Raf kinase activity. Nature **394:**88-92.
246. **Uma, S., S. D. Hartson, J. J. Chen, and R. L. Matts.** 1997. Hsp90 is obligatory for the heme-regulated eIF-2alpha kinase to acquire and maintain an activable conformation. J Biol Chem **272:**11648-56.
247. **Uma, S., R. L. Matts, Y. Guo, S. White, and J. J. Chen.** 2000. The N-terminal region of the heme-regulated eIF2alpha kinase is an autonomous heme binding domain. Eur J Biochem **267:**498-506.
248. **Uma, S., V. Thulasiraman, and R. L. Matts.** 1999. Dual role for Hsc70 in the biogenesis and regulation of the heme-regulated kinase of the alpha subunit of eukaryotic translation initiation factor 2. Mol Cell Biol **19:**5861-71.
249. **Usui, H., R. Inoue, O. Tanabe, Y. Nishito, M. Shimizu, H. Hayashi, H. Kagamiyama, and M. Takeda.** 1998. Activation of protein phosphatase 2A by cAMP-dependent protein kinase-catalyzed phosphorylation of the 74-kDa B" (delta) regulatory subunit in vitro and identification of the phosphorylation sites. FEBS Lett **430:**312-6.
250. **Vainberg, I. E., S. A. Lewis, H. Rommelaere, C. Ampe, J. Vandekerckhove, H. L. Klein, and N. J. Cowan.** 1998. Prefoldin, a chaperone that delivers unfolded proteins to cytosolic chaperonin. Cell **93:**863-73.
251. **Valay, J. G., M. Simon, M. F. Dubois, O. Bensaude, C. Facca, and G. Faye.** 1995. The KIN28 gene is required both for RNA polymerase II mediated transcription and phosphorylation of the Rpb1p CTD. J Mol Biol **249:**535-44.
252. **Walker, A. I., T. Hunt, R. J. Jackson, and C. W. Anderson.** 1985. Double-stranded DNA induces the phosphorylation of several proteins including the 90 000 mol. wt. heat-shock protein in animal cell extracts. Embo J **4:**139-45.
253. **Walsh, A. H., A. Cheng, and R. E. Honkanen.** 1997. Fostriecin, an antitumor antibiotic with inhibitory activity against serine/threonine protein phosphatases types 1 (PP1) and 2A (PP2A), is highly selective for PP2A. FEBS Lett **416:**230-4.
254. **Wang, X., N. Grammatikakis, and J. Hu.** 2002. Role of p50/CDC37 in hepadnavirus assembly and replication. J Biol Chem **277:**24361-7.

255. **Welch, W. J., J. I. Garrels, G. P. Thomas, J. J. Lin, and J. R. Feramisco.** 1983. Biochemical characterization of the mammalian stress proteins and identification of two stress proteins as glucose- and Ca2+-ionophore-regulated proteins. J Biol Chem **258:**7102-11.
256. **Whitelaw, M. L., K. Hutchison, and G. H. Perdew.** 1991. A 50-kDa cytosolic protein complexed with the 90-kDa heat shock protein (hsp90) is the same protein complexed with pp60v-src hsp90 in cells transformed by the Rous sarcoma virus. J Biol Chem **266:**16436-40.
257. **Whitesell, L., E. G. Mimnaugh, B. De Costa, C. E. Myers, and L. M. Neckers.** 1994. Inhibition of heat shock protein HSP90-pp60v-src heteroprotein complex formation by benzoquinone ansamycins: essential role for stress proteins in oncogenic transformation. Proc Natl Acad Sci U S A **91:**8324-8.
258. **Wiech, H., J. Buchner, R. Zimmermann, and U. Jakob.** 1992. Hsp90 chaperones protein folding in vitro. Nature **358:**169-70.
259. **Xu, Z., J. K. Pal, V. Thulasiraman, H. P. Hahn, J. J. Chen, and R. L. Matts.** 1997. The role of the 90-kDa heat-shock protein and its associated cohorts in stabilizing the heme-regulated eIF-2alpha kinase in reticulocyte lysates during heat stress. Eur J Biochem **246:**461-70.
260. **Yamano, H., K. Ishii, and M. Yanagida.** 1994. Phosphorylation of dis2 protein phosphatase at the C-terminal cdc2 consensus and its potential role in cell cycle regulation. Embo J **13:**5310-8.
261. **Young, J. C., and F. U. Hartl.** 2000. Polypeptide release by Hsp90 involves ATP hydrolysis and is enhanced by the co-chaperone p23. Embo J **19:**5930-40.
262. **Young, J. C., I. Moarefi, and F. U. Hartl.** 2001. Hsp90: a specialized but essential protein-folding tool. J Cell Biol **154:**267-73.
263. **Young, J. C., W. M. Obermann, and F. U. Hartl.** 1998. Specific binding of tetratricopeptide repeat proteins to the C-terminal 12-kDa domain of hsp90. J Biol Chem **273:**18007-10.
264. **Young, J. C., C. Schneider, and F. U. Hartl.** 1997. In vitro evidence that hsp90 contains two independent chaperone sites. FEBS Lett **418:**139-43.
265. **Zhang, F., A. Strand, D. Robbins, M. H. Cobb, and E. J. Goldsmith.** 1994. Atomic structure of the MAP kinase ERK2 at 2.3 A resolution. Nature **367:**704-11.
266. **Zhang, X., C. J. Herring, P. R. Romano, J. Szczepanowska, H. Brzeska, A. G. Hinnebusch, and J. Qin.** 1998. Identification of phosphorylation sites in proteins separated by polyacrylamide gel electrophoresis. Anal Chem **70:**2050-9.
267. **Zhao, S., and A. Sancar.** 1997. Human blue-light photoreceptor hCRY2 specifically interacts with protein serine/threonine phosphatase 5 and modulates its activity. Photochem Photobiol **66:**727-31.
268. **Zhao, Y. G., R. Gilmore, G. Leone, M. C. Coffey, B. Weber, and P. W. Lee.** 2001. Hsp90 phosphorylation is linked to its chaperoning function. Assembly of the reovirus cell attachment protein. J Biol Chem **276:**32822-7.
269. **Zhu, X., X. Zhao, W. F. Burkholder, A. Gragerov, C. M. Ogata, M. E. Gottesman, and W. A. Hendrickson.** 1996. Structural analysis of substrate binding by the molecular chaperone DnaK. Science **272:**1606-14.

270. **Ziegelhoffer, T., P. Lopez-Buesa, and E. A. Craig.** 1995. The dissociation of ATP from hsp70 of Saccharomyces cerevisiae is stimulated by both Ydj1p and peptide substrates. J Biol Chem **270:**10412-9.
271. **Zimmerman, S. B., and S. O. Trach.** 1991. Estimation of macromolecule concentrations and excluded volume effects for the cytoplasm of Escherichia coli. J Mol Biol **222:**599-620.
272. **Zuo, Z., G. Urban, J. G. Scammell, N. M. Dean, T. K. McLean, I. Aragon, and R. E. Honkanen.** 1999. Ser/Thr protein phosphatase type 5 (PP5) is a negative regulator of glucocorticoid receptor-mediated growth arrest. Biochemistry **38:**8849-57.

VITA

Jieya Shao 2

Candidate for the Degree of

Doctor of Philosophy

Thesis: CHARACTERIZATION OF THE MOLECULAR CHAPERONE HSP90 COHORTS, p50^{CDC37} AND PROTEIN PHOSPHATASE 5, AND THEIR DIFFERENTIAL REGULATION OF THE BIOGENESIS OF THE HEME-REGULATED eIF2α KINASE

Major Field: Biochemistry and Molecular Biology

Biographical:

Personal Data: Born in Tianjin, China, on April 1, 1973, the daughter of Minyi Shao and Shuzhen Chen.

Education: Graduated from Tianjin Number One High School, Tianjin, China in July 1992; received Bachelor of Science Degree in Biochemistry from Nankai University, Tianjin, China in July 1996; completed requirements for the Doctor of Philosophy Degree with a major in Biochemistry and Molecular Biology at Oklahoma State University in December 2002.

Experience: Half-time Research Assistant, Department of Biochemistry and Molecular Biology, Oklahoma State University, Stillwater, Oklahoma, May 1997-December 2002; Quarter-time Research Assistant, Laboratory of MALDI-TOF Mass Spectrometry, Core Facility, Department of Biochemistry and Molecular Biology, Oklahoma State University, Stillwater, Oklahoma, January 2002-December 2002.